UNIVERSITY OF OKLAHOMA

GRADUATE COLLEGE

EFFECT OF DIOIC ACIDS ON FERRIC IRON REDUCTION BY *SHEWANELLA ONEIDENSIS* MR-1 AND CARBON STEEL CORROSION

A THESIS

SUBMITTED TO THE GRADUATE FACULTY

in partial fulfillment of the requirements for the

Degree of

MASTER OF SCIENCE

By

HATICE NURSAH KOKBUDAK
Norman, Oklahoma
2017

EFFECT OF DIOIC ACIDS ON FERRIC IRON REDUCTION BY *SHEWANELLA ONEIDENSIS* MR-1 AND CARBON STEEL CORROSION

A THESIS APPROVED FOR THE
SCHOOL OF CIVIL ENGINEERING AND ENVIRONMENTAL SCIENCE

BY

_____
Dr. Mark A. Nanny, Chair

_____
Dr. Joseph M. Suflita

_____
Dr. Robert W. Nairn

Acknowledgements

I would like to thank my parent, Ayfer and Suleyman Kokbudak who supported me and gave me unconditional love during my life. I also want to thank my grandparent, Yuksel and Giyaseddin Horozoglu taught me the importance of education and supported me during my college life.

I would like to thank my thesis advisor, Dr. Mark A. Nanny for accepting me as his graduate student and supporting me through my project as well as teaching me to be a better student.

I would also like to thank Dr. Joseph M. Suflita and Dr. Robert W. Nairn for their assistance and patience as well as for serving on my committee. I also wish to express special thanks to Dr. Jizhong Zhou for accepting me his laboratory and Dr. Aifen Zhou for assist me with laboratory procedures. I would like to thank Yan Li for being there whenever I need her help. I also want to thank the summer visitor researcher, Shawn Cusack for his input and help to my project.

Finally, I would like to express a very special thanks to Kilean Lucas for supporting me emotionally and companionship through all the good and bad times.

Table of Contents

List of Tables

List of Figures

Abstract

Corrosion represents a tremendous burden on infrastructure and industries such as the oil and gas industry. According to National Association of Corrosion Engineers (NACE), total annual cost of steel corrosion in the oil and gas production industry is estimated to be $1.372 billion and over 20% of the corrosion cost is through microbially induced corrosion (Jahaverdashti, 2008). Production water tanks, oil wells and pipes are critical components in the oil and gas industry and are among objects that are most susceptible to corrosion. Maintaining or replacing these can place significant financial strain on the industry. Hence, it is important to determine the cause(s) and the underlying mechanism(s) behind the biological corrosion that occurs in field. Aqueous samples taken from water oil wells and pipes from Putumayo Basin located in Colombia show an abundance of bacterial species such as *Shewanella* spp, a facultative anaerobic iron-reducing bacteria (IRB). In addition, a number of dicarboxylic (dioic) acids were detected in these tanks that are proposed to arise from the aerobic degradation of hydrocarbons that are present in the environment. In this work, we propose a new microbially influenced corrosion (MIC) mechanism by which dioic acids solubilize ferric iron from a steel surface and the soluble ferric iron is respired by iron reducing bacteria that are present, allowing unbinding of the dioic acid for further ferric iron solubilization, thus increasing the rate of carbon steel corrosion. We studied the effects of three dioic acids that have been found in the production water environment (oxalic acid, malonic acid and succinic acid) as well as two reference ligands (citric acid and nitrilotriacetic acid (NTA)) on this proposed IRB MIC mechanism. Our results show that in the presence of bacteria, the dioic acids increase the concentration of dissolved ferric iron more than in an abiotic environment (oxalate shows nearly a 3-fold increase in dissolved ferric iron concentration). We also observe a decrease on $E_{corrosion}$ with oxalate suggesting that the removal efficiency of ferric oxyhydroxide layer from steel surface increased and *S. oneidensis* MR-1 respiration facilitated. We conclude that our mechanism is valid as a basic mechanism of IRB MIC, but the system is likely more complex due to the adsorption of ligands on the surface and the formation of biofilms.

Chapter 1 : Introduction

1.1 Introduction to Iron Reducing Bacteria and Carbon Steel Corrosion

Microbially induced carbon steel corrosion has been a documented problem in a variety of industries including oil field production and natural gas transmission. According to National Association of Corrosion Engineers (NACE), total annual cost of corrosion in the oil and gas production industry is estimated to be $1.372 billion with over 20% of the corrosion costs due to microbially induced corrosion (Jahaverdashti, 2008). Hence, it is imperative to determine the factors that affect the development of carbon steel corrosion and control its rate under microbial influence.

The most well-known microbial agents affecting corrosion are sulfate reducing bacteria (SRB) that have been shown to be the driving force for corrosion in many aquatic environments (Enning & Garrelfs, 2014). SRB can reduce sulfate with organic compounds or hydrogen, which causes the production of hydrogen sulfide. Hydrogen sulfide is an indirect corrosive chemical agent; it is a byproduct of the SRB that causes corrosion and not the SRB themselves in a process commonly called chemical microbially influenced corrosion (CMIC). Some species of SRB can also attack iron via withdrawal of electrons, which occurs through direct metabolic coupling, and this process is electrical microbially influenced corrosion (EMIC). In many cases, corrosion of iron by SRB is due in part to the formation of ferrous sulfides (FeS), which help to thermodynamically drive the oxidation reactions that are the cause of steel corrosion (Enning & Garrelfs, 2014).

However, it is suspected that other microbes besides SRBs may be able to facilitate

MIC. Based upon production water samples in the Putumayo Basin, Colombia strongly suggest a different microbial corrosion mechanism. These samples showed 11 μM sulfate and no SRB activity or sulfide was detected from sulfate reduction assay. Additionally, the production water showed a dissolved iron concentration exceeding 25 mM, which is significantly higher than what is defined as corrosion (>90 μM). This is very unusual for a SRB driven corrosion mechanism, as ferrous ions typically precipitate with sulfite (Nanny, 2015). A phenanthroline colorimetric test on the samples showed that all the dissolved iron present in the ferric iron state. Also, the production water was found to be ~ pH 7 and the amount of solubilized ferric iron was 10^{14} times higher than the equilibrium concentration found in solubility diagrams (Stumm et al., 1996). Even though the well water samples were exposed to atmosphere for 5 days, no precipitation occurred. The stable, high concentration of ferric iron was hypothesized to result from the presence of organic ligands such as dioic acids (oxalic acid, malonic acid and succinic acid), which chelate with ferric iron, forming a stable iron complex.

The origin of these dioic acids is hypothesized to be related to the presence of aerobic hydrocarbon degrading microbes, which, due to the presence of petroleum products at the research site, can initiate the degradation process. It has been shown that some aerobic microbes are capable of enzymatically degrading n-alkanes – via hydroxylases, alcohol dehydrogenases, and aldehyde dehydrogenases – into easily metabolizable substrates such as dioic acids (Broadway et al., 1993). This is important because alkanes are typically a major fraction (50%) of crude oil, depending on the oil source (Labinger et al., 2002). Ferric iron can be stable in aqueous solution once it forms a complex with

organic chelators even when they exposed to atmosphere (Paris et al., 2013). Both a variety and abundance of organic molecules were present in samples from Putumayo Basin including α-hydroxy carboxylic acids, dioic acids, 2,2'-oxybis acetic acid, and polyethylene glycerol (PEG)-carboxylic acids (Duncan and Nanny, 2015). It hypothesized that these acids are capable of complexing with ferric iron, leading to an increase in dissolved iron concentrations. Similar compounds were found in natural gas production water tank samples taken from Barnett Shale in North Texas (Duncan and Nanny, 2015). Based on the findings from two research cites, this research focuses on the organic ligand composition of the well water samples that may facilitate a new mechanism of microbial induced corrosion.

Based on the Putumayo and North Texas data there is a new proposed microbially induced corrosion mechanism involving iron reducing bacteria (IRB) as demonstrated in Figure 1.1. The mechanism proposes that organic ligands, produced by the aerobic microbes, can chelate with ferric iron from a ferric oxyhydroxide layer on the steel surface and solubilize a ferric ion, which can be used as terminal electron acceptor by IRB. Once the ligand is released it may re-adsorb to the oxidized steel surface to solubilize more ferric ions. This cycling mechanism removes most of the ferric oxyhydroxide layer from the production water pipes or tanks. Removal of the water from the production tank allows for periodic input of dissolved oxygen. Dissolved O_2 is prevented from diffusing through the ferric oxide layer to the bare steel surface, which then decreases corrosion rate. However, organic ligands can remove this layer by solubilizing ferric iron. When there is a periodic input of O_2, it can oxidize the metallic iron from steel surface further since the protective ferric oxyhydroxide layer has been

removed and the overall corrosion rate is going to be a function of the efficiency of removal of ferric oxyhydroxide layer and amount of O_2 put into production water tank.

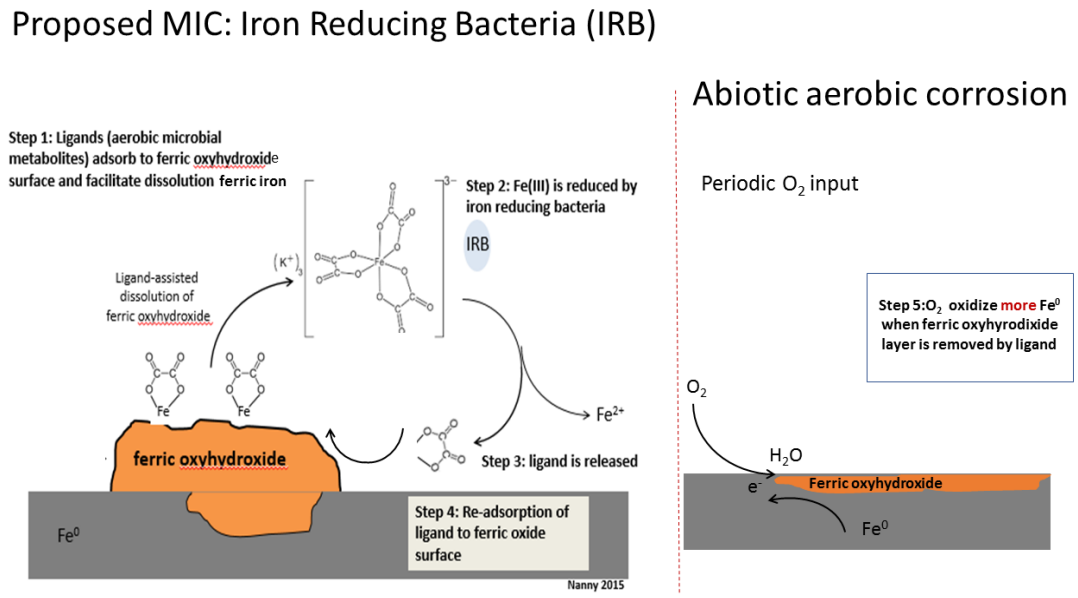

Figure 1.1 A) Ligands increase soluble ferric iron concentration which can be used as TEA by IRB This process decreases ferric oxyhydroxide layer on steel surface. **B)** O_2 reacts with metal iron and forms H_2O and Fe^{+3} that will produce ferric oxyhydroxide.

Three dioic acids that have been identified in both Putumayo Basin and Barnett Shale production waters are oxalic acid, malonic acid and succinic acid. While these acids have been identified, their concentrations in these environments has not been measured with the exception of oxalate in Barnett Shale production water, where it was measured to be 1 mM. However, in the literature, these dioic acids are reported to be among the highest concentration dioic acids in water samples from 40 petroleum wells located in the San Joaquin, Santa Maria and northern Gulf of Mexico basins (Kharaka et al., 1993), where they have been measured at values up to 50 mM for oxalate and 250 mM for malonate (Kharaka et al., 1993).

For this reason, concentrations varying between 0.1 mM and 50 mM of these dioic acids

were used for this study. Another property of these dioic acid is that they are relatively small (their molecular weights are between 90-118 gram/mole) organic acids known to chelate ferric iron with known binding constants, which are log β_3 = 20.20 (oxalate), log β_3 = 16.6 (malonate) and log β_3 = 6.88 (succinate). These binding constants are directly correlated to the strength of the bonds in the complex and their definition is given in Figure 2. Dioic acids chelate with iron in a 3:1 ratio. For oxalic acid, this forms three 5-membered rings around Fe^{3+} ion as shown in Figure 2.

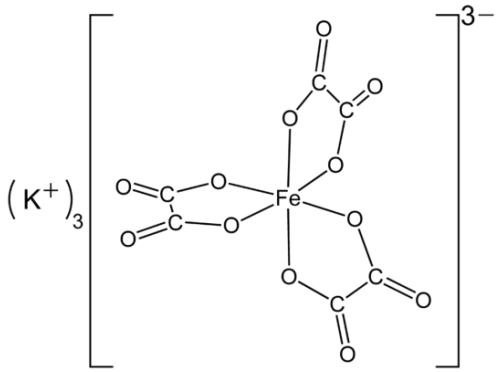

Figure 1.2 Oxalic acid complex with Fe^{3+} with β_3 = 20.20.

The iron reducing mechanism and its effect on corrosion isn't clearly proven in literature (Nanny et al. 2016). Figure 1.3 demonstrates two possible IRB mechanisms. Pathway 1 demonstrates the iron chelation hypothesis and pathway 2 demonstrates the microbial-mineral direct contact mechanism. Pathway 1 shows that ferric iron is chelated by an organic ligand thereby increasing its solubility. The amount of available free energy for ferric iron respiration is -36 kJ/mole for the ligands citrate and nitrilotriacetic acid (NTA) (Bird at al., 2011). Pathway 2 shows that the amount of available free energy varies from -9 to + 60 kJ/mole for mineral-microbial direct

contact, depending upon the solubility of the ferric oxide phase being reduced. This is a much less favorable free energy range than for the iron chelation mechanism, suggesting direct microbial contact with solid-phase ferric oxides is not a highly productive mechanism for respiration of ferric iron since IRB respiration depends on the solubility of mineral ferric iron (Bird et al., 2011). When we compare the two pathways, chelated ferric iron reduction is energetically more favorable, which can be postulated to be true even for ligands other than citrate and NTA. Moreover, the maximum rate for soluble chelated ferric iron is one to three orders of magnitude greater than that of iron respiration occurring through direct contact between the microbe and the ferric oxide solid phase (Bonneville et al., 2004). Because these mechanisms are still largely unconfirmed, we tried to elucidate the difference between the two pathways by using organic metabolites as model chelators found in field samples (dioic acids with $6 < \log \beta_3 < 21$) and comparing them with ferric oxyhydroxide microbial-mineral respiration.

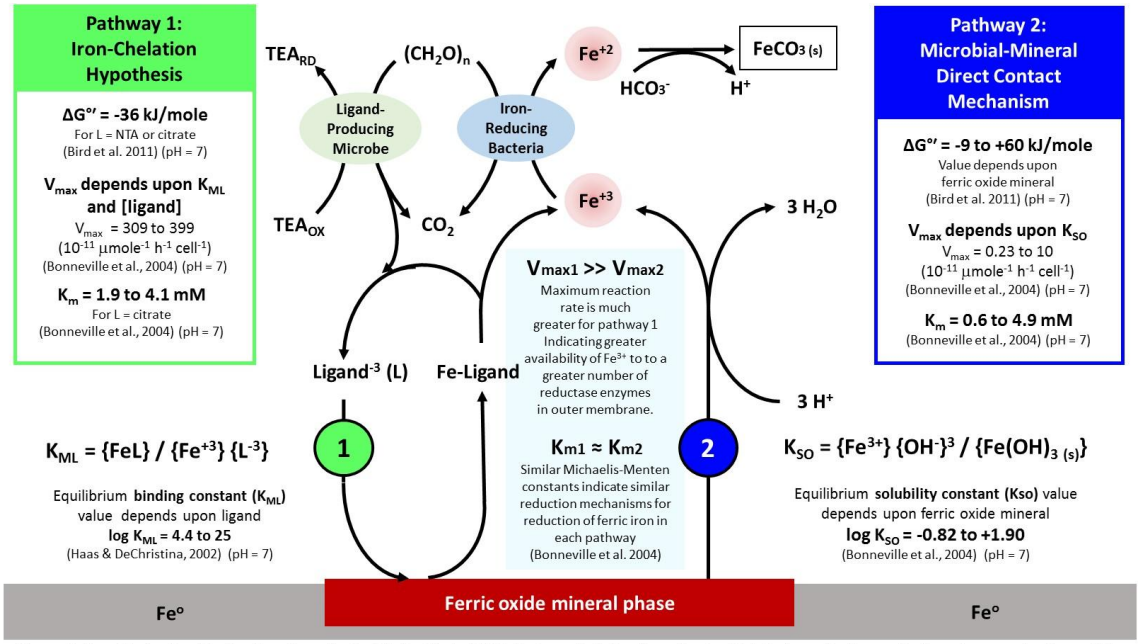

Figure 1.3 Iron reduction mechanisms hypothesized to facilitate MIC: (**Pathway 1**) the iron-chelation hypothesis which is dependent upon the ligand concentration and its binding constant with ferric iron, and the microbial mineral direct contact mechanism (**Pathway 2**) which is dependent upon the equilibrium concentration of dissolved ferric iron and the dissolution rate of ferric oxide.

When choosing a model organism for this research, we turn to data from production water environments to determine the most likely culprits of this iron reducing behavior. It has been shown that most of the microbial community found in the Putumayo Basin belongs to the *Shewanella* genus, which are facultative anaerobic bacteria that may use ferric iron as a terminal electron acceptor (TEA) under anaerobic conditions (Nanny et al. 2015), (Wiatrowski et al., 2006). This means that it utilizes O_2 as the terminal electron acceptor for its metabolism in aerobic environment, but in the lack of O_2 *Shewanella* will utilize iron as the terminal electron acceptor (Hecherl et al., 2003). This bacterium facilitates its ferric iron respiration through the release of siderophores, which are organic ligands that chelate iron and solubilize it with high stability (Bird et al.,

2011). Siderophores are a common component in the respiration of ferric iron in both iron reducing bacteria and sulfate reducing bacteria (Gram, 1994). However, there is not any evidence of siderophores present in Putumayo Basin (Nanny et al., 2016). Additionally, Putumayo Basin data demonstrates an abundance of dissolved ferric iron that hypothesized to be due to an abundance of organic chelators. *Shewanella* doesn't require producing siderophores and have instead been hypothesized to use organic chelators if the conditions are right (Bird et al., 2011). This is a major advantage over sulfate reducing bacteria, as producing siderophores is very energetically demanding. Because of this, ferric iron intake with siderophores typically only occurs in dissolved ferric iron poor environments (Bird et al., 2011). The Putumayo Basin well is a dissolved ferric iron rich environment and for this reason IRB can respire dissolved ferric ion without the formation of siderophores, giving them a huge advantage over SRB. These results indicate that it may be *Shewanella* that is the culprit in the corrosion of steel in these systems. Based on the aforementioned findings and conclusions we choose *Shewanella oneidensis* MR-1 as our model IRB. I tested *S. oneidensis* MR-1 respiration in the presence of three dioic acids –oxalic acid, malonic acid, and succinic acid – and look at the effects of the acid binding constant (log β_3), the acid's ability to dissolve ferric iron and bio-available ferric iron for *S. oneidensis* MR-1 respiration to determine if it plays a role in the corrosion of steel in these production water environments.

Pipelines and water tanks that are used at oil production sites are typically exposed to the atmosphere. This constant exposure to oxygen naturally leads to the formation of a ferric oxyhydroxide layer on the steel surface, which passivates the steel, preventing

further corrosion. However, the presence of this passivation layer makes using total corrosion products as a measure of corrosion an impractical method as the initial oxidation layer will vary from surface to surface depending on oxygen flow.

For this reason, electrochemical techniques are often employed to measure corrosion rates independent of these complicating factors. Linear polarization resistance (LPR) is used that can provide instantaneous results of corrosion rate. This technique measures changes in the electrode (steel coupon) current as a function of changing the electrode potential. From this data, the resistance to polarization can also be determined. By using the polarization resistance (R_p), the corrosion rate (often reported in milli-inches per year [mpy]) can be calculated using the Stern-Geary equation (Stern et al., 1957) by Gamry Framework Software.

1.2 Hypothesis and Objectives

1.2.1 Goal

The goal of this research is to test a newly proposed mechanism of microbially induced corrosion (MIC) that involves interactions between organic ligands and iron reducing bacteria (IRB) found to be present in production well environments. The proposed mechanism is that organic ligands solubilize ferric iron from an oxidized steel surface, which is then reduced by IRB under anaerobic conditions. Once the oxidized layer (ferric oxyhydroxide) is consumed by the ligand (that is being constantly recycled to solubilize more ferric iron), periodic oxygen input would cause the further oxidation of the metal, starting the cycle over again. It is proposed that this mechanism contributes to increasing the overall corrosion process. This research will focus on the interactions between *S. oneidensis* MR-1 (our model IRB) and low molecular weight dioic acids

(oxalic acid, malonic acid and succinic acid) that have a range of binding constants ($6 < \log \beta_3 < 21$).

1.2.3 Hypotheses

Previous studies from two regions –Barnett Shale in North Texas and Putumayo Basin in Colombia – have provided information that allows us to propose the different corrosion mechanism in this research. It has been shown that the concentration of dissolved ferric iron was 25 mM, which is 10^{14} times higher than the equilibrium concentration of ferric iron at pH 7. Additionally, organic ligands that can chelate with ferric iron – increasing their solubility – such as dioic acids have been found in oil and gas production water, along with evidence of microbial activity. A majority of the microbial community found in the Putumayo Basin belongs to the *Shewanella* genus, which are also well studied IRBs. Based on these findings, the overall hypothesis of this research is: the binding constants of three dioic acids found in production water environments are in the range that they can stably bind with and solubilize ferric iron present on a steel surface, making the ferric iron available for subsequent respiration by a model IRB (*S. oneidensis* MR-1). It is hypothesized that these three ligands have binding constants strong enough to allow them to bind ferric iron and solubilize it from a steel surface, but weak enough that it can release the ferric iron for respiration/reduction by the bacteria. To fully test this hypothesis, it has been broken down into three smaller aims:

1. The three dioic acids of choice (oxalic acid, malonic acid and succinic acid) have binding constants that allow solubilizing of ferric iron from an oxidized layer that has formed on a steel coupon under aerobic conditions in an abiotic

environment.

2. The iron reducing bacteria *S. oneidensis* MR-1 respires ferric iron that has been solubilized by the dioic acids (oxalic acid, malonic acid and succinic acid) for both ferric oxyhydroxide and from an oxidized steel surface under anaerobic conditions.

3. The solubilization of ferric iron from an oxidized steel surface by dioic acids and its subsequent respiration/reduction by *S. oneidensis* MR-1 causes an increase in corrosion rate of the carbon steel sample in anaerobic conditions.

1.2.4 Objective

The objective of this research was to design and carry out experiments that allowed us to answer the overall research question of whether the presence of dioic acids combined with the iron reducing bacteria *S. oneidensis* MR-1 increased the rate of corrosion of steel under anaerobic conditions. The objective was carried out first by studying the efficiency of the selected dioic acids at solubilizing ferric iron. This was done by studying the interaction between carbon steel and the individual dioic acids at various concentrations under aerobic conditions for both clean and oxidized carbon steel. The total corrosion was quantified by either measuring the corrosion products for ferric iron concentration using atomic absorption spectroscopy (AAS) or electrochemical techniques such as linear polarization resistance. After this, the effect of various concentration dioic acids on the solubilization of ferric oxyhydroxide and *S. oneidensis* MR-1 respiration in an anaerobic environment was tested. *S. oneidensis* MR-1 respiration was measured using a ferrozine based colorimetric assay. Finally, the effects of dioic acid solubilization of ferric iron and *S. oneidensis* MR-1 respiration on

the corrosion of steel were investigated. The system was studied both with and without the dioic acids to determine their role in the corrosion process. This was achieved through AAS measurement of the corrosion products as well as linear polarization electrochemical methods.

Chapter 2 : Literature Review

The study of the different aspects of steel corrosion has a variety of applications in a multitude of fields including the petroleum, auto, and civil engineering industries. This literature review highlights current knowledge of the effects that small organic acids (e.g. acetic acid, formic acid and dioic acids) have on the corrosion behavior of equipment in these industries. Additionally, the present understanding of the role of *S. oneidensis* MR-1 in carbon steel corrosion is highlighted. This shows what is currently known and how our work impacts the understanding of these processes in the field.

2.1 Monocarboxylic Organic Acid Interactions on Steel Surfaces:

Steel surfaces in the oil and gas industry are exposed to a multitude of environments and conditions throughout their lifetimes. The interactions of these surfaces and various components (such as organic acids) in the production water that pass over them can play a significant part in determining how the material will resist and/or succumb to corrosion. Over the course of prolonged exposure to even minimally corrosive conditions (e.g. weak acids, the presence of oxygen gas, etc.), it is common to observe the formation of a ferric hydroxide passivation layer on the steel surfaces in these systems. The interactions of small organic monocarboxylic acids – that are commonly found in production water environments, arising as the metabolic products of *Acetobacter* species present (Williamson et al., 2015) – with this layer have previously been investigated and described in below.

In production water environments, organic acids are often found at concentrations around 1 mM, which encompasses all the organic acids present (Tran et al., 2013). It has been shown that the most common low molecular weight organic acid in these

environments is acetic acid (CH_3COOH, or HAc), which is found to be in the range of 50-90% of the total organic acids (Gunaltun & Larrey, 2000), (Dougherty, 2004). Acetic acid is a weak acid with pKa=4.76 and it will dissociate depending on the temperature and pH of water. Due to the frequency of its occurrence, there are many studies investigating the effects of acetic acid on mild steel corrosion in aqueous environments. Studies have proposed two mechanistic ways in which acetic acid increases the rate of corrosion (Dougherty, 2004). These proposed mechanisms show that acetic acid accelerates the cathodic reactions at the steel surface. The first mechanism, known as direct reduction, is the dissociation of acetic acid at the metal surface where it oxidizes metallic iron to ferrous iron as shown in Equation 1:

$$CH_3COOH + e^- \rightarrow CH_3COO^- + H_{ads} \quad (1)$$

where H_{ads} is the adsorbed hydrogen. The other mechanism is acetic acid dissociation near the metal surface providing additional hydrogen ions for the cathodic reduction of hydrogen ions, which is known as the buffering effect (Tran et al., 2013). Only the hydrogen ions need to be considered in this mechanism, as the role of acetic acid is solely to provide hydrogen, thus acting as a buffer. This is shown in Equation 2.

$$H^+(aq) + e^- \rightarrow H_{ads} \quad (2)$$

While acetic acid is the most common low molecular weight organic acid identified in production water, there are other acids present that also contribute to the corrosion of the steel surfaces. These other acids include formic acid (CH_2O_2, pKa = 3.75) and propionic acid (CH_3CH_2COOH, pKa = 4.76). Studies have shown that these acids also influence the corrosion of carbon steel, as well as an impact on the formation of a

ferrous carbonate passivation layer on the steel surface (Rivera, 2011). The conclusion from this other work is that organic acids increase the required time to form a ferrous carbonate layer, which would passivate the steel surface when pH is below their pKa values (Rivera, 2011). This means that it takes longer to reach low corrosion rates in the presence of these organic acids, signaling that their presence generally indicates an increase in the rate of corrosion of steel surfaces. When the pH is above their pKa values, organic acids do not affect the solubility of iron carbonate directly but rather they diffuse through pores in the protective layer and adsorb the bare steel (Rivera, 2011).

2.2 Ferric Dissolution and Surface Passivation by Dicarboxylic (Dioic) Acids:

Organic acids present in production water are not limited to only monocarboxylic acids. Production waters also contain dicarboxylic acids, the most abundant of which are oxalic (C2), malonic (C3), succinic (C4), and glutaric (C5) acids (Kawamura et al., 1996). Dioic acids may have an important role in the dissolution of ferric iron because of their ability to form metal complexes with ferric ions (Okochi et al., 2002). Dioic acids, such as malonic acid (pKa_1 = 2.83, pKa_2 = 5.69) and oxalic acid (pKa_1 = 1.23, pKa_2 = 4.19), form complexes with ferric iron, even at low concentrations (Paris et al., 2013). In addition, these dioic acid-iron complexes have high stability constants. The stability (binding) constant is defined previously in Figure 1.2, and is the stability of the metal-ligand complex and for ferric iron. The stability constant of acetic acid-iron and formic acid-iron complexes are log β_3 = 3.2 and log β_3 = 3.1 respectively (Perrin, 1959). In comparison, the stability constants for dioic acid-ferric iron complexes are several orders of magnitude larger, for example, malonic acid-iron and oxalic acid-iron, the

stability constants (typically reported as log β_3) are 16.6 and 20.2 respectively (Okochi et al., 2002).

In addition to the high stability constant, it has been shown that oxalate, malonate and succinate enhance iron solubility, resulting in an increase of dissolved ferric iron concentrations, with a positive linear relationship between ferric solubility and ligand concentration as shown in Figure 2.1 (Paris et al., 2013). Also, increasing the number of carbon atoms in organic molecules i.e. for dioic acid species oxalate (C2) to succinate (C4) decreases ferric solubility, as shown in Figure 2.2 (Wang et al., 2017). It has been reported that the effects of ligands on ferric dissolution decrease with the increase in the chain length for aliphatic, dicarboxylic ligands due to the decreasing of electron donor capacity (Wang et al., 2017).

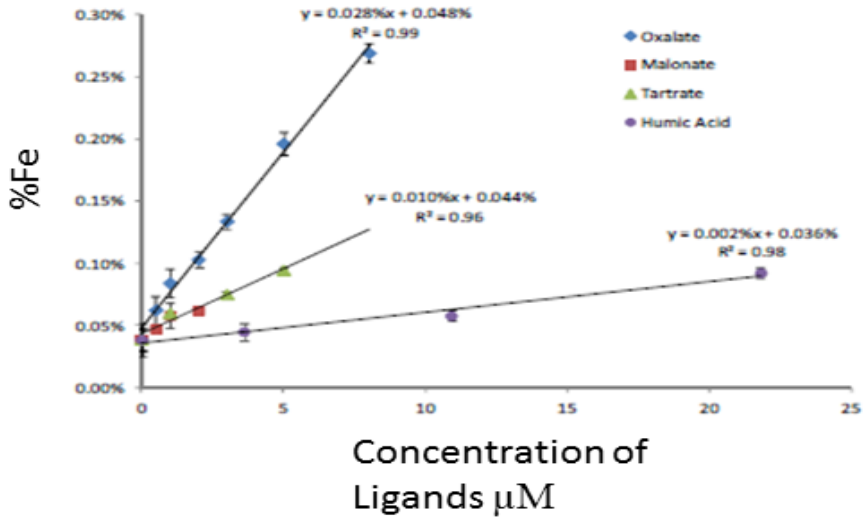

Figure 2.1 Iron solubility (%) vs organic species concentration (µM) at pH 4.7 (Paris et al., 2011).

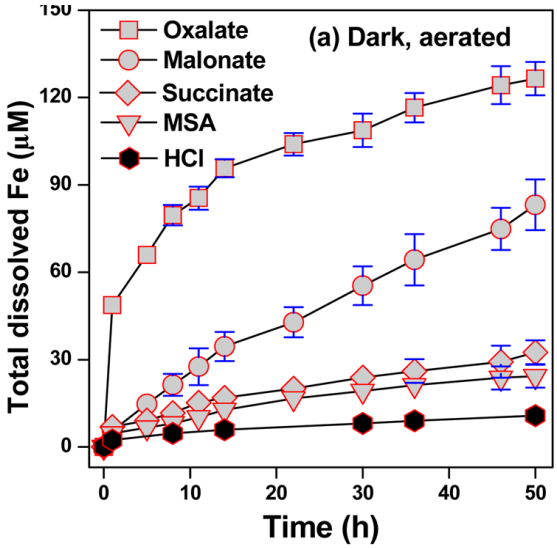

Figure 2.2 Comparison of Fe dissolution as a function of time in the presence of oxalate, malonate and succinate at pH =3 (Wang et al., 2017).

Despite the evidence for increased ferric iron solubilization in the presence of dicarboxylic acids, studies have shown that dioic acids, such as oxalate, malonate and succinate can passivate carbon steel surfaces and inhibit corrosion. For example, it was demonstrated that the inhibition efficiency of corrosion increases with increasing succinic acid concentration, increasing pH of the solution and time of incubation (Amin et al, 2006). When the succinate concentration is higher than 10 mM, corrosion rate decreases 97% (Amin et al, 2006). In another study, it was shown that low concentration oxalic acid – in the range of 10^{-7} – 10^{-3} M – inhibits carbon steel corrosion in sulphuric acid solution – ranging from 50-85% – when pH > 3, whereas for pH < 3 solutions, it was found that the corrosion rate increased (Giacomelli et al., 2004).

The presence of a passivation layer – often in the form of ferric oxyhydroxides – is important to understanding the effects of dicarboxylic acids on steel corrosion. Ferric oxyhydroxide particles have been shown to have an impact on the fate of anionic

ligands in the natural environment as well as oil/gas industrial processes (Brown et al., 1999). Ferric oxyhydroxide has a large surface area so it can act as an efficient sorbent and control organic ligand concentration via a range of sorption process at pH 4 (Simanova et al., 2011). It was claimed by Simanova et al., 2011 that previous studies have shown oxalate cannot solubilize ferric iron because dissolved ferric iron readsorbs as labile iron-oxalate complexes on the surface. However, they concluded that ferric iron in a ternary ligand complex is more labile so it is more bioavailable than ferric oxide (Simanova et al., 2011).

In summary, it has been demonstrated that dicarboxylic acids have both an inhibitory effect and also a potential deleterious effect (through the dissolution of iron) on the corrosion of carbon steel. These are two conflicting results from different research experiments depending on the environment those acids are found. Also, it isn't understood what effects these dioic acids have on the corrosion of carbon steel in the presence of IRB. For this reason, this research provides better understanding of the effects of these components for abiotic systems by changing a single parameter (dioic acid concentrations) under aerobic and anaerobic conditions.

2.3 Equilibrium of Free Fe(III) and Fe(III)-Ligand Controls *Shewanella* Respiration

Shewanella is a genus of facultative anaerobic bacteria. In the lack of oxygen, *Shewanella* can utilize ferric iron as a terminal electron acceptor (Hacherl et al., 2003). In addition, *Shewanella* is a well characterized organism in that it's genome is known and there exist many mutant strains. Therefore, understanding the mechanism of steel

corrosion in the presence of iron-reducing microbes is an important topic, and as such, *Shewanella* provides an excellent microbial model for study. There are three proposed mechanisms for electron transfer from *Shewanella* and *Geobacter*, microbes to terminal electron acceptors. These are: (i) directly from outer membrane c-type cytochromes to ferric oxide minerals, (ii) indirectly via electron shuttles such as (riboflavin and flavin mononucleotides) or (iii) indirectly via the solubilization of ferric iron by organic chelators (may be exogenous substances or produced by the organisms themselves (Bird et al., 2011) (Newman, 2001). However, utilization of ferric iron as a terminal electron acceptor as in mechanism (i), the respiration of IRB requires direct contact with the ferric oxyhydroxide surface, which is a severely limiting mechanism because in theory, direct electron transfer requires that the donating cytochrome to be within 20 Å of solid ferric iron (Bird et al., 2011). *Shewanella* is capable of secreting riboflavins and flavin mononucleotides when it grows with fumarate, ferric iron and electrode (Canstein, 2008). Production of flavins support ferric iron reduction via electron shuttles and be reduced at the cell surface (mechanism ii) (Bird et al., 2011). It was also reported that *S. putrefaciens* and *S. oneidensis* species can produce organic chelators (i.e. siderophores) in the presence of insoluble ferric iron (Taillefert et al., 2007). In iron limiting conditions, *S. putrefaciens* can produce siderophores to solubilize ferric iron and reduce it (Gram, 1994). On the other hand, it has been reported siderophores are not necessary for ferric solubilization during anaerobic ferric respiration by *S. oneidensis* MR-1 (Fennessey, 2010). Based on the literature, it is apparent that multiple mechanisms are available for solid ferric respiration by *Shewanella* genus (Bird et al., 2011), however, it is not fully understood how environmental parameters favor *Shewanella* to favor one

mechanism over another. However, it is clear that siderophore production requires energy consumption, therefore, if organic ligands are present that can chelate ferric iron and increase its bio-availability, *Shewanella* can use this dissolved ferric iron for respiration. It has been shown *S. oneidensis* MR-1 respires ferric-citrate and ferric-NTA without any indicator of ferric-hydroxamate reductase (i.e., necessary for the formation of siderophores) activity (Fennessey, 2010)

One of the proposed mechanisms by which organic ligands and iron chelators such as siderophores or oxalate facilitate microbial induced corrosion is through the chemical equilibrium that exists between freely dissolved ferric iron and ligand-bound iron according to the following equation:

$$3\ \text{ligand} + \text{Fe(III)} \leftrightharpoons \text{Fe(III)-(ligand)}_3 \qquad (3)$$

In this case, IRB, such as *S. oneidensis,* bind to the free Fe(III), the concentration of which is determined by the equilibrium constant of the above equation. . Therefore, a lower equilibrium binding constant (log K_{ML}) between Fe(III) and a ligand shifts the equilibrium to the left. This will increase the free ferric iron concentration in solution which further facilitates iron reduction by *Shewanella*, as shown by Simanova et al., 2011. In Haas and DiChristina's research (2002), where *Shewanella putrefaciens* was anaerobically inoculated with Fe(III)-ligands (ligand = citrate (log $\beta_3 = 11.5$), NTA (log $\beta_3 = 15.9$), and EDTA (log $\beta_3 = 25$) as the sole terminal electron acceptor, showed *S. putrefaciens* respire dissolved ferric iron but this respiration is restricted by the presence of strong Fe(III)-chelating agents (Haas and DiChristina, 2002). This says that even though NTA and citrate form less stable complexes with ferric iron – due to their lower binding constants compared to EDTA – they will result in faster Fe(III) reduction rates

by IRB by providing greater bioavailability of ferric iron in being able to bind and unbind more rapidly. This statement questioned the effect of binding constant dioic acids ferric iron solubility and *S. oneidensis* MR-1 respiration. In abiotic environment, dissolved ferric iron (ferric-ligand complex) concentration increases with increasing binding constant in following order succinate ($\log \beta_3 = 6.88$), malonate ($\log \beta_3 = 16.20$) and oxalate ($\log \beta_3 = 20.20$). However, binding constant as high as EDTA ($\log \beta_3 = 25$) do not provide enough free ferric iron for *S. oneidensis* MR-1 respiration even though EDTA can produce ferric-EDTA complex. The ferric iron solubilization from the ferric oxyhydroxide layer of a steel and ferric respiration by *S. oneidensis* MR-1 both depend on the binding strength of organic ligands. Citrate ($\log \beta_3 = 11.5$) and NTA ($\log \beta_3 = 15.9$) were described as ideal chelators since they form less stable ferric iron complexes compared to EDTA, which makes free ferric iron more bioavailable for *S. oneidensis* MR-1 respiration. This is the motivation that then led to testing whether or not dioic acids exhibit the same relationship for binding constant and solubilized ferric iron as shown by Haas and DiChristina, (2002).

2.4 Effect of Iron Reducing Bacteria on Steel Corrosion

Microorganisms can change electrochemical properties of (corrosion potential, corrosion rate) at the metal-solution interface by producing biofilm (Videla, 2009)**.** This biofilm production on steel surface can range from induction or acceleration of corrosion, to corrosion inhibition (Videla, 2009). IRB can use ferric iron as a terminal electron acceptor in anaerobic environment and for this reason it is very important to understand and study their effect of steel corrosion. The literature illustrates the corrosion of different *Shewanella* species on steel corrosion (Arnold, 1990) (Little,

2007). Steel corrosion in the presence of bacteria depends both on media and the type of organism (Herrera, 2009). In the oil and gas industry, the dominant microbial species are likely to vary from one site to another site depending on the physiochemical characteristics of the production water (Herrera, 2009). However, it is expected to find facultative anaerobic IRB as *Shewanella* or *Vibrio* more commonly than strictly anaerobic IRB as *Geobacter* as the oxygen concentration might vary in production water (Herrera, 2009). It has been reported that the corrosion rate was higher in field with mixed IRB communities than pure culture corrosion, as shown in Figure 2.1.

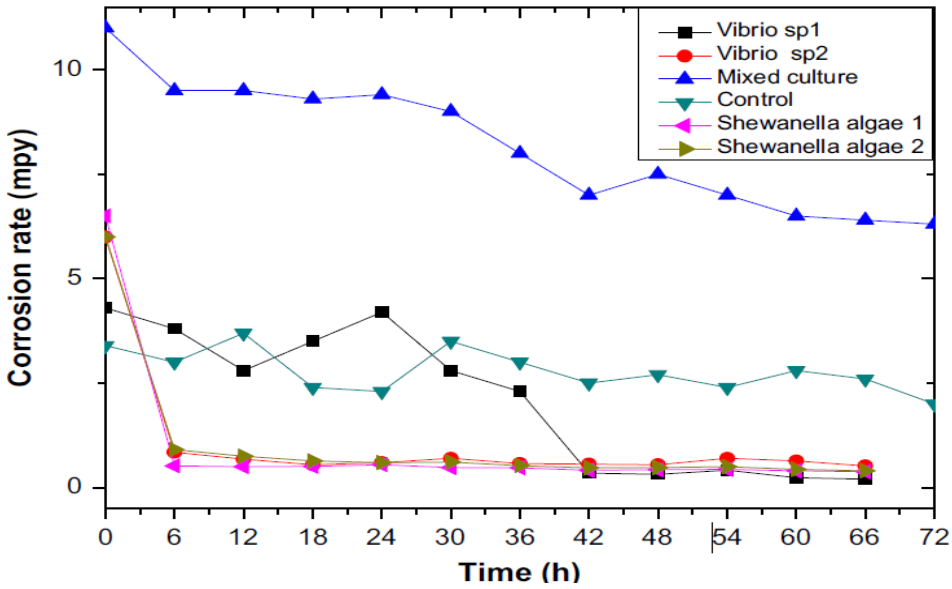

Figure 2.3 Corrosion rate of API X52 steel in pure and mixed cultures of isolated bacteria (Herrera, 2009).

Since the genome of *S. oneidensis* MR-1 was sequenced and mutants in specific genes (e.g. corrosion related genes) are easily prepared, it has been used as model IRB organism (Dubiel, 2002). Previous studies have tested the corrosion of stainless steel under aerobic condition with wild and mutant type (not capable to form a biofilm) of *S. oneidensis* MR-1 in a media (Dubiel, 2002). They found that *S. oneidensis* MR-1

reduced the corrosion rate under their experimental condition (Dubiel, 2002) due to the consumption of oxygen in media and reduction of ferric iron from ferric oxyhydroxide layer.

On the other hand, ferric respiration may serve to dissolve the ferric oxyhydroxide protective layer, thus enhancing corrosion of the steel (S. Belkaid, 2012). Another study reported previously formed rust can be completely removed by *S. oneidensis* from carbon steel surface under anaerobic conditions (Starosvetsky, 2016) which leads to further oxidation of metallic iron. In their study, mild steel was corroded via atmospheric exposure and pre-corroded coupons were exposed to *S. oneidensis* and *G. sulfurreducens* without adding any extra external ferric sources in media (Starosvetsky, 2016). After three weeks of incubation, most of the oxidized layer on coupons were removed in comparison with abiotic control (Starosvetsky, 2016). Also, mass loss measurement of carbon steel showed addition of bacterial cultures increased mass loss 5-6 times higher compared to coupon incubated in abiotic media (Starosvetsky, 2016). Figure 2.1 shows the coupons after incubation with abiotic media and cultures (Starosvetsky, 2016). The difference between coupons were visually distinguishable which supported that IRB can remove oxidized layer from steel surface.

Figure 2.4 (Left) pre-oxidized coupons incubated in media and (right) after incubated with *G. sulfurreducens* and *S. oneidensis* cultures incubated in media for 3 weeks (Starosvetsky, 2016).

Thus, it has been demonstrated that IRBs can inhibit or facilitate steel corrosion. Present knowledge suggests that the corrosion behavior depends on steel surface area, microbial cell concentration and the composition of the growth medium (Herrera, 2009). Having a thorough understanding of the underlying mechanisms of corrosion helps to better address and solve this problem by designing agents or utilizing mechanisms that either impede or reverse the corrosion processes (Fajardo et al., 2007). This research was done with the purpose of contributing to closing some of the gaps in the understanding of the mechanism by which the dioic acids: oxalic acid, malonic acid, and succinic acid, contribute to carbon steel corrosion in the presence of *S. oneidensis MR*-1.

Chapter 3 : Methodology

This chapter explains the research methodology implemented to test main research hypothesis which was tested with abiotic and biotic corrosion experiments. Tests were conducted to study the effect of dioic acids on corrosion of clean/oxidized steel under aerobic conditions and the effect of microbial respiration on corrosion under anaerobic conditions, created with the addition of *S. oneidensis* MR-1.

In this section, abiotic experiments were done with clean and oxidized steel surface in presence of dioic acids as well as NTA and citrate. Then, biotic experiments were done with ferric oxyhydroxide and oxidized steel to measure respiration rate of *S. oneidensis* MR-1 with the presence of same ligands. Also, corrosion rate was measured for both abiotic and biotic steel corrosion experiments.

3.1 Clean Steel Surface Corrosion Experiments with Dioic Acids, citrate and NTA

In this section, the effect of dioic acids on the solubility of ferric iron was tested. Increase in the solubility of ferric iron supposed to increase the corrosion rate of a clean steel surface under aerobic conditions. Tested dioic acids were oxalate, malonate and succinate in concentration range of (0.01 mM, 0.1 mM, 1 mM, 10 mM and 50 mM) as well as 50 mM citrate and NTA. Steel coupons were incubated with different concentrations of ligands for 8 days. Then, dissolved iron and total iron loss were measured as a determination of ferric iron solubility and corrosion rate.

The carbon steel (1018) used for this study had a composition of 0.14–0.20% C, 0.6–0.9% Mn, 0.035% maximum S, 0.030% maximum P, and the remainder Fe. It was cut into small round coupons with diameters of 10 mm and a thickness of approximately 1 mm. The coupons have weight of 0.5253±0.0077 grams. Right before coupons used,

they were sonicated for 15 minutes in acetone and then submerged in pure ethanol for 5 minutes and dried immediately with N_2. Clean carbon steels were incubated with varying concentrations (0 mM, 0.01 mM, 0.1 mM, 1 mM, 10 mM and 50 mM) of dioic acids; oxalate, malonate, succinate as well as citrate (50 mM) and NTA (50 mM) for 8 days at room temperature. At the end of the experiment dissolved iron and total iron were measured.

As stock solution 250 mM oxalate malonate, succinate, citrate and NTA were prepared in 100 ml volumetric flask and pH adjusted to 7 with 10 N NaOH. Also, pH of NANOpure water adjusted to 7 with 0.1 N NaOH. From those stock solutions, 50, 10, 1, 0.1 and 0.01 mM dioic acids were diluted by using class A glass pipettes with pH 7 NANOpure water in 100 ml class A volumetric flask. Stock solution of ligands filter by using 0.2 μm filter into sterile 100 ml autoclaved and crimp-sealed glass bottles.

Figure 3.1 demonstrates the experiment steps for aerobic corrosion of a clean carbon steel. In detail, carbon steel coupons were transferred into individual autoclaved Balch tubes. Deprotonated dioic acids (0-50 mM), 50 mM citrate and 50 mM NTA was transferred into the Balch tubes. The Balch tubes were sealed with rubber septa and covered with aluminum crimp seals. 23G X 1 needle was inserted into the septa and a 0.2 μm sterile filter was attached to the needle to preserve the sterility of the Balch tubes. The point of this process is to incubate clean coupons with organic acid under aerobic conditions without contaminating the experimental samples. Carbon steel coupons were incubated in variety of ligand at different concentrations for 8 days at room temperature. After incubation, total iron and dissolved iron samples were needed to be extracted from solution. First dissolved iron sample was prepared. For dissolved

iron, 1.5 ml aliquots were filtered using a 0.2-µm filter and acidified with highly concentrated nitric acid (5-10% v/v). Then, coupons were removed from liquid and washed with 1 ml NANOpure water in a way that washed water went into remaining liquid in Balch tube. By doing washing, easily removable corrosion products on coupon surface was removed and added into incubated liquid samples. After visible products appeared to have been removed, the coupons were soaked in 15 ml Falcon tube with 3 ml cleaning acid solution for 5 minutes at room temperature. The protocol for cleaning acid solution was followed the ASTM Standard G1-03 (G1-03, 2003). The acid cleaning solution (3.5 g/l of hexamethylene tetramine in 6M HCl) was prepared to remove accumulated corrosion product from the coupon surface. This cleaning solution was designed to remove only iron oxide (rust) not the uncorroded metal. After this step, 3 ml the soaked cleaning solution will be transferred into Balch tubes. Falcon tubes washed with 1 ml NANOpure water and transfer into Balch tubes. For total iron, total volume of samples (8.5 ml) were acidified with highly concentrated nitric acid (5-10% v/v). Acidified dissolved iron and total iron samples were vortexed and they incubated at room temperature at least 24 hours to provide enough time to solubilize any precipitates. For dissolved iron, usually 24 hours incubation is enough if there was not any precipitation occurred. However, total iron may need to incubate at room temperature more than 48 hours to dissolve all the corrosion products. Before doing any dilutions, precipitation should be check. If there is still precipitation at the end of 48 hours, acid percentage can be increase up to 10%.

Dissolved iron samples dilute between 0-50 fold and total iron samples dilute 100-10,000 fold with class A glass pipettes and volumetric flasks. Iron in liquid samples

were analyzed with a Varian AA240FS and GTA120 Atomic Absorption Spectrophotometer.

Cleaned coupons were dried with nitrogen gas and stored in a vacuum desiccator, as carbon steel will immediately begin forming a new corrosion (red) layer upon exposure to air. The carbon steel was incubated in desiccator for further analysis if it is necessary.

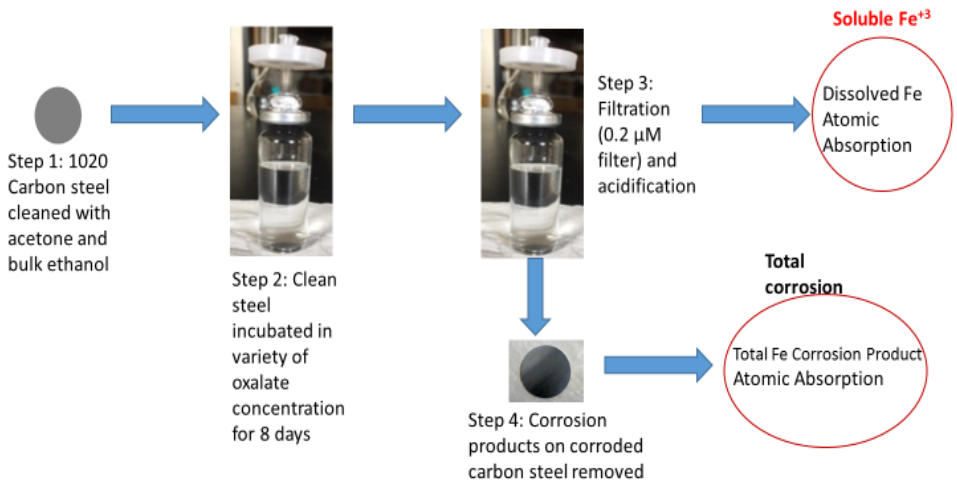

Figure 3.1 Abiotic corrosion experiment with a variety of oxalate concentrations, incubated for 8 days. Total iron and dissolved ferric iron were measured at the end of experiment.

3.2 Oxidized Steel Surface Corrosion Experiments with Dioic Acids, citrate and NTA

Since many steel pipelines, production water tanks have dissolved O_2 in the system, they oxidized and formed ferric oxyhydroxide layer on carbon steel surface. In this section, oxidized carbon steel used for corrosion experiments to create more realistic

scenario to replicate corrosion problem based on the two basins that were described previously. When oxidized steel is used, it is not applicable to measure total corrosion product with AAS as the amount of oxidized metal may vary from one steel surface to other. For this reason, electrochemical measurements were useful to identify surface potential and calculate corrosion rate. In this section tested hypothesis was addition of 50 mM ligands such as oxalate, malonate, succinate, citrate and NTA will change corrosion rate and dissolved ferric iron depending on their binding constant. These experiments, two oxidized steel coupons incubated in electrolyte solution under O_2 rich environment until they reached similar corrosion potential ($E_{corrosion}$). Then addition of ligands demonstrated the effect of them to oxidized steel corrosion.

EuroCell electrochemical cell kit was purchased from Gamry Instrument. The working electrode used in these experiments was carbon steel (1018) with composition of 0.22–0.38% C, 0.12-0.14 % Mn, 0.03% maximum S, 0.030% maximum P, and the remainder Fe. The dimensions of carbon steel were 0.95 cm x 1.27 cm and a surface area of 4.5 cm^2. The working electrode assembly washed with acetone and sterilized in 100% ethanol for 5 minutes. In EuroCell electrochemical kit, oxidized carbon steel used as a working electrode, a standard calomel electrode (SCE) was used a reference electrode and graphite electrode was used a counter electrode. Electrolyte solution was 0.1 M $NaNO_3$ prepared at pH 7 with 0.1 N NaOH. Figure 3.2 demonstrates the experiment's steps. In detail, clean carbon steel was incubated with 10 ml 0.1 M $NaNO_3$ solution at room temperature for 4 days. After surface oxidize, carbon steels washed with NANOpure water and dried. Their weight measured and recorded as a control steel working electrode and ligand-tested steel working electrode. To clean the

electrochemical cells, EuroCell kits were incubated with 6 M HCl to remove any iron residual and washed with NANOpure water. The control EuroCell filled with 200 ml electrolyte and ligand testing EuroCell filled with 160 ml electrolyte solution. The oxidized working electrode, a reference electrode and a counter electrode were placed in Eurocell and connected to Gamry Potentiostat with the Reference 3000 main cell cable kit. A gas bubbler was connected to the gas cylinder to provide oxygen flow during the experimental period. Also, the electrolyte solution was stirred between the waiting times of measurement to eliminate mass diffusion limitations at experiment. Stirrer was connected to the timer and electrolyte solution was stirred during the measurements. Linear polarization resistance (LPR) curves were recorded corrosion potential ($E_{corrosion}$) every 10 minutes during the 60 hours. The potential was swept ±10 mV above and below the $E_{corrosion}$ at a rate of 0.125 mV/s by using Gamry Potentiostat (600+ Reference) and Gamry Framework Software. Tafel slop regions were used to extrapolate resistance polarization (R_p) values within ± 5 mV of $E_{corrosion}$. The corrosion rate was derived by taking the inverse of R_p. The control and ligand test experiments were set up to run for 60 hours by using Gamry Framework DC corrosion linear polarization resistance method. After two oxidized steel surfaces reached the similar $E_{corrosion}$ and R_p (usually within 10 hours), 250 mM 40 ml oxalate, malonate, succinate, citrate or NTA added into one of the EuroCell to determine the effect of the compound on an oxidized steel surface. To measure dissolved ferric iron concentration from electrochemical cells, 2 ml aliquots will be harvested at time 10, 30 and 60 hours from both control and ligand test EuroCell and filter through the 0.2 μm polyethersulfane membrane filter. Samples were acidified for (5-10% v/v) and dissolved ferric iron

concentration was measured with AAS. The oxidized steel coupons were incubated in 3 ml cleaning solution as it described previous section (G1-03, 2003) and dried with N_2 gas. Then, their mass was measured and total mass loss was calculated.

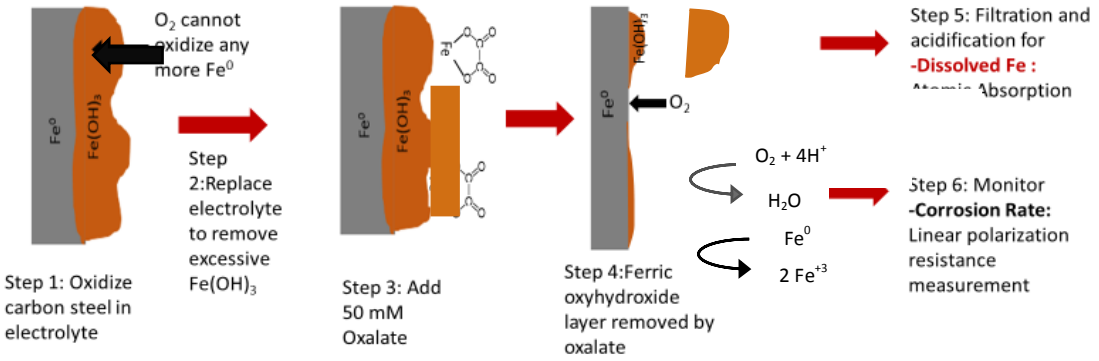

Figure 3.2 Mechanism of abiotic electrochemical corrosion experiment with oxalate. Oxalate will remove the ferric oxyhydroxide layer, allowing O_2 gas to oxidize more bare iron from steel surface. Dissolved ferric iron concentration and corrosion rate are measured during the experiment.

3.3 Carbon Steel Corrosion with the Presence of *S. oneidensis* MR-1 and Dioic Acids under Anaerobic Conditions

It was hypothesized that, *S. oneidensis* MR-1 respiration with the presence with organic ligands such as oxalate, malonate, succinate, NTA and citrate increase corrosion rate. The relationship between binding constant, ferric solubility and ferric bio-availability for respiration were studied in this section. *S. oneidensis* MR-1 respiration was tested with laboratory prepared 25 mM ferric oxyhydroxide and corroded steel surface. Later, corrosion rate of steel surface also measured with the presence of *S. oneidensis* MR-1 and dioic acids.

3.3.1 *S. oneidensis* MR-1 Growth Curve with 25 mM Fumarate, Ferric-citrate and Ferric-NTA

S. oneidensis MR-1 was obtained from Dr. Zhou's lab. The anaerobic MR-1 minimal media had 50 mM lactate as electron donor and 60 mM fumarate as the terminal electron acceptor. This media was modified and prepared without any electron acceptor. The stock *S. oneidensis* MR-1 culture (in 50% glycerol broth) was frozen at -80°C. To start a culture, 150 µL of the stock culture was incubated anaerobically for 24 hours at 32°C in 10 mL MR-1 minimal media (Appendix 1) which includes 50 mM lactate as electron donor and 60 mM fumarate as terminal electron acceptor. At the end of incubation, optical density (OD_{600}=0.8) was measured with a spectrophotometer. Media with MR-1 was centrifuged at 5000 rpm for 10 minutes. Supernatants disposed and cells will wash with 10 ml 50 mM PIPES buffer (pH=7) for 2 times (Patil, 2013) and they were suspended in minimal MR-1 media without any electron donor and OD was measured between 0.76-0.80. Balch tubes were St sterilized with anaerobic minimal media having 50 mM lactate as electron donor. After autoclaving the media, 25 mM solid ferric oxyhydroxide, 25 mM ferric-citrate, 25 mM ferric-NTA or 25 mM fumarate were added to media and media volume was 10 ml. *S. oneidensis* MR-1 (100µL) was added to media and inoculated at 32ºC in dark incubator. Their growth was measured at time 0,4,8,12,22 and 26 hours of incubation. At the end of the experiment, 0.5 ml aliquot samples were filtered through 0.2 µm filter and acidified with 10 µl HCl and ferrous concentration was measured. The growth of 25 mM ferric oxyhydroxide media was not able to be measured by OD_{600} due to ferric particles, so microbial respiration (ferrous concentration) was the only measured parameters.

3.3.2 Ferric Oxyhydroxide Respiration of *S. oneidensis* MR-1 with 5-50 mM Oxalate, Malonate, Succinate, Citrate and NTA

For these experiments, the dissolution of solid ferric oxyhydroxide tested with ligands: succinate (log β_3 = 6.88), citrate (log β_3 = 11.5), NTA (log β_3 = 15.9), malonate (log β_3 = 16.6) and oxalate (log β_3 = 20.20) with presence of *S. oneidensis* MR-1.The independent parameters of this experiment were a variety of chelators (succinate, citrate, NTA, malonate, and oxalate) with different binding constants and the dependent parameter is ferrous concentration, which is an indicator of respiration.

The stock *S. oneidensis* MR-1 culture (in 50% glycerol broth) was frozen at -80°C. To start a culture, 150 µL of the stock culture was incubated anaerobically for 16-18 hours at 32°C in 10 mL MR-1 minimal media which includes 50 mM lactate as electron donor and 60 mM fumarate as terminal electron acceptor. At the end of incubation, optical density (OD_{600} = 0.76-0.80) was measured with a spectrophotometer. Balch tubes were prepared with anaerobic minimal media having 50 mM lactate as electron donor and 25 mM solid ferric oxyhydroxide as terminal electron acceptor. Varying concentrations of oxalate, malonate, succinate, citrate and NTA (5 and 50 mM) were added into the media. Then, 500 µL (OD_{600}=0.8) *S. oneidensis* MR-1 was inoculated into 50 mL anaerobic media and bottles were incubated at 32°C for 36 hours in dark. During the incubation, at time 0, 1, 3, 6, 9 and 12 hours, 0.5 mL aliquots were filtered through a 0.2 µm filter and acidified with 10 µL of highly concentrated HCl. Acidified samples were used for ferrozine assays to analyze the ferrous concentration of the samples, which is an indicator of *S. oneidensis* MR-1 respiration. Also, total dissolved ferric iron samples were taken at the end of 12 hours-period. Aliquot samples were filtered through a 0.2

μm filter and acidified (5-10%v/v) with highly concentrated HNO_3. Dissolved iron samples were diluted between 0-50 fold and with class A glass pipettes and volumetric flasks. Total dissolved iron in liquid samples were analyzed with Varian AA240FS and GTA120 Atomic Absorption Spectrophotometry.

3.3.3 *S. oneidensis* MR-1 Respiration of Oxidized Steel Coupons with Dioic Acids

The carbon steel (1018) used for this study had a composition of 0.14–0.20% C, 0.6–0.9% Mn, 0.035% maximum S, 0.030% maximum P, and the remainder Fe. It was cut into small round coupons with diameters of 10 mm and a thickness of approximately 1 mm. The coupons have weight of 0.5253±0.0077 grams. Right before coupons used, they were sonicated for 15 minutes in acetone and then submerged in 100% ethanol for 5 minutes to sterilize steel and transfer into autoclaved Balch tubes and filled with 1 ml NANOpure water. The Balch tubes was sealed with rubber septa and covered with aluminum crimp seals. A needle was inserted into the septa and a 0.2 μm sterile filter attached to the needle to preserve the sterility of the Balch tubes. After corrosion product formed (3 days), carbon steel and NANOpure water transferred into 40 ml MR-1 minimal media without any electron donor. Oxygen was removed from the media by vacuuming and flushing nitrogen. Then, 250 mM stock dioic acid was added into the media. Experiments were run with both 5 and 50 mM dioic acids.

The stock *S. oneidensis* MR-1 culture (in 50% glycerol broth) was frozen at -80°C. To start a culture, 150 μL of the stock culture was incubated anaerobically for 16-18 hours at 32°C in 10 mL MR-1 minimal media (Appendix 1) which includes 50 mM lactate as electron donor and 60 mM fumarate as terminal electron acceptor. At the end of incubation, optical density (OD=0.76-0.80) was measured with a spectrophotometer.

Media with MR-1 was centrifuged at 5000 rpm for 10 minutes. Supernatants disposed and cells were washed with 10 ml 50 mM PIPES buffer (pH=7) for 2 times (Patil, 2013) and they were suspending in minimal MR-1 media without any electron donor and OD was measured between 0.76-0.80. Then, 500 µL *S. oneidensis* MR-1 incubated into 50 mL prepared anaerobic media and incubated at 32°C for 36 hours in a dark environment. Ferric iron samples were taken at 2, 6, 12, 24 and 36 hours. Total dissolved iron was toked at the end of 36 hours.

For ferrous iron, 0.5 mL aliquots will be filtered through a 0.2 µm filter and acidified with 10 µL of highly concentrated hydrochloric acid. Acidified samples will be used for ferrozine assays to analyze the ferrous concentration of samples, which is indicator of *S. oneidensis* MR-1 respiration. For total dissolved iron, 2 mL aliquots were filtered through a 0.2 µm filter and acidified with 50 µL of highly concentrated nitric acid. Total dissolved iron was measured with AAS.

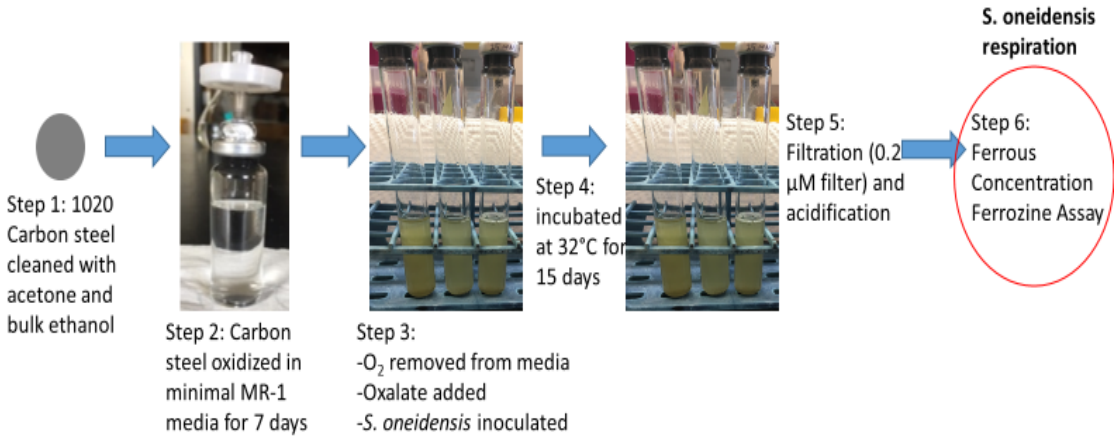

Figure 3.3 Biotic experiment with oxalate in presence of carbon steel coupon. A steel coupon is incubated with oxalate under aerobic conditions and *S. oneidensis MR-1* is inoculated in the media. *S. oneidensis MR-1* respiration and total dissolved iron are measured at the end of the experiment.

3.4 Corrosion Rate Measurements with *S. oneidensis* MR-1 and 50 mM Dioic Acids

The final set of experiments that were performed to test whether dioic acids facilitate *S. oneidensis* MR-1 respiration and thereby increase the corrosion rate of carbon steel. The independent parameters of this experiment are the dioic acids and the dependent parameters are the corrosion rate and the dissolved ferric iron concentration. This experiment was performed in two different ways to measure corrosion rate of oxidized steel coupon as it shown in Figure 3.4. In both ways carbon steel coupons were oxidized in 0.1 M $NaNO_3$ electrolyte solution under aerobic conditions and they transfer in anaerobic chamber. In both experiments, oxidized steel coupons were reached equilibrium with MR-1 media solution, which was called phase 1. For experiment A, *S. oneidensis* MR-1 was added into both cells and after they reached the same potential again, 50 mM oxalate, malonate or succinate was added into one of the cell. In experiment B, 50 mM dioic acids were added to both electrochemical cells and it followed by addition of *S. oneidensis* MR-1 into a cell.

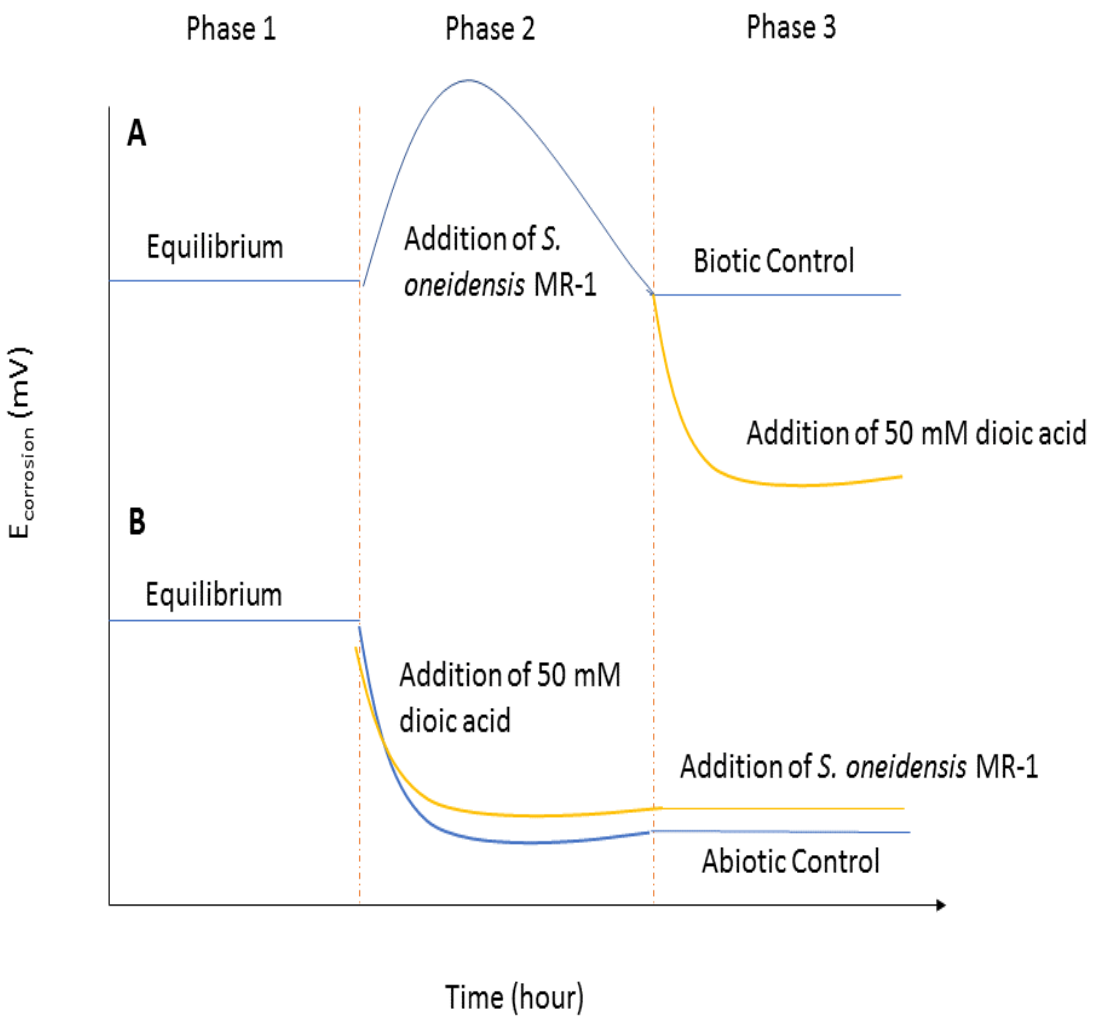

Figure 3.4 Schematic demonstration of changing $E_{corrosion}$ by time with the presence of *S. oneidensis* MR-1 and dioic acids. A) Oxidized steels were incubated in MR-1 media until they reached to equilibrium and *S. oneidensis* MR-1 was added to both of cells and later, 50 mM dioic acid added into a cell. B) Oxidized steels were incubated in MR-1 media until they reached to equilibrium and 50 mM ligands were added to both of cells and later, *S. oneidensis* MR-1 was added into a cell.

EuroCell electrochemical cell kit was purchased from Gamry Instruments. Working electrode used in experiments was carbon steel (1018) with composition of 0.22–0.38% C, 0.12-0.14 % Mn, 0.03% maximum S, 0.030% maximum P, and the remainder Fe. The dimensions of carbon steel were 0.95 cm x 1.27 cm and a surface area of 4.5 cm^2.

In EuroCell electrochemical kit, oxidized carbon steel used as a working electrode, a standard calomel electrode (SCE) was used a reference electrode and graphite electrode was used a counter electrode. Electrolyte solution was sterile MR-1 media at pH 7. EuroCell kit was washed with 6 N HCl and NANOpure water. All the glassware was autoclaved before their used. The working electrode (carbon steel) washed with acetone and sterilized in 100% ethanol for 5 minutes. Clean carbon steel was incubated with 10 ml 0.1 M $NaNO_3$ solution at room temperature for 4 days. After surface oxidize, carbon steels washed with NANOpure water and dried. Both of EuroCell filled with 200 ml MR-1 media in anaerobic chamber. The oxidized working electrode, a reference electrode and a counter electrode were placed in Eurocell and connected to Gamry Potentiostat with Reference 3000 main cell cable kit. The electrolyte solution was stirred between the waiting times of measurement to eliminate mass diffusion limitations in the experiment. Stirrer was connected to the timer and electrolyte solution was stirred during the measurements. Linear polarization resistance (LPR) curves were recorded corrosion potential ($E_{corrosion}$) every 10 minutes during the 40 hours. The potential was swept ±10 mV above and below the $E_{corrosion}$ at a rate of 0.125 mV/s by using Gamry Potentiostat (600+ Reference) and Gamry Framework Software. After two oxidized steel surfaces reached the similar $E_{corrosion}$ and R_p (within 17 hours), *S. oneidensis* MR-1 was added to both of the EuroCell in experiment A. After $E_{corrosion}$ and R_p reached similar values again, 50 mM dioic acids were added into one of the cell to compare the effect of dioic aids to corrosion in the presence of *S. oneidensis* MR-1. Total dissolved ferric iron and ferrous iron samples were taken at 15, 18, 24 and 40 hours. Total dissolved iron acidified with highly concentrated HNO_3 and diluted up to

50-fold. Iron concentration was measured with AAS. Ferrous concentration was analyzed with Ferrozine assay.

In experiment B, 50 mM dioic acids were added to both of EuroCell as a phase 2 after two oxidized steel surfaces reached the similar $E_{corrosion}$ and R_p (within 7 hours). In phase 3 (within 17 hours), *S. oneidensis* MR-1 was added into one of the cell to understand the effect of *S. oneidensis* MR-1 to corrosion rate. Total dissolved ferric iron and ferrous iron samples were taken at 16, 22 and 40 hours. Total dissolved iron acidified with highly concentrated HNO_3 and diluted up to 50-fold. Iron concentration was measured with AAS. Ferrous concentration was analyzed with ferrozine assay.

The oxidized steel coupons were incubated in 3 ml cleaning solution as it described previous sections (G1-03, 2003) and dried with N_2 gas. Then, they incubated in desiccator if further analysis is required.

Chapter 4 : Results

4.1 Abiotic Clean Steel Surface Corrosion Experiment with Dioic Acids under Aerobic Conditions

Understanding the interactions between the ligand and the steel surface is important to develop our understanding of how the proposed corrosion mechanism can be validated. To begin this investigation, it is important to determine the interactions between the dioic acids (and control ligands) and a clean steel surface. The purpose of this experiment is to establish a baseline for the dissolution of ferric iron from the clean steel surface in the presence of oxygen. For these experiments, it is hypothesized that the dissolution of ferric iron concentration increases with increasing chelator binding constant and chelator concentration. Based on this hypothesis, the concentration of dissolved ferric iron should increase with binding constant at constant ligand concentration. Succinate ($\log \beta_3 = 6.88$) will dissolve the least amount of ferric iron from the clean steel followed by citrate ($\log \beta_3 = 11.5$), NTA ($\log \beta_3 = 15.9$), malonate ($\log \beta_3 = 16.6$) and finally oxalate ($\log \beta_3 = 20.20$).

Figure 4.1 illustrates that for 50 mM of ligands, there is not a correlation between ligand binding constant and dissolved iron concentration. Chelators (succinate and citrate) with a binding constant lower than $\log \beta_3 = 11.5$ solubilize very small amounts (~ 1 μM) of iron as compared to chelators with a binding constant above $\log \beta_3 = 11.5$. However, the trend of increase stops after NTA, which has a binding constant of $\log \beta_3 = 15.9$. After this, the amount of dissolved ferric iron decreases as the binding constant increases. While NTA solubilizes 10.2 ± 0.29 μM of ferric iron, malonate ($\log \beta_3 = 16.6$) and oxalate ($\log \beta_3 = 20.2$) solubilize 6.5 ± 0.25 μM, and 5 ± 0.50 μM of ferric iron

respectively. This result suggests that there is not a direct linear relationship between log β_3 and dissolved iron concentration but log β_3 need to be higher than 15 to solubilize iron.There might be other factors that are important to determining the dissolved iron concentration due to differences in ligands chemical structure.

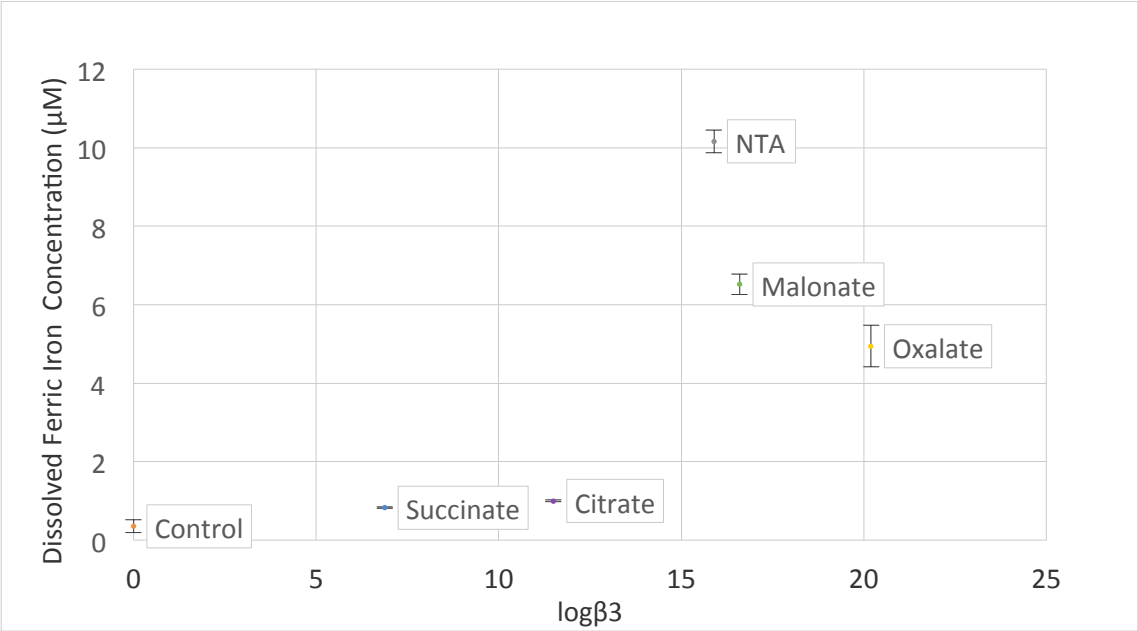

Figure 4.1 Dissolved ferric iron concentration after incubation of clean steel (1.6 cm^2) in 50 mM dioic acids, NTA and citrate at pH=7 for 192 hours at 24ºC.

In addition to the dissolved ferric iron concentration, the total iron concentration was measured as an extent of corrosion. For this measurement, it was hypothesized that the extent of corrosion will be directly related to the binding constant and concentration of the chelator. Figure 4.2 shows that a direct relationship doesn't exist, except for the control, the ligands follow the same trend as dissolved iron concentration. The lower binding constant ligands produce less total iron while NTA has the maximum total iron followed by a drop off in total iron concentration for malonate and oxalate. Succinate and citrate have a total dissolved iron concentration of less than the control, which suggests passivation of the surface so that it cannot interact with oxygen.

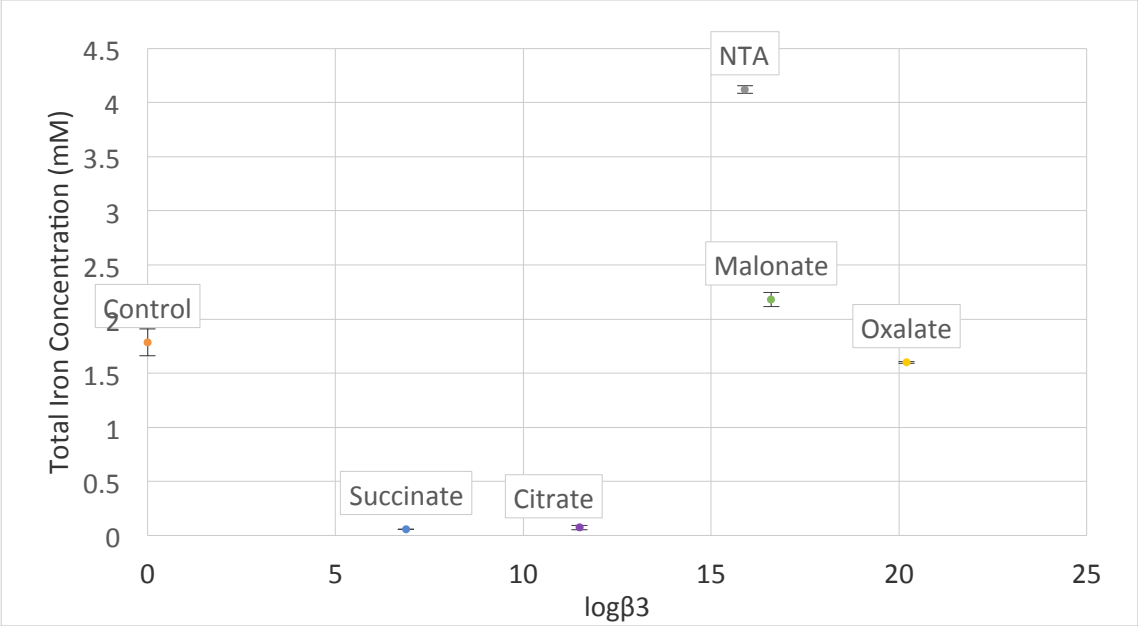

Figure 4.2 Total iron concentration after clean steel (1.6 cm^2) incubated in 50 mM dioic acids, NTA and citrate at pH=7 for 192 hours at 24ºC.

The main conclusions from Figures 4.1 and 4.2 are: 1) binding constant controls the dissolved ferric iron concentration and the presence of dissolved oxygen controls the extend the corrosion, 2) low binding constant chelators (succinate and citrate) do not solubilize ferric iron very effectively, nor do they produce much total iron suggesting that they form a passivation layer on the surface of the steel and 3) initially there is an increasing trend in dissolved ferric iron and total iron, but at a binding constant higher than ~16, the trend begins to decrease suggesting some solubilization of the steel, but also passivation of the steel surface.

The experiments performed previously used ligands at a concentration of 50 mM. The purpose of this was to test the effect of maximum concentration of ligands that have been seen in oil and gas industry (Kharaka, Ambats, & Thordsen, 1993). It is also important to determine the range of dioic acid concentrations that produced a

measurable response, a set of experiment was performed where the concentration was varied as 0 mM, 0.01 mM, 0.1 mM, 1 mM, 10 mM and 50 mM.

Figure 4.3 illustrates that ligand concentration needs to be higher than 1 mM to measure an observable effect on dissolved ferric iron concentration. For concentrations of dioic acid between 0.01 – 1 mM, the amount of dissolved ferric iron concentration remained around 100 nM. However, when the dioic acid concentration was increased to 10 mM, then the amount of dissolved ferric iron in the system increased to near 1 mM and became 8 mM at 50 mM. This suggests that there is no measurable effect of dioic acids on the solubilization of ferric iron when concentrations of dioic acid is lower than ~1 mM. Additionally, for almost all of the concentrations succinate did not solubilize as much ferric iron as oxalate and malonate (for 0.1 mM dioic acids, the amount of dissolved iron for oxalate and succinate were the same).

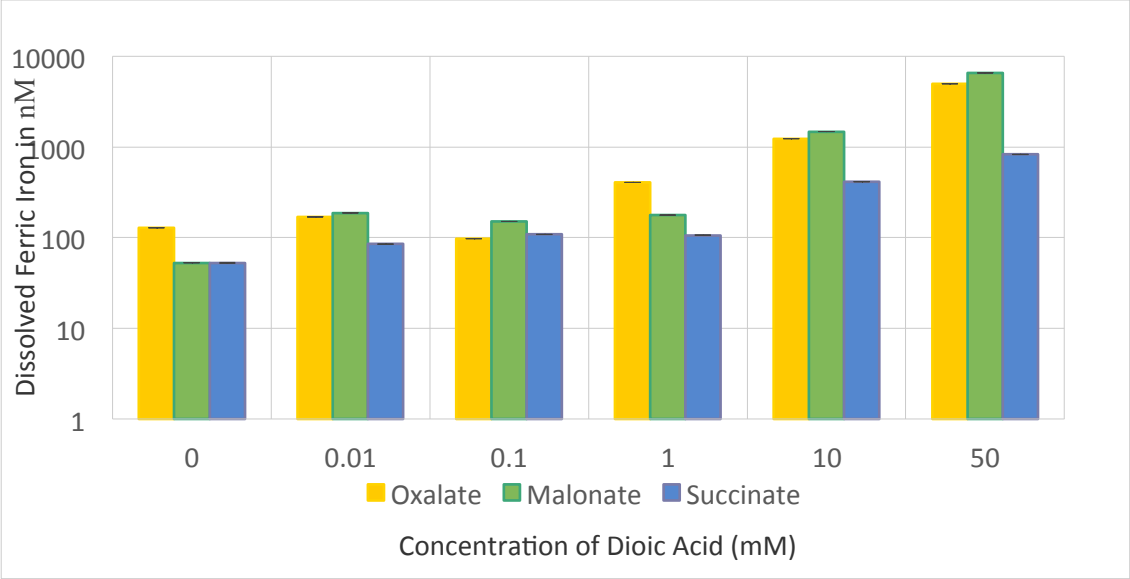

Figure 4.3 Log scale dissolved ferric iron concentration of clean steel surface area (1.6 cm^2) with varying concentration of dioic acids at pH=7 for 192 hours at 24ºC under aerobic conditions.

Figure 4.4 demonstrates that increasing dioic acid concentration has much less influence on total iron concentration. Overall, each concentration tested for each dioic acid produced at least 1 mM of total dissolved iron, suggesting that there is at least some corrosion of the steel surface occurring. There is one outlier to this data, which is the 50 mM succinate sample. This sample did not produce a measurable amount of total iron, is similar to what was observed in Figure 4.2, further suggesting that at a concentration of 50 mM succinate passivates the steel surface rather than promotes corrosion.

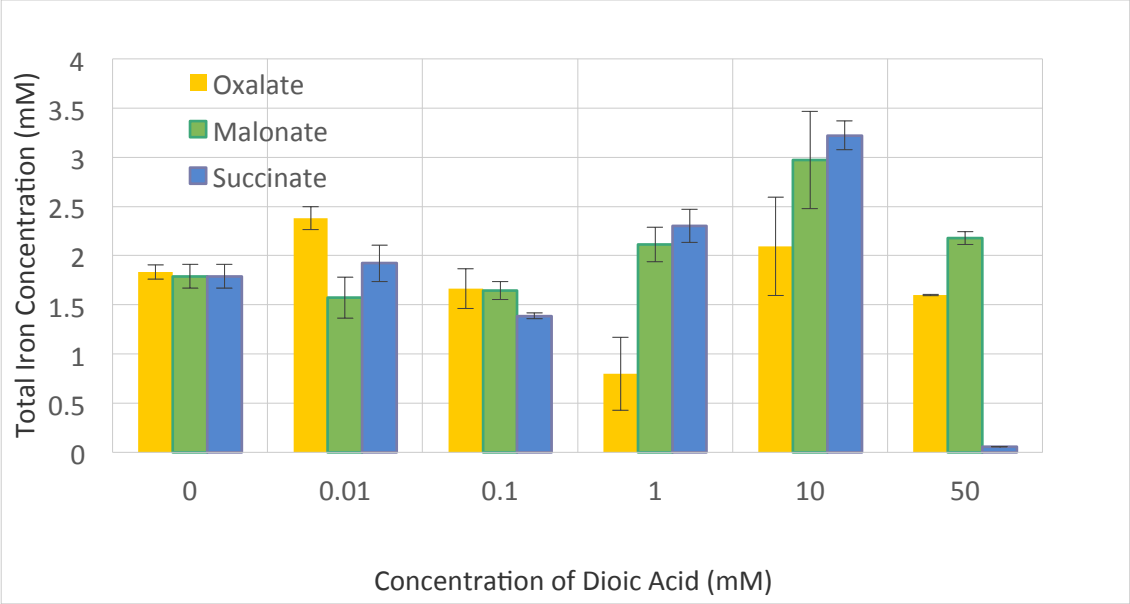

Figure 4.4 Total iron concentration of clean steel surface area (1.6 cm^2) with varying concentration of dioic acids at pH=7 for 192 hours at 24ºC under aerobic conditions.

The main conclusions from Section 4.1 are: 1) the hypothesized trend of a higher binding constant producing a higher concentration of dissolved ferric iron does not hold due to additional factors besides binding constant, 2) dioic acid concentrations greater than ~1 mM result in increasing dissolved iron concentration and 3) 50 mM succinate appears to passivate the surface of a clean steel coupon. The results of this section provided a baseline for how the ligand interacts with a clean steel surface and the next step was to determine their behavior in the presence of oxidized steel.

4.2 Abiotic Oxidized Steel Surface Corrosion Experiment with Dioic Acids

Since oxidized steel surfaces, i.e. ferric oxyhydroxide coating, are often present in carbon steel infrastructure, effect of dioic acids to oxidized steel surfaces was investigated. Linear polarization measurements were used to measure corrosion

potential ($E_{corrosion}$) and polarization resistance (R_p) in order to obtain corrosion rate over time.

4.2.1 Dissolved Ferric Iron with 50 mM Dioic Acids, Citrate and NTA on Oxidized Steel

Figure 4.5 shows that dioic acids, citrate and NTA resulted in an increase in dissolved ferric iron concentration although all five ligands exhibited different behavior over 50 hours of incubation**.** Over the course of the experiment, the dissolved ferric concentration does not change in the control. Figure 4.5 B shows that the addition of 50 mM oxalate increased the dissolved ferric concentration immediately (at 1 minute after addition) to 3.10 ± 0.02 μM., 4.47 ± 0.18 μM at the end of 30 hour. At the end of 50 hours however, it decreased to 1.96 ± 0.03 μM. The addition of 50 mM malonate solubilized 2.12 ± 0.07 μM of ferric iron (at 1 minute after the addition) and 5.24 ± 0.05 μM at the end of 30 hour. At the end of 60 hour the dissolved ferric iron concentration decreased to 3.9 ± 0.1 μM. The dissolved ferric iron concentration did not show an immediate response to the succinate addition (within 1 minute after the addition) nor was there a response after 20 hours. This is a significantly different response than was observed with the oxalate and malonate experiments. At the end of the incubation, the results deviated from the trend, showing an increased concentration of dissolved iron (3.0 ± 0.04 μM) for succinate. Figure 4.5 A shows addition of NTA or citrate increased dissolved ferric iron concentration more than dioic acids. Initially citrate could solubilize 1.78 ± 0.32 μM of ferric iron. This increased to 56.82 ± 1.46 μM after 20 hours and 63.45 ± 1.51 μM after 50 hours. NTA could solubilize the most ferric iron from oxidized steel surface. It increased the ferric solubility to 26 ± 0.32 μM

immediately after addition and finally to 65.42 ± 4.63 µM at the end of the 50 hour experiment.

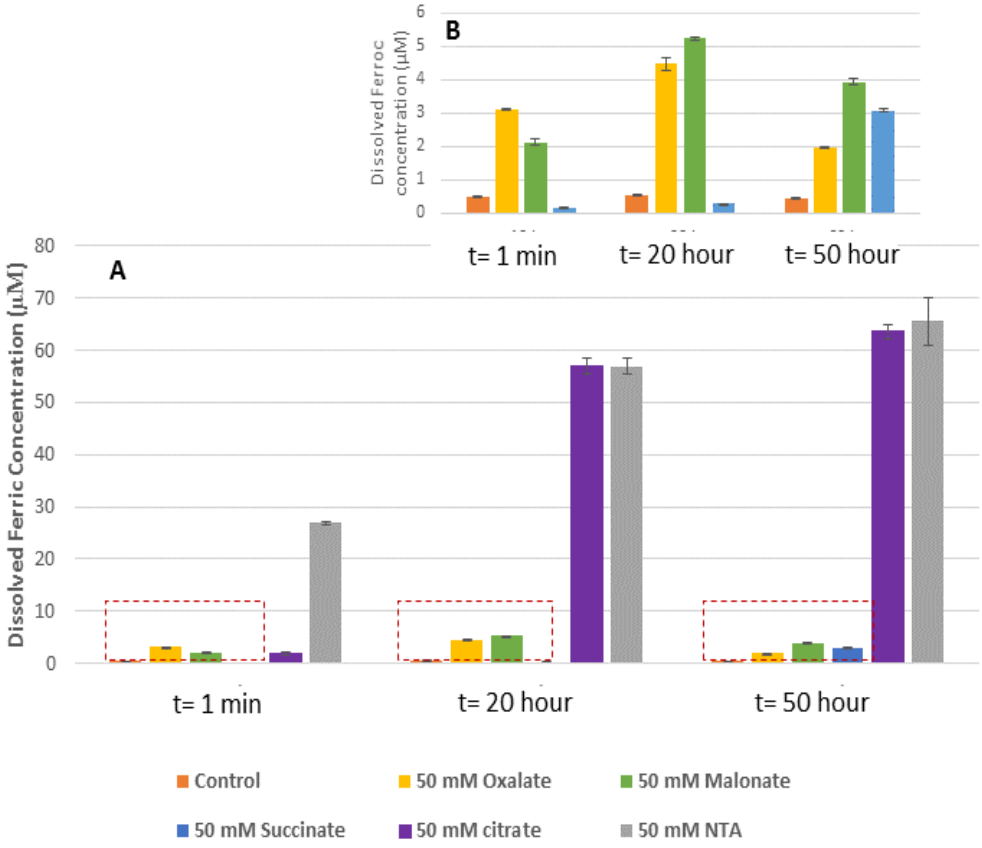

Figure 4.5 A) Dissolved ferric iron concentration of oxidized steel (4.5 cm^2) incubated in 50 mM dioic acids, citrate, NTA and control at pH=7 for 50 hours **B)** Dissolved ferric iron concentration of oxidized steel incubated in 50 mM dioic acids and control at pH=7 for 50 hours.

The important conclusions from this experiment are: 1) the addition of oxalate causes the amount of dissolved ferric iron to increase more rapidly than malonate and succinate immediately after addition, 2) malonate has a delayed response, but in keeping with the data from experiments in section 4.1 at longer time points it solubilizes the most ferric iron from the surface, 3) succinate initially passivates the surface and then gradually begins to solubilize ferric iron from the ferric oxyhydroxide layer, and 4) the reference

ligands are capable of solubilizing significantly more ferric iron than the dioic acids (a maximum of 65.42 ± 4.63 μM at t = 50 hr for NTA vs. a maximum of 5.24 ± 0.05 μM at t = 20 hr for malonate.

4.2.2 Corrosion Potential of Oxidized Steel with 50 mM Dioic Acids, Citrate and NTA under Aerobic Conditions

Corrosion potential ($E_{corrosion}$) measurements during the corrosion process measure the change in electrode (steel sample) potential over time. $E_{corrosion}$ can be used as an indicative if steel sample is corroding or passivating. Increases in $E_{corrosion}$ indicate that it is more difficult to remove electrons from the steel surface, so oxygen cannot oxidize metallic iron from steel surface very readily. Decreases in $E_{corrosion}$ indicate the accumulation of negative charge on steel surface, leading to a build up of electrons on the sample surface which allows for easier interaction with dissolved oxygen.

Figure 4.6 illustrates that each ligand has a unique influence on $E_{corrosion}$. For the abiotic dioic acid experiments, the $E_{corrosion}$ is shown in Figure 4.6. The $E_{corrosion}$ of the control steel remained in the range of -440 mV to -465 mV for each experiment. When 50 mM oxalate was added to the EuroCell (t = 10 hr), the $E_{corrosion}$ immediately shifted in the positive direction, from -420 mV to -320 mV, as shown in Figure 4.6 A. For the remainder of the experiment, $E_{corrosion}$ remained between -320 mV and -340 mV. Figure 4.6 B shows the addition of malonate caused the $E_{corrosion}$ of the steel to decrease to nearly -600 mV from -400 mV. After the addition of the 50 mM succinate (Figure 4.6 C), the $E_{corrosion}$ initially shifted to -200 mV, which was higher than the control potential (-420 mV). It then switches and becomes more negative (-600 mV). After addition of citrate (Figure 4.6 D), $E_{corrosion}$ became -391 mV from -425 mV. After 10 hours, it

stabilized around -530 mV. The addition of NTA (Figure 4.6 E) shifted $E_{corrosion}$ to -700 mV from 425 mV and after 45 hours $E_{corrosion}$ increased to -470 mV.

The addition of 50 mM oxalate caused an increase in $E_{corrosion}$ suggesting that it was harder for oxygen to oxidize metallic iron from the steel surface. The addition of malonate caused a decrease in $E_{corrosion}$ suggesting that there were residual electrons from the oxidation of the steel. The addition of succinate caused first an increase in $E_{corrosion}$ and then a decrease suggesting that initially the steel sample was more difficult to oxidized, but later it became easier for oxidation to occur. Both reference ligands caused a general decrease in $E_{corrosion}$ suggesting that both samples were oxidized more in the presence of a ligand.

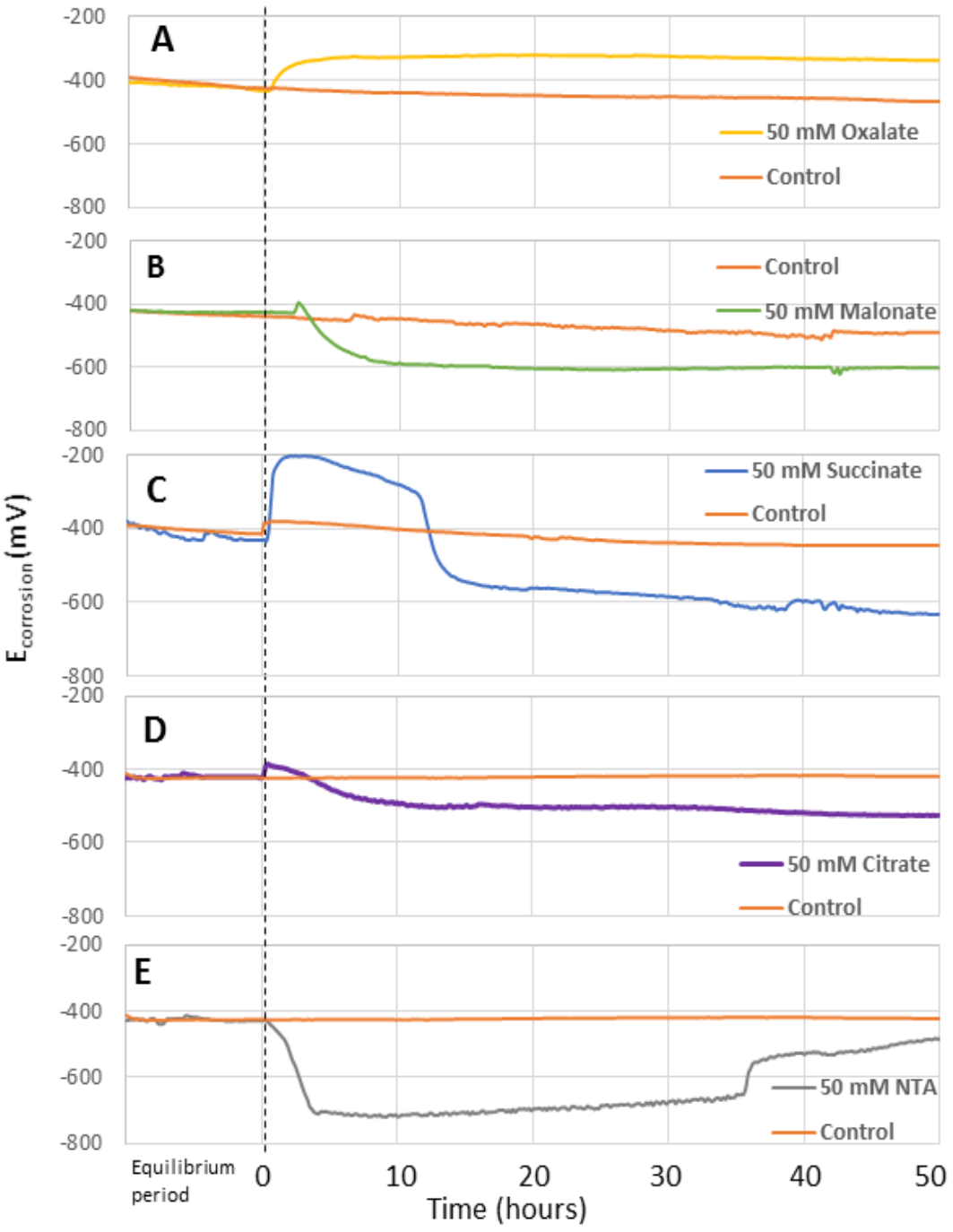

Figure 4.6 Corrosion potential ($E_{corrosion}$) of the samples plotted versus time. Oxidized steel incubated in 50 mM (A) oxalate, (B) malonate, (C) succinate, (D) citrate and (E) NTA for 50 hours. Black line is an indicator of the time point of ligands were added to system (0 hour).

4.2.3 Polarization Resistance of Oxidized Steel with 50 mM Dioic Acids, Citrate and NTA under Aerobic Conditions

When taking a linear polarization resistance measurement, the potential of the sample is plotted vs. the current. The slope of the resulting linear data is the polarization resistance (which fits with Ohm's Law). The polarization resistance can be used as a measure of the resistance to corrosion of the sample: i.e. the higher the polarization resistance, the less the sample will be likely to corrode.

Figure 4.7 shows the polarization resistance data from the oxidized steel samples. For each experiment, the control had an average R_p between 40 and 60 ohms, which remained constant throughout the course of the experiment. Figure 4.7 A shows that the addition of 50 mM of oxalate caused a rapid increase of R_p from 50 ohms to an average of 350 ohms. Figure 4.7 B shows that the addition of 50 mM malonate did not change the R_p (60 ohms) immediately. However, after 10 hours R_p decreased to 24 ohms. Figure 4.7 C shows the addition of 50 mM succinate increased to R_p from 60 ohms to 150 ohms but this then decreased to around 40 ohms at t = 10 hours after the addition of succinate). Figure 4.7 D shows the addition of 50 mM citrate caused R_p increased but R_p was not stable until t = 20 hours. The polarization resistance measurements were very noisy and could not provide an average value. After 20 hours, R_p became stable again and was similar to R_p of the control experiment (60 ohms). Figure 4.7 E shows the addition of 50 mM NTA decreased the resistance from 40 ohms to an average of 20 ohms. There were random increases in the resistance, but these were brief and the resistance remained lower than the control for the majority of the experiment.

The addition of oxalate causes R_p to increase, which follows the increase in corrosion potential of the sample to indicate that there is passivation occurring. The addition of malonate causes R_p to decrease, which again confirms the potential data in suggesting corrosion of the sample. The succinate initially causes an increase in R_p which then reverses and decreases, showing initial passivation and then eventual corrosion of the surface.

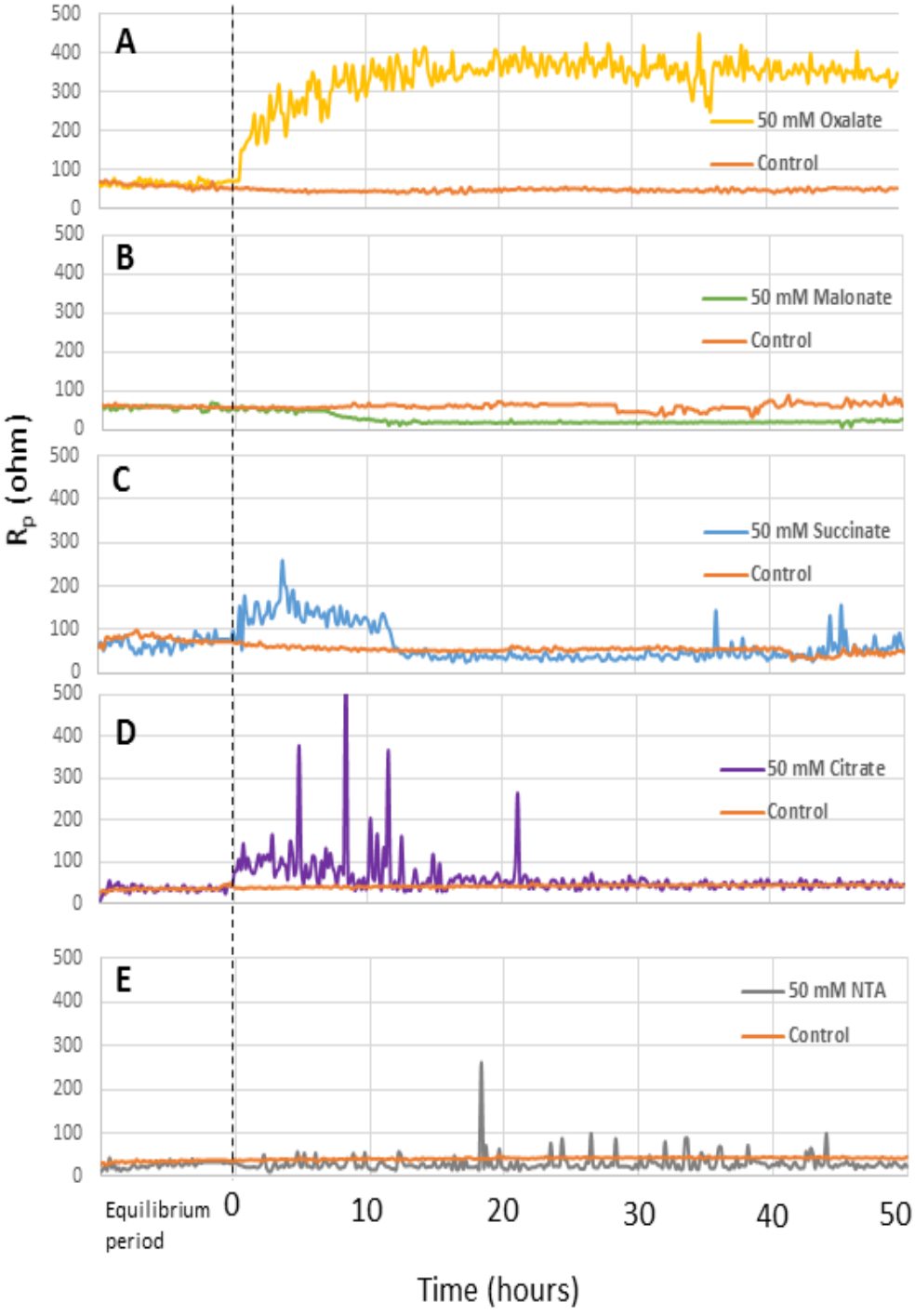

Figure 4.7 Polarization resistance (R_p) of the samples plotted versus time. Oxidized steel incubated in 50 mM (A) oxalate, (B) malonate, (C) succinate, (D) citrate and (E) NTA for 50 hours. Black line is indicator of the time point of ligands were added to system (0 hour).

4.2.4 Corrosion Rate of Oxidized Steel with 50 mM Dioic Acids, Citrate and NTA under Aerobic Conditions

The corrosion rate in milli-inches per year (mpy) was calculated from $E_{corrosion}$ and R_p, this calculation is performed in the Gamry software and is plotted for each sample in Figure 4.8.

Figure 4.8 shows that for all the samples, the average corrosion rate of the control sample remained between 50 mpy and 70 mpy. All the dioic acids were added at t = 0 hour. With the addition of oxalate, the corrosion rate of the sample decreased from 40 mpy to 10 mpy (Figure 4.8 A). The addition of 50 mM malonate (Figure 4.8 B) did not affect the corrosion rate immediately, but it showed a gradual increase from ~50 mpy to 100 mpy. However, at the end of the experiment (t = 50 hr) the corrosion rate became the same as the control (70 mpy). The addition of 50 mM succinate (Figure 4.8 C) first caused the corrosion rate to decrease from 50 mpy to 20 mpy. After 10 hours, the corrosion rate increased to 70 mpy before finally stabilizing at 50 mpy. After 50 mM citrate was added (Figure 4.8 D), the corrosion rate initially decreased to ~20 mpy and then increased to 50 mpy. When NTA was added (Figure 4.8 E), the average corrosion rate increased from 70 mpy to 110 mpy. Over a 6-hour period, the corrosion rate showed significant variation, but it eventually settled down around 110 mpy again.

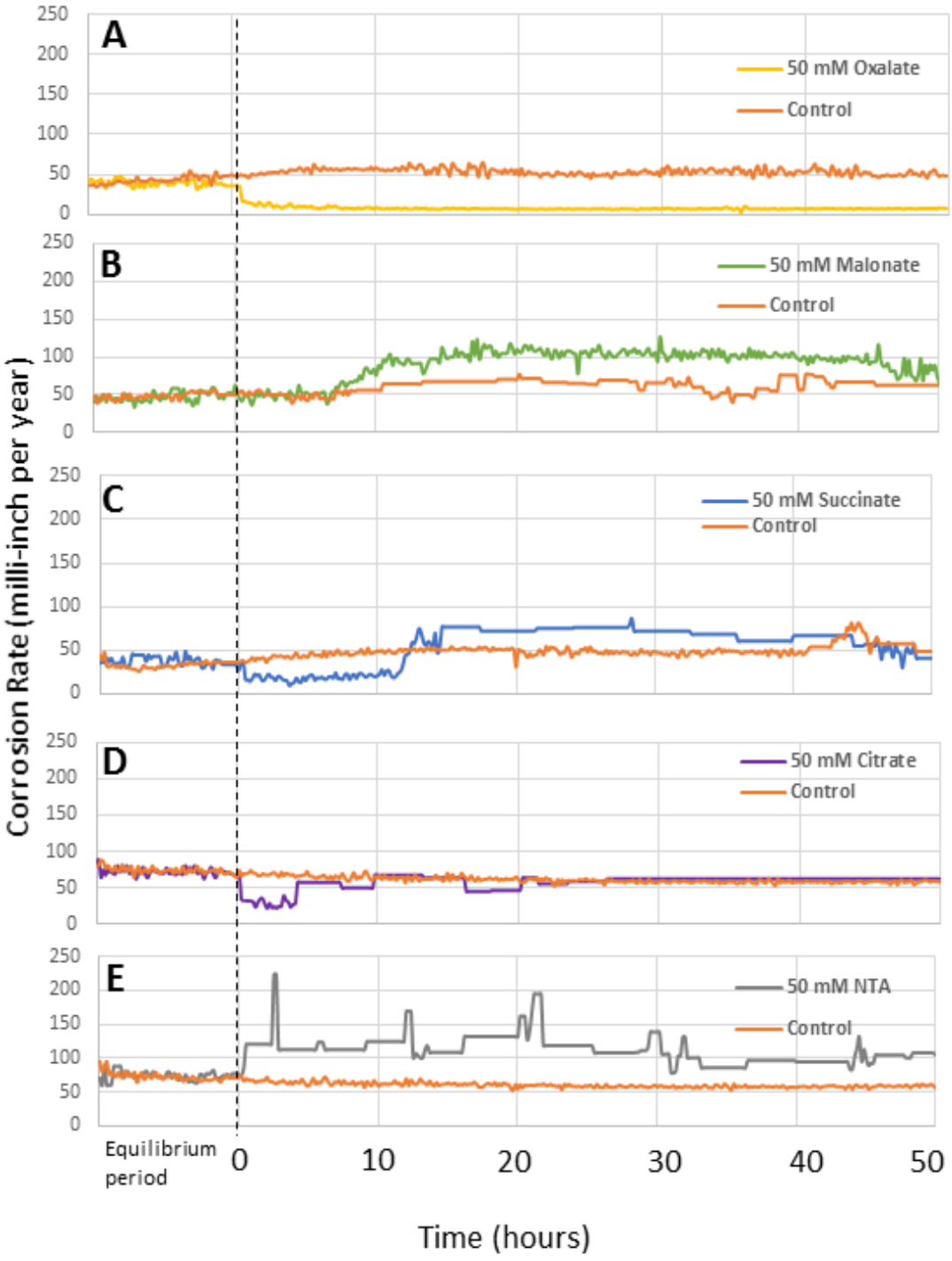

Figure 4.8 Corrosion rate of the samples plotted versus time. Oxidized steel incubated in 50 mM (A) oxalate, (B) malonate, (C) succinate, (D) citrate and (E) NTA for 50 hours. Black line is an indicator of time point where ligands were added to a system (0 hr).

The conclusions from this section are: 1) confirming the results from sections 4.2.1, 4.2.2 and 4.2.3, the corrosion rate with oxalate decreases, suggesting that there is passivation of the steel sample, 2) malonate again confirms the results of the previous three sections that it causes an increase in the corrosion rate of the steel sample, 3) succinate does indeed show that it first passivates the steel sample, but then causes an increase in the corrosion of the sample, 4) citrate has a minimal effect on the corrosion rate of the steel sample, but it does cause a slight increase in the corrosion, 5) NTA has the highest average corrosion rate of the steel and 6) ligands that most increased the corrosion rate of the steel samples were, in decreasing order, NTA > malonate > citrate > succinate > oxalate.

4.2.5 Mass Loss Measurements of Oxidized Steel with 50 mM dioic acids, citrate and NTA under aerobic conditions.

A final method of measuring the corrosion of the steel samples (used for LPR experiments) is using mass loss. The mass of the oxidized steel was recorded before and after incubation with the ligands. This measurement gives the overall loss of mass of the sample, which is the amount of iron that has been removed.

The mass loss of the ligand samples (Table 4.1) shows that mass loss is dependent upon the ligand. It was compared to the mass loss of a ligand free control, which over the course of the experiment (60 hours) lost 45 mg. The steel coupon incubated with 50 mM oxalate lost 21 mg of iron. The steel coupon incubated with 50 mM malonate showed a loss of 55 mg. The steel coupon incubated with 50 mM succinate lost 44 mg

of iron. The steel sample incubated with 50 mM citrate lost 60 mg of iron and the steel sample incubated with 50 mM NTA lost 190 mg of iron.

The mass loss data fit with LPR results. For the dioic acids investigated, the sample with 50 mM oxalate has a smaller mass loss than the control sample and 50 mM malonate has the most effect on increasing the corrosion of a steel surface. The steel sample incubated with 50 mM succinate was very similar to the control steel sample. Citrate increases the corrosion of the steel samples, but not as significantly as NTA, which confirms the previous results. This again indicates that NTA increases the corrosion of a steel surface most of the ligands.

Table 4-1 Mass loss of oxidized carbon steel during the electrochemical experiment (60 hour) at pH=7

Sample	**Mass loss (mg)**
Control	46
50 mM Oxalate	21
50 mM Malonate	55
50 mM Succinate	44
50 mM Citrate	60
50 mM NTA	190

The takeaways of Section 4.2 are: 1) malonate has the effect of increasing the corrosion of steel samples, while oxalate has the effect of passivating the steel samples, 2) succinate has an overall neutral effect on the corrosion of steel samples and 3) malonate has the most dissolved iron and also the highest mass loss of the dioic acid samples, while oxalate has the second highest dissolved ferric iron, but the lowest mass loss.

These results suggest that, for abiotic experiments, malonate has the greatest effect on increasing the corrosion rate of the steel, while oxalate has the best passivation effect on the oxidized steel. This indicates that the amount of corrosion will increase with increasing binding constant, but there is a maximum value and past that passivation becomes dominant.

4.3 Carbon Steel Corrosion with the presence of *S. oneidensis* MR-1 and Dioic Acids under Anaerobic Conditions

The previous section showed the results for abiotic experiments that tested the response of the corrosion of steel samples incubated with the selected organic ligands (the dioic acids oxalate, malonate and succinate, citrate and NTA). The next step was to show how the corrosion of the steel samples was affected when bacteria were present in addition to the organic ligands. The results of this would demonstrate the relationship between the organic ligand and the respiration of ferric iron by the facultative anaerobic iron reducing bacteria *S. oneidensis* MR-1.

4.3.1 S. oneidensis MR-1 Growth Curve with 25 mM Fumarate, Ferric-citrate and Ferric-NTA

Before testing the effects of the bacteria and ligand on corrosion, the first step was to determine how the growth of *S. oneidensis* MR-1 was affected when it was grown on ferric iron as the terminal electron acceptor (TEA) with two different binding constants rather than the fumarate that is typically used as the TEA.

Figure 4.9 shows the growth curves of *S. oneidensis* MR-1 for two ferric iron TEAs and fumarate. Based on this figure, *S. oneidensis* MR-1 growth with 25 mM ferric-citrate reached stationary phase earlier than any other electron donor (t = 6 hr) and

furthermore, it had a very short stationary phase. Ferric-NTA had lower growth (OD = 0.11) compared to ferric-citrate (OD = 0.3) and fumarate (OD = 0.25). However, the time to reach the stationary and death phase for both ferric-NTA and fumarate are similar (t = 14 hr and t = 24 hr, respectively). The control did not contain any electron acceptor so there was no growth of *S. oneidensis* MR-1.

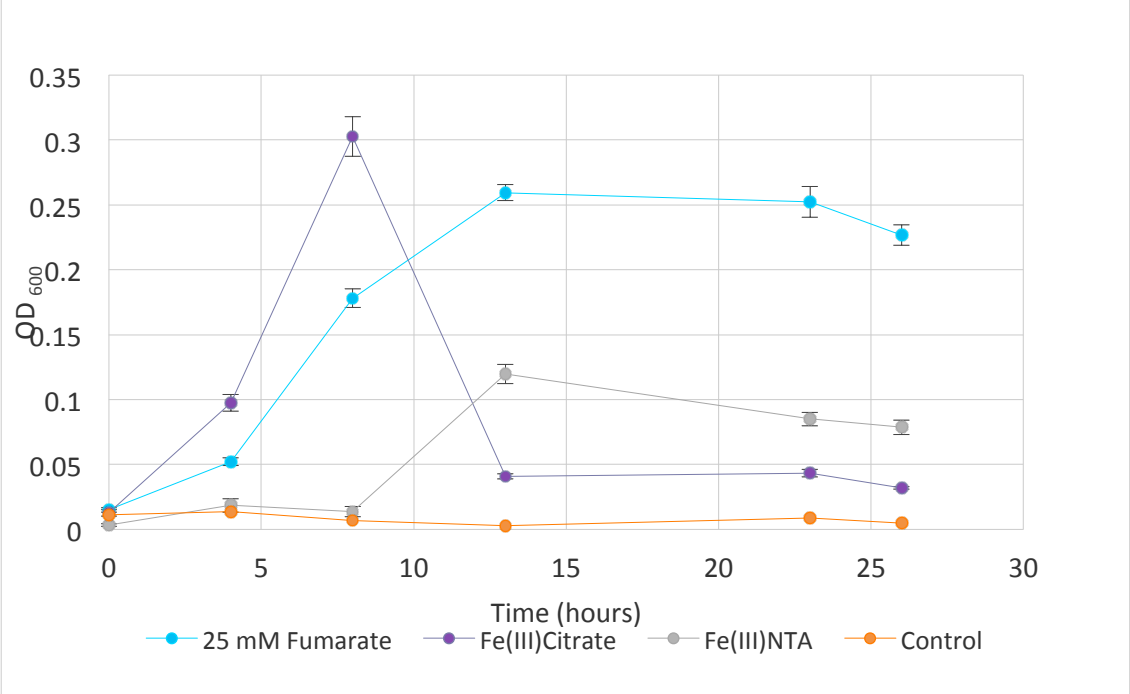

Figure 4.9 Growth curve of *S. oneidensis* MR-1with different terminal electron acceptors at pH 7 and 32º C.

S. oneidensis MR-1 was also inoculated with 25 mM solid ferric oxyhydroxide but optical density could not be measured due to the solid ferric iron particles in media.

At the end of a 26-hour inoculation, the ferrous concentration from media with 25 mM ferric oxyhydroxide, ferric-citrate and ferric-NTA were measured as shown in Figure 4.10. The purpose of this was to observe how much ferric iron was respired by the bacteria and converted to ferrous iron. *S. oneidensis* MR-1 with 25 mM ferric-citrate as the TEA provides more available free ferric iron due to a low binding constant and it

produced an average of 5.82 ± 2.8 mM ferrous iron while *S. oneidensis* MR-1 with 25 mM ferric-NTA produced an average of 2.19 ± 1.2 mM ferrous iron. The respiration of 25 mM ferric oxyhydroxide was the lowest, having produced < 1 mM of ferrous iron. Control (ferric oxyhydroxide) experiments showed *S. oneidensis* MR-1 is capable of respiring solid ferric iron but growth is expected to be much lower than other electron acceptors due to a low ferrous iron concentration. The ferrous iron concentration for the control experiment was 0.74 ± 0.013 mM.

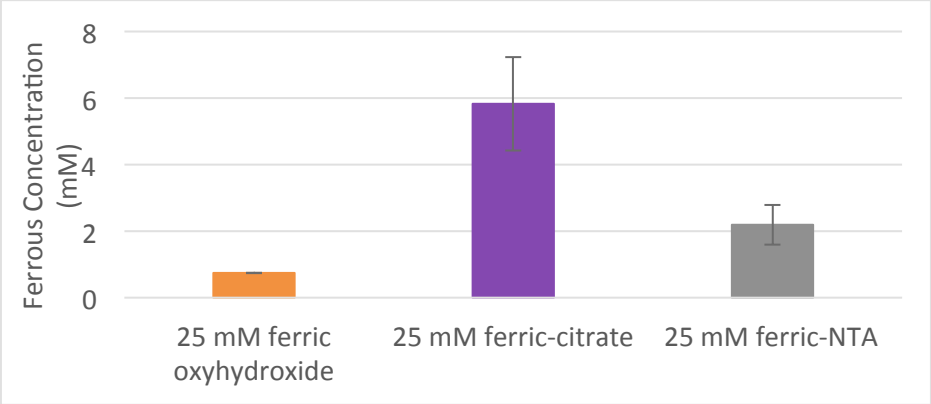

Figure 4.10 Ferrous concentration of *S. oneidensis* MR-1with addition of different terminal electron acceptor incubated for 36 hours at pH 7 and 32º C.

The main conclusions from this section are: 1) *S. oneidensis* MR-1 are capable of using ferric iron as a TEA, but their growth was severely limited compared to cultures grown on fumarate suggesting that they should not be grown for experiments on this TEA and 2) during their growth on the ferric iron complexes, *S. oneidensis* MR-1 respired ferric iron, converting it to ferrous iron. To produce the best cultures (with high yield and long stationary phase) for these experiments, cultures were grown with fumarate as the TEA and then washed to remove the fumarate, which is also a dioic acid before using it for my further experiments.

4.3.2 Ferric Oxyhydroxide Respiration by S. oneidensis MR-1

The purpose of this section was to determine how each ligand affects the respiration of ferric iron by *S. oneidensis* MR-1. The hypothesis is that the presence of ligand increases the dissolved ferric iron concentration and soluble ferric iron will facilitate *S. oneidensis* MR-1 anaerobic respiration. Also, ferric iron reduction will increase with increasing concentration of ligand due to the higher concentration of ferric iron. The section 4.1 abiotic experiments showed that the minimal amount of ligand required to dissolved higher concentration of ferric iron than control was ~1 mM. Increasing the concentration of ligand increased the amount of dissolved ferric iron concentration. The following experiments were performed with 5 mM or 50 mM ligands to determine if there was a different effect when the system contained bacteria.

S. oneidensis MR-1 (OD_{600} = 0.8) was incubated with 25 mM ferric oxyhydroxide for 24 hours at 32º C with 5 and 50 mM of either dioic acids, citrate or NTA. Figure 4.11 shows the change in ferrous iron concentration during 12 hours of *S. oneidensis* MR-1 respiration in the presence of 5 mM of the respective ligands. It can be seen that in the presence of 5 mM NTA, *S oneidensis* MR-1 had the greatest respiration of ferric iron. At the end of 12 hours, the ferrous iron concentration was 3.06 ± 0.11 mM in the presence of 5 mM NTA and 2.90 ± 0.30 mM in the presence of 5 mM citrate. The ferrous iron concentration with 5 mM dioic acids (oxalate, malonate, and succinate) were 0.96 ± 0.03 mM, 0.92 ± 0.13 mM and 0.73 ± 0.08 mM respectively. The control experiment (without any ligands) had a ferrous iron concentration of 0.72 ± 0.03 mM.

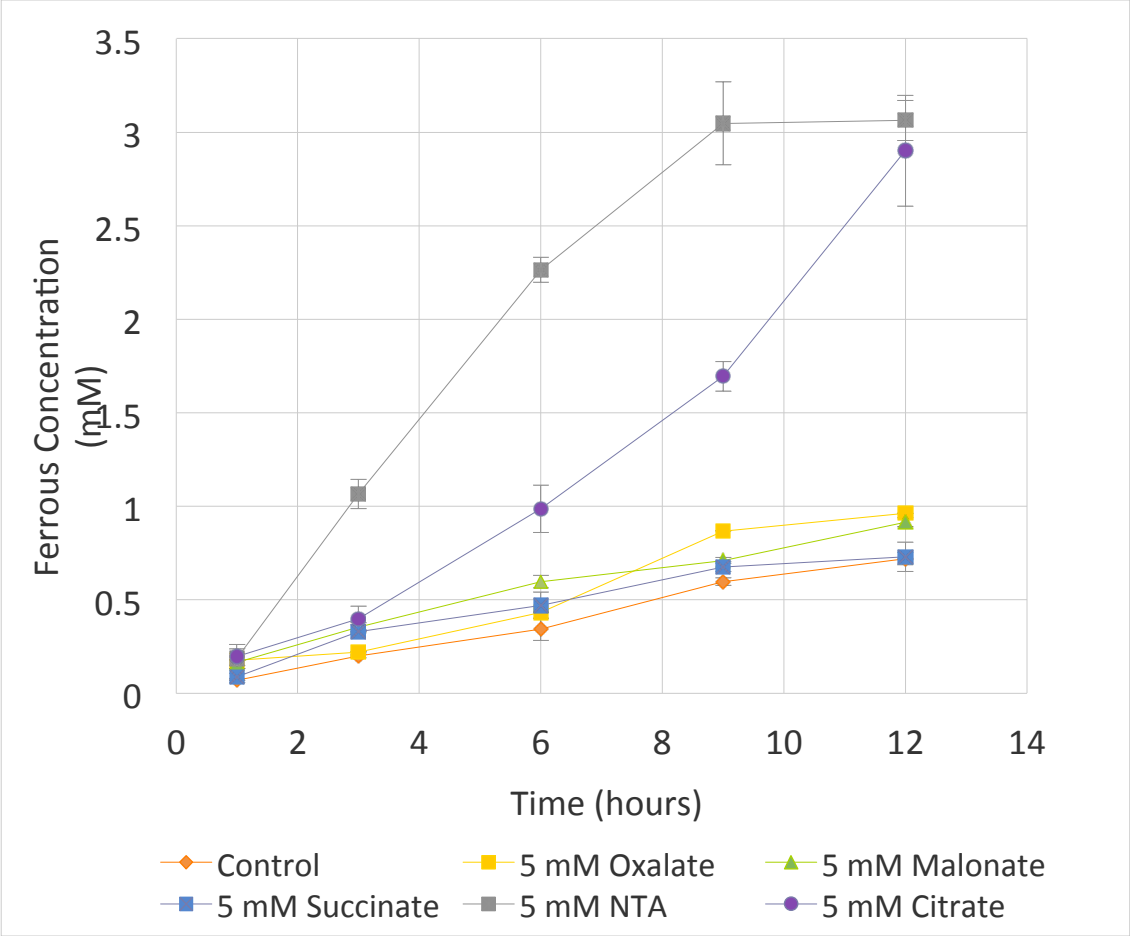

Figure 4.11 *S. oneidensis* MR-1 respiration of 25 mM ferric oxyhydroxide with addition of 5 mM oxalate, malonate, succinate, citrate and NTA incubated in dark for 12 hours at pH 7 and 32º C.

Figure 4.12 shows the changing ferrous iron concentration during 12 hours of *S. oneidensis* MR-1 respiration in the presence of 50 mM ligands. The same trend was observed as with 5 mM ligands but the effect on respiration was much greater. At the end of 12 hours, the ferrous iron concentration was 5.77 ± 0.31 mM in the presence of 50 mM NTA and 9.72 ± 0.17 mM in the presence of 50 mM citrate. Ferrous concentration with 50 mM dioic acids (oxalate, malonate, and succinate) were 2.72 ± 0.09 mM, 1.57 ± 0.16 mM and 0.72 ± 0.05 mM respectively. The control experiment (with only ferric oxyhydroxide) had a ferrous iron concentration of 0.57 ± 0.06 mM.

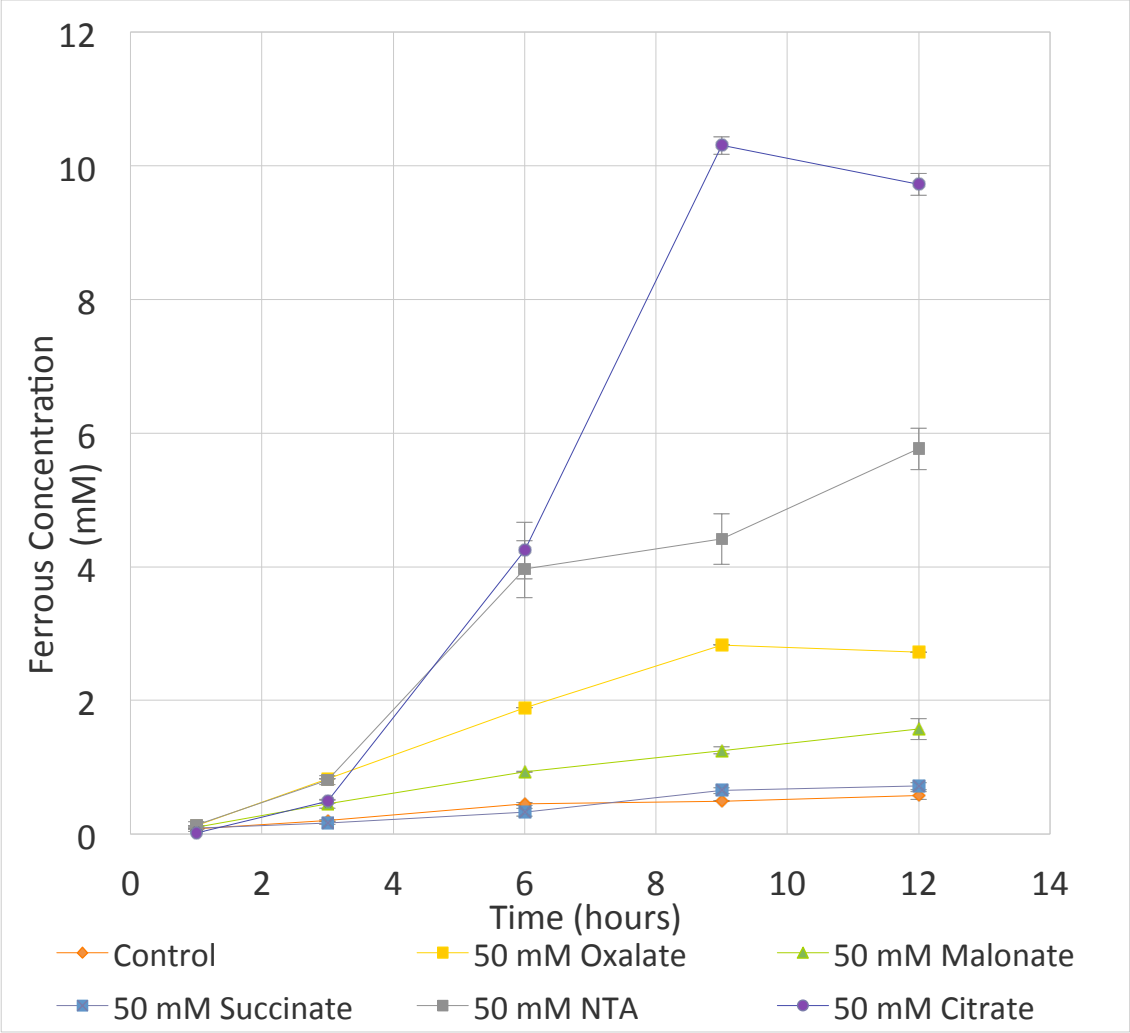

Figure 4.12 *S. oneidensis* MR-1 respiration of 25 mM ferric oxyhydroxide with addition of 50 mM oxalate, malonate, succinate, citrate and NTA incubated in dark for 12 hours at pH 7 and 32º C.

The conclusions are: 1) higher concentrations of ligands allow for more respiration of ferric iron (producing ferrous iron), 2) at lower concentrations of ligand, NTA gives the best respiration of ferric iron, which agrees with the data from the previous experiments suggesting that it produced the highest amount of dissolved ferric iron, 3) at concentrations of 5 mM, the respiration with oxalate and malonate slightly higher than succinate and control, 4) at concentration of 50 mM the respiration rate with oxalate and malonate much higher than control and succinate, 5) at higher concentrations the effect

of binding constant becomes more apparent, as it was shown in Figure 4.5 that citrate and NTA were capable of solubilizing nearly similar amounts of ferric iron and when *S. oneidensis* MR-1 is present, because citrate has a lower binding constant than NTA thus allowing the disassociation from the ligand/ferric iron complex, but 6) for the dioic acids, the binding constant does not affect the respiration in this way; instead the amount of ferric iron respiration increases with increasing binding constant, supporting our hypothesis.

Figure 4.13 shows the dissolved ferric iron and dissolved ferrous iron from ferric oxyhydroxide in the presence of different ligands, in the presence or absence of S. oneidensis MR-1 in order to assess any microbial influence on the total dissolved iron. The ferrous iron concentration was too low to detect in the abiotic samples (below the detection limit of 50 μM). In the presence of *S. oneidensis* MR-1, ferric iron concentration increased, showing that ferric iron solubilization by organic ligands is improved in the presence of bacteria. Abiotic 5 mM dioic acids (oxalate, malonate, and succinate) could solubilize 0.40 ± 0.003 mM, 0.17 ± 0.005 mM and 0.09 ± 0.008 mM respectively. When *S. oneidensis* MR-1 was present, the amount of solubilized ferric iron became 0.54 ± 0.013 mM, 0.53 ± 0.225 mM and 0.27 ± 0.018 mM respectively. Similar trends were observed with citrate and NTA. Abiotic samples with citrate and NTA solubilized 0.50 ± 0.045 mM and 1.00 ± 0.068 mM ferric iron. When *S. oneidensis* MR-1 was present, the ferric iron concentration for both citrate and NTA increased to 1.94 ± 0.025 mM and 2.01 ± 0.05 mM respectively. Ferrous iron concentration also increased with increasing solubilized ferric iron.

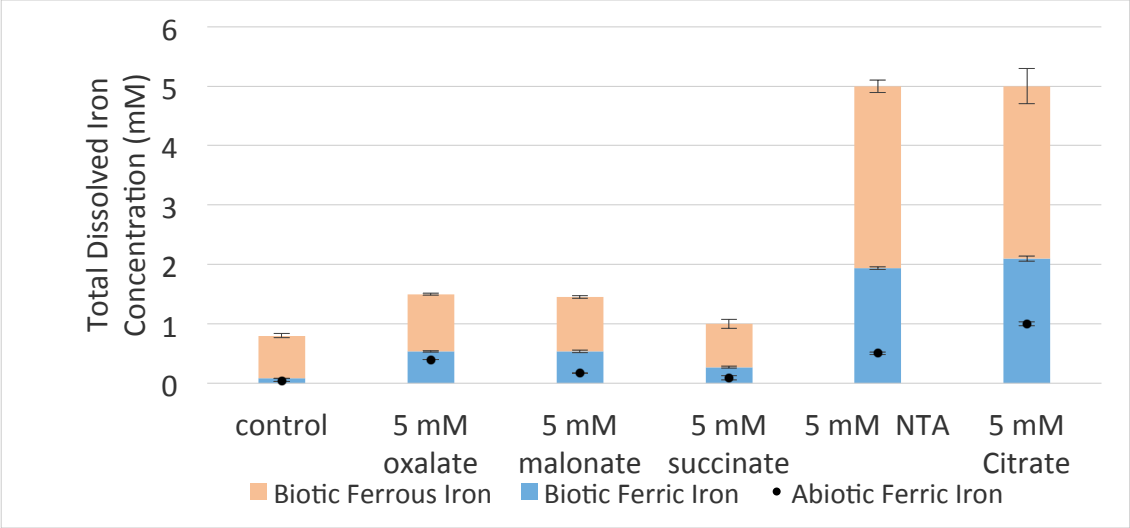

Figure 4.13 Biotic and abiotic (sterile) total dissolved iron concentration at the end of 12 hours incubation with 25 mM ferric oxyhydroxide and 5 mM ligands (oxalate, malonate, succinate, NTA and citrate) at pH 7 and 32º C. Ferrous iron was not detected in abiotic samples.

Figure 4.14 shows the similar data as Figure 4.13, but this time for 50 mM ligands. The ferrous iron concentration was not detected (below 50 µM) in the abiotic samples so it did not plot. Figure 4.13 shows that the ferric iron concentration increased in the presence of *S. oneidensis* MR-1, as it did with the 5 mM for all ligands. Abiotic 50 mM dioic acids (oxalate, malonate and succinate) solubilized 0.71 ± 0.005 mM, 0.21 ± 0.008 mM and 0.09 ± 0.008 mM respectively. When *S. oneidensis* MR-1 was present, the amount of solubilized ferric iron increased to 1.99 ± 0.60 mM, 1.18 ± 0.48 mM and 0.29 ± 0.031 mM respectively. Similar behaviors were again observed with citrate and NTA since abiotic samples solubilized 1.16 ± 0.031 mM and 3.44 ± 0.065 mM of ferric iron. When *S. oneidensis* MR-1 was present, the ferric iron concentration for both citrate and NTA increased to 8.08 ± 0.015 mM and 7.60 ± 0.831 mM respectively.

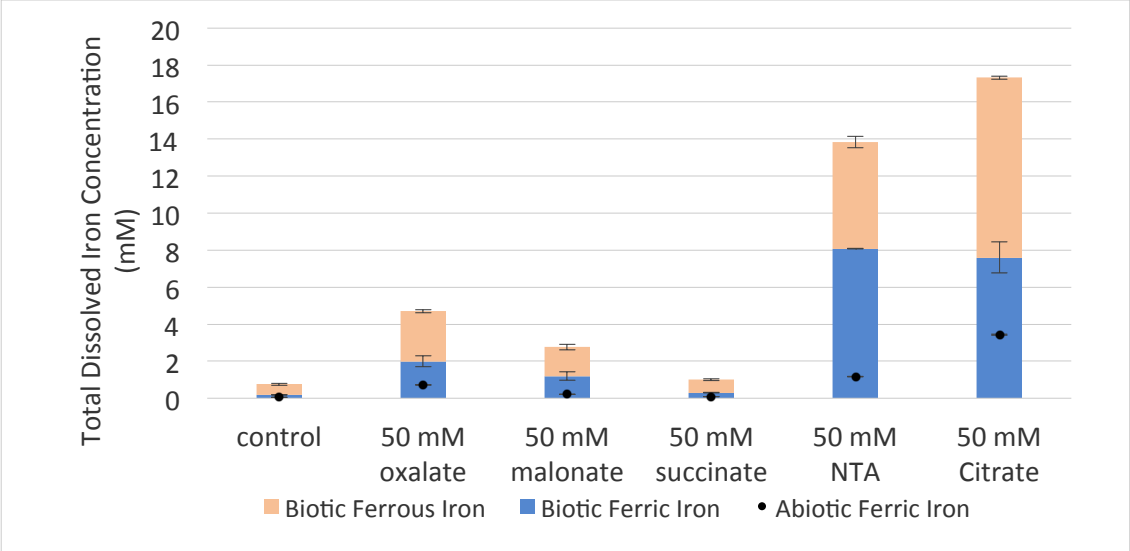

Figure 4.14 Biotic and abiotic (sterile) total dissolved iron concentration at the end of 12 hours incubation with 25 mM ferric oxyhydroxide and 50 mM ligands (oxalate, malonate, succinate, NTA and citrate) at pH 7 and 32º C. Ferrous iron was not detected in abiotic samples.

Conclusions from Figures 4.13 and 4.14 are: 1) the presence of *S. oneidensis* MR-1 greatly affects the ligand-ferric chelation, producing more dissolved ferric iron and ferrous iron than abiotic controls.

Conclusions from this section are: 1) in the presence of low concentration ligands, *S. oneidensis* MR-1 respiration of ferric iron was the highest with NTA due to its higher binding constant than citrate, but for concentrations of 50 mM, citrate produced the highest ferric iron respiration (shown by Figure 4.12 and Figure 4.14); which is most likely due to the higher availability of soluble ferric iron allowing the lower binding constant citrate to bind more and then release more ferric iron while at lower concentrations due to its higher binding constant NTA is better at solubilizing ferric iron when it is not freely available in solution, 2) for both the 5 mM and 50 mM concentrations, the dioic acids produced the results hypothesized; the amount of dissolved ferric iron increased with increasing binding constant, but the ferrous iron

production (respiration) also increased with increasing binding constant and 3) as was shown previously, higher concentrations of ligand produced higher concentrations of dissolved ferric iron and better ferric iron respiration (production of ferrous iron). However, it should be noted that these results are for ferric oxyhydroxide particles and there is no steel surface. The next step was to therefore repeat these experiments with oxidized steel coupons in the place of the ferric oxyhydroxide in order to show the effects of *S. oneidensis* MR-1 respiration on the oxidized steel surface.

4.3.3 S. oneidensis MR-1 Respiration of Oxidized Steel with Dioic Acids

The oxidized steel surface has varying types of ferric iron in the formation of ferric hydroxide layer. For this reason, it is important to test the respiration of ferric iron by *S. oneidensis* MR-1 with oxidized steel samples where the ligand and bacteria interact with oxidized steel. As it was shown in the previous section that the dioic acids increases soluble ferric iron concentration and it facilitate *S. oneidensis* MR-1 respiration.

Figure 4.15 shows the changing ferrous iron concentration over the course of 36 hours of *S. oneidensis* MR-1 respiration in the presence of 5 mM ligands and an oxidized steel coupon. The ferrous iron concentrations for 5 mM dioic acids (oxalate, malonate and succinate) were 0.36 ± 0.03 mM, 0.39 ± 0.013 mM and 0.32 ± 0.05 mM respectively. The control experiment (without any ligands) had a ferrous iron concentration of 0.29 ± 0.02 mM. At the end of 12 hours, the ferrous iron concentration was 0.57 ± 0.10 mM for the 5 mM NTA system.

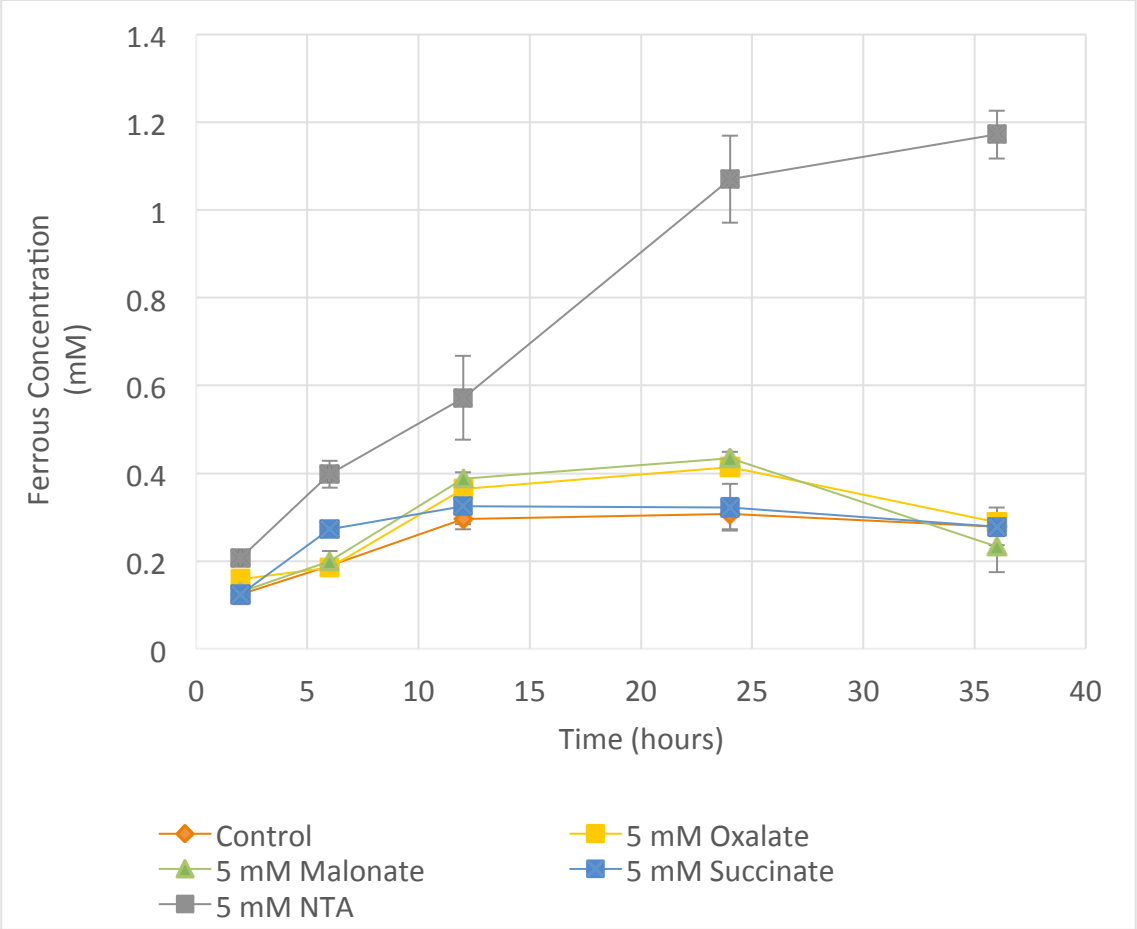

Figure 4.15 Ferrous concentration of oxidized steel coupon (1.6 cm^2) incubated in *S. oneidensis* MR-1with addition of 5 mM dioic acids for 24 hours at pH 7 and 32º C.

Figure 4.16 shows the changing ferrous concentration during 36 hours of *S. oneidensis* MR-1 respiration in the presence of 50 mM dioic acids. The ferrous iron concentration with 50 mM dioic acids (oxalate, malonate and succinate) was 0.65 ± 0.05 mM, 0.35± 0.08 mM and 0.32± 0.04 mM respectively. The control experiment (without any ligands) had a ferrous iron concentration of 0.25 ± 0.04 mM.

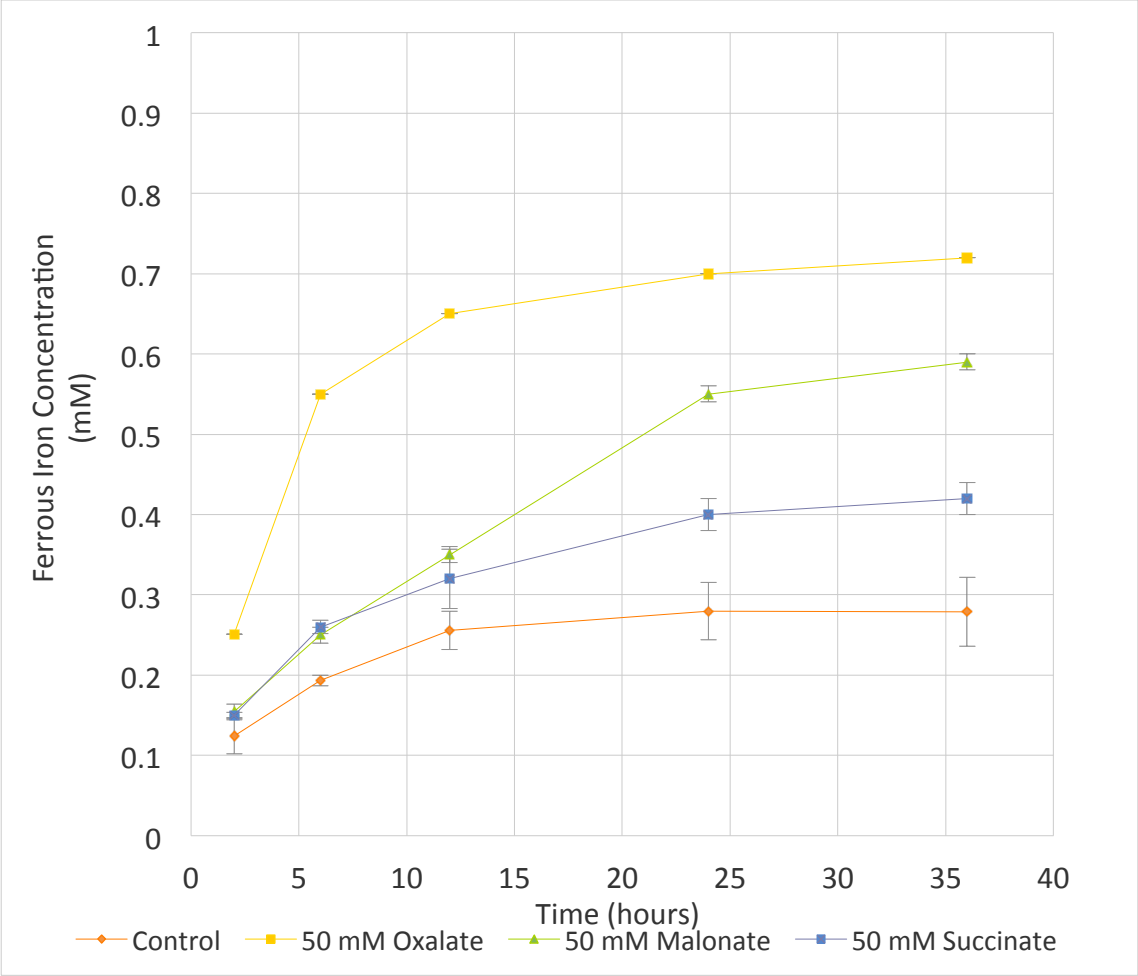

Figure 4.16 Ferrous concentration of oxidized steel coupon (1.6 cm^2) incubated in *S. oneidensis* MR-1 with addition of 50 mM dioic acids for 12 hours at pH 7 and 32º C.

The conclusions for Figures 4.15 and 4.16 are: 1) dioic acids had smaller effect on *S. oneidensis* MR-1 respiration with oxidized steel for 5 mM concentrations, 2) for 50 mM ligand concentrations, all of the dioic acids facilitated ferric iron respiration by *S. oneidensis* MR-1 where oxalate again allowed for the highest production of ferrous iron (~0.7 mM at t = 36 hr), followed by malonate and then succinate, supporting the hypothesis that a higher binding constant increases the concentration of dissolved ferric iron (as shown indirectly through ferrous iron production).

Figure 4.17 compares the total iron concentrations for abiotic samples and biotic samples with 5 mM ligands that were incubated with oxidized steel coupons. The results show that abiotic samples have higher concentrations of dissolved ferric iron than biotic samples, which is the opposite of what was observed with the experiments with ferric oxyhydroxide. In this experiment, the initial concentration of ferric hydroxide on steel surface was unknown. As seen in Figure 4.17, 5 mM NTA and 5 mM oxalate solubilize the most ferric iron with each solubilizing 0.57 ± 0.19 mM and 0.30 ± 0.03 mM respectively. *S. oneidensis* MR-1 respiration increased with 5 mM NTA. Even though 5 mM oxalate solubilized more ferric iron than 5 mM malonate and succinate, the ferrous iron concentration of the samples are very similar in concentration (not shown). Again, the abiotic ferrous iron concentrations were below detectable limits for these samples.

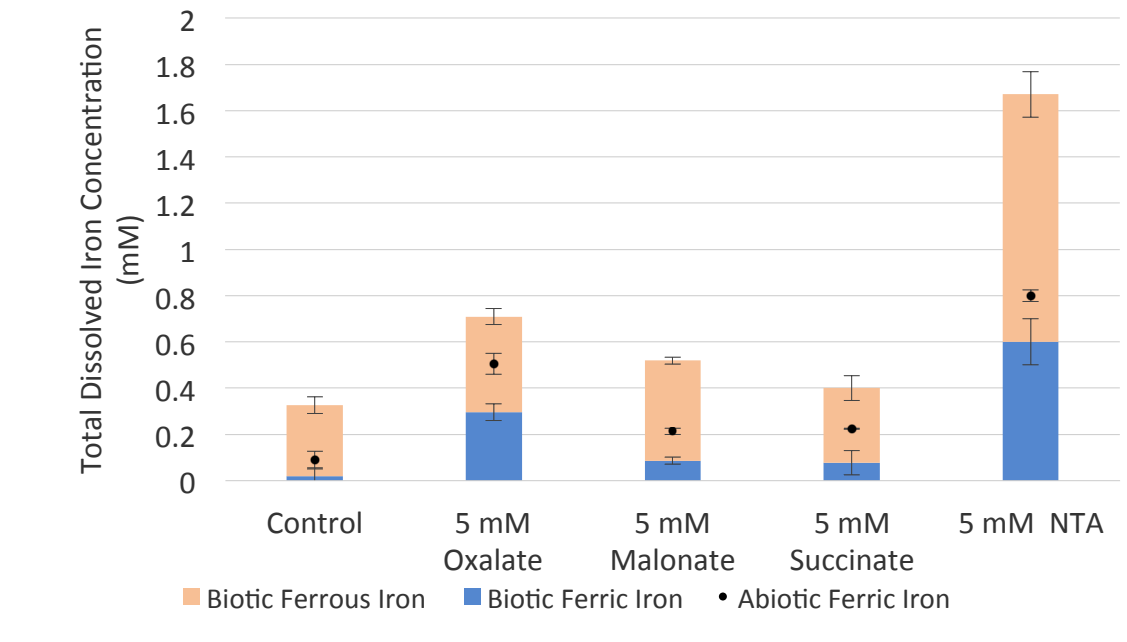

Figure 4.17 Biotic and abiotic (sterile) total dissolved iron concentration at the end of 12 hours incubation with oxidized steel coupon and 5 mM ligands (oxalate, malonate, succinate, NTA and citrate) at pH 7 and 32° C. Ferrous iron was not detected in abiotic samples.

Figure 4.18 shows the total iron concentrations for abiotic samples and biotic samples with 50 mM ligands that were incubated with oxidized steel coupons. Ferrous iron concentrations were below detectable limits in the abiotic samples. This experiment shows that increasing the ligand concentration increases ferric and ferrous iron formation in biotic samples. The highest concentration of total iron (both ferric and ferrous) was obtained with 50 mM oxalate at the end of a 12-hour incubation (~1 mM).

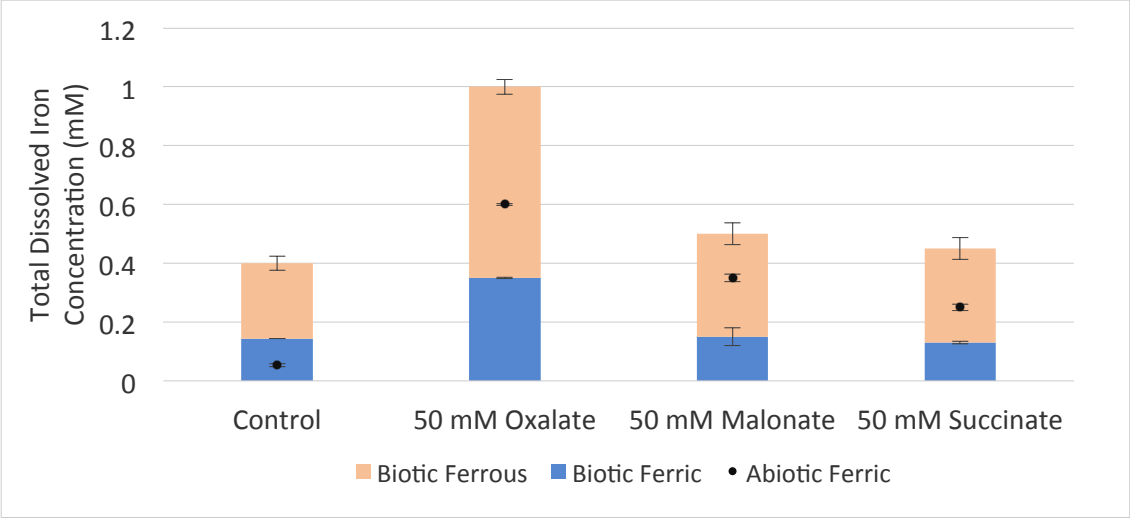

Figure 4.18 Biotic and abiotic (sterile) total dissolved iron concentration at the end of 12 hours incubation with oxidized steel coupon and 50 mM dioic acids at pH 7 and 32º C. Ferrous iron was not detected in abiotic samples.

The conclusions from Figure 4.17 and 4.18 are: 1) for oxidized steel coupons, the concentration of ligand (5 mM vs. 50 mM) did not significantly affect the amount of total iron but there were higher ferrous iron concentrations at ligand concentrations of 50 mM, suggesting that increasing dioic acid concentration facilitates *S. oneidensis* MR-1 respiration, 2) oxalate had the highest effect, producing the most dissolved ferric iron and total iron, suggesting that even though it had the highest binding constant and solubilized the most ferric iron, it also facilitated *S. oneidensis* MR-1 respiration the

best and 3) the abiotic ferric iron production was higher than the biotic ferric iron production for the oxidized steel samples. This suggests that the consumption of ferric iron *S. oneidensis* MR-1 is faster than ferric iron solubilization by dioic acids from the steel surface.

To determine how much the presence of ligand facilitated *S. oneidensis* MR-1 respiration with either ferric oxyhydroxide or an oxidized steel sample with 5 mM and 50 mM ligands, ferrous formation rates were calculated. The reason for reporting rate as ferrous iron formation was that oxidized steel had unknown type and amount of ferric oxides. They were calculated by linear-least square regression of ferrous iron concentration versus time over the duration of experiment. The order of the reaction could be determined by fitting the ferrous iron concentration data as a function of time. Since the data were a linear fit when plotting the concentration vs. time, then the reaction was zero order. Additionally, ferrous iron formation rates with oxidized steel and ferric oxyhydroxide in the presence of ligands were compared.

Table 4.2 shows the ferrous iron formation rate. The R-squared values show that the regression fits the data with high agreement, suggesting that the reaction is zero order. For dioic acids, 50 mM oxalate increased the ferrous iron formation rate to 0.353 mM/hr. For the other dioic acids at 50 mM, the reaction rate decreased with decreasing binding constant in both the ferric oxyhydroxide and oxidized steel coupon systems. However, for 5 mM dioic acids, it was more difficult to discern a distinct relationship between binding constant and the reaction rate. For 5 mM of dioic acids with the oxidized steel coupons, they didn't make much difference in the rates compared to the respective due to the low concentration of ferric iron. The highest rate of ferrous iron

formation was obtained with 50 mM citrate and NTA, which are already known as facilitative ligands for *S. oneidensis* MR-1 respiration as shown in literature (Haas & Dichristina, 2002). For these experiments, the ferrous iron formation rate with 50 mM NTA is 0.7890 mM/hr and 0.8770 mM/hr with 50 mM citrate. Also, control data shows ferrous formation rate with ferric oxyhydroxide is approximately 6 times higher than the oxidized steel.

Table 4-2 Zero order ferrous formation rate for both oxidized coupons and 25 mM ferric oxyhydroxide over 12 hours.

		25 mM Ferric Oxyhydroxide		**Oxidized Steel Coupon**	
		Ferrous form. rate (mM/hr)	R-squared value	Ferrous form. rate (mM/hr)	R-squared value
50 mM Ligands	Control	0.076 ± 0.011	0.994	0.013 ± 0.003	0.979
	Oxalate	0.353 ± 0.003	1.000	0.381 ± 0.027	0.852
	Malonate	0.166 ± 0.006	1.000	0.193 ± 0.003	0.999
	Succinate	0.048 ± 0.006	0.996	0.164 ± 0.008	0.922
	Citrate	0.877 ± 0.379	0.909	-	-
	NTA	0.789 ± 0.239	0.942	-	-
5 mM Ligands	Control	0.064 ± 0.010	0.986	0.017 ± 0.001	1.000
	Oxalate	0.087 ± 0.032	0.919	0.021 ± 0.011	0.919
	Malonate	0.069 ± 0.016	0.967	0.026 ± 0.007	0.980
	Succinate	0.087 ± 0.015	0.919	0.019 ± 0.013	0.863
	Citrate	0.190 ± 0.032	0.982	-	-
	NTA	0.360 ± 0.049	0.988	0.036 ± 0.009	0.980

The main conclusions of the reaction order experiment are: 1) the reaction is zero order, suggesting that the rate of reaction was independent of the ligand concentration in the system but ferric solubility is depending on ligand concentration 2) 5 mM dioic acid samples did not give consistent rate results, indicating that this concentration was too low to provide reliable measurements for the dioic acids chosen and therefore 50 mM concentrations were used, 3) for the oxidized steel coupon and the ferric oxyhydroxide, the reaction rates were very similar for oxalate and malonate, suggesting that the reaction is independent of whether or not the ferric iron is present as a steel or as a ferric oxyhydroxide particle because they had the same capability of solubilize ferric iron from two different surface 4) of the three dioic acids, oxalate has the highest reaction rate followed by malonate and then succinate for both ferric oxyhydroxide and oxidized steel.

4.3.4 Respiration Rate Measurements with S. oneidensis MR-1 and 50 mM Ligands with Previous Inoculation of Ligand

In Section 4.3.2, the ligands and *S. oneidensis* MR-1 were inoculated with ferric oxyhydroxide at the same time. To test the hypothesis that the respiration rate is not limited by the dissolution of ferric oxyhydroxide, 25 mM ferric oxyhydroxide was initially incubated with 50 mM ligands for 12 hours. Then *S. oneidensis* MR-1 was inoculated into the system and the ferrous iron concentration was measured over the next 12 hours. Figure 4.19 shows ferrous iron formation as a function of time with ferric oxyhydroxide. Comparing Figure 4.19 to Figure 4.12 (ligand and microbe inoculated at the same time), it was obvious that the trend of ferrous iron formation for each ligand

was very similar. For the dioic acids, oxalate again had the highest ferrous iron formation followed by malonate and then succinate. 50 mM citrate had the highest rate of ferrous iron formation followed by 50 mM NTA. This was the same result seen in Figure 4.12.

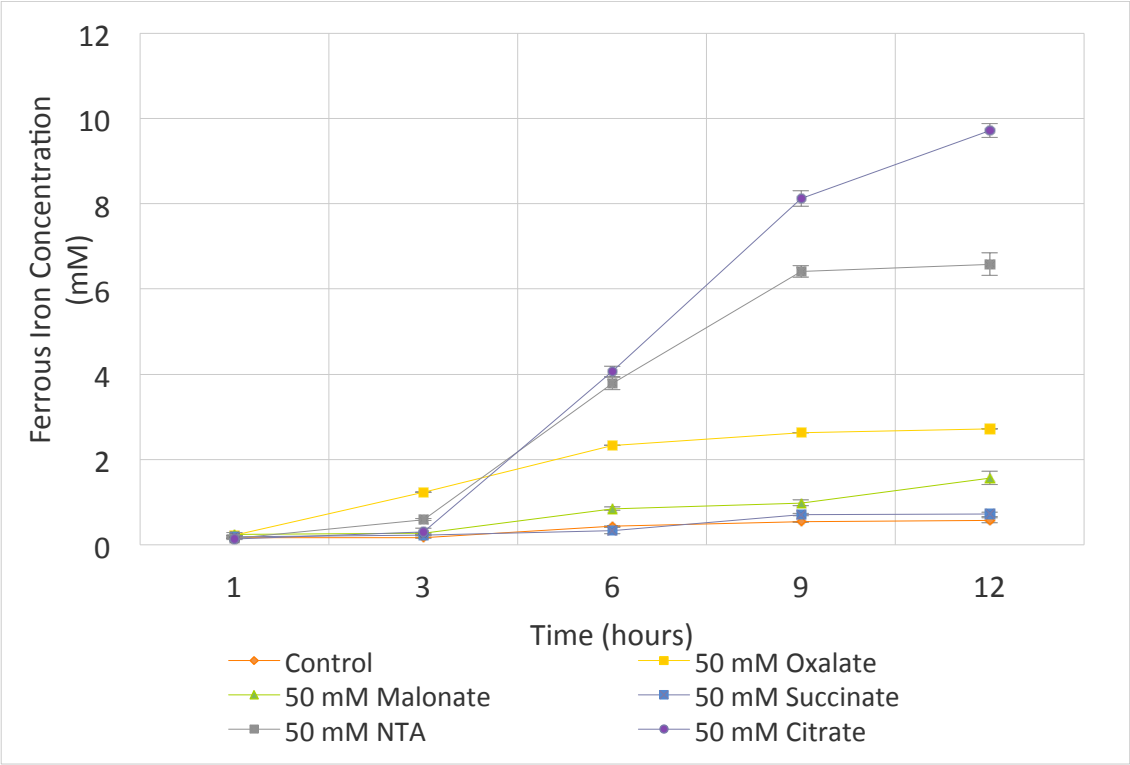

Figure 4.19 50 mM ligands were incubated with 25 mM ferric oxyhydroxide in sterile media for 12 hours. *S. oneidensis* MR-1 was added in media and then samples were incubated in the dark for another 12 hours at pH 7 and 32ºC. The ferrous iron formation rate was measured from the concentration as a function of time.

Figure 4.20 further shows the total iron concentration for the experiments where *S. oneidensis* MR-1 was added 12 hours after the addition of the ligand. As can be seen the results were almost exactly the same as observed in Figure 4.14, further indicating that the addition of bacteria after the ligand and ferric oxyhydroxide have been incubated for 12 hours does not affect the respiration of ferric iron.

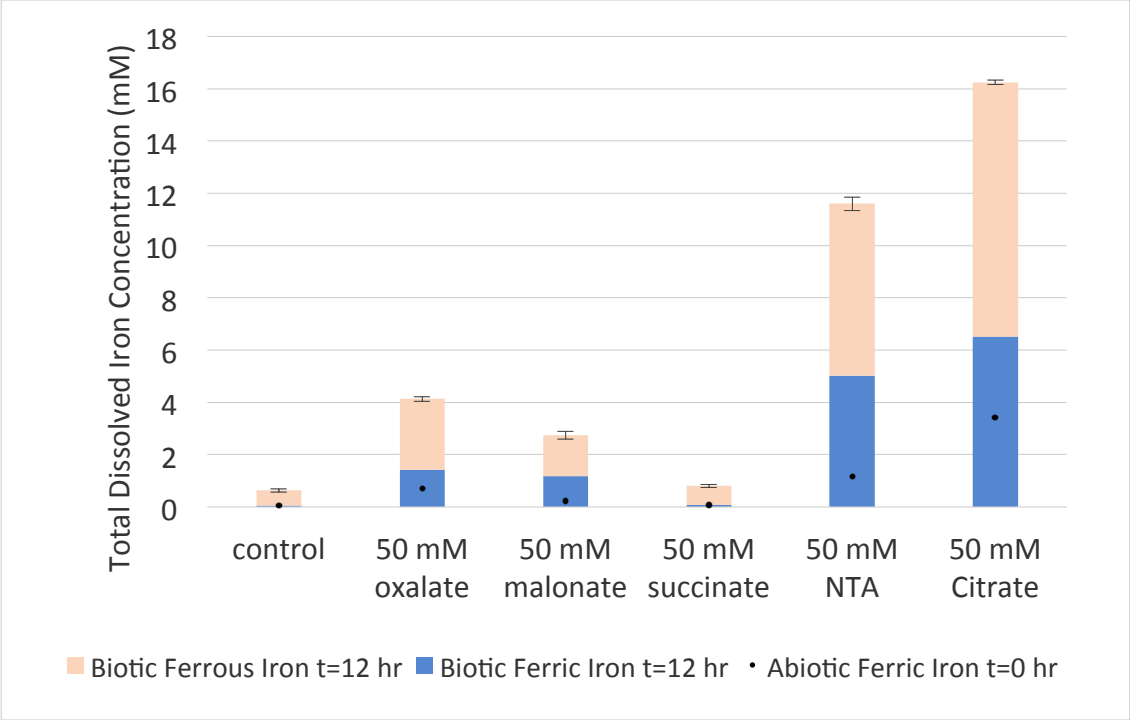

Figure 4.20 Biotic and abiotic (sterile) total dissolved iron concentration at the end of 12 hours incubation with 25 mM ferric oxyhydroxide and 50 mM dioic acids at pH 7 and 32º C. Ferrous iron was not detected in abiotic samples.

The reaction rate was calculated from the linear region (first three-time point) of the data in Figure 4.19 and reported in Table 4.3. The ferrous iron formation rate for the experiments incubated for 12 hours with the ligands before the addition of *S. oneidensis* MR-1 and the experiments where the ligand and *S. oneidensis* MR-1 were added as the same time showed similar ferrous iron formation rates. This means reaction rate is not limited by solubilization of ferric iron solubility.

Table 4-3 Comparison effect of different incubation time of 50 mM dioic acids to *S. oneidensis* MR-1 respiration.

Zero order rate		**25 mM ferric oxyhydroxide incubated with ligands for 0 hr before *S. oneidensis* MR-1 added**		**25 mM ferric oxyhydroxide incubated with ligands for 12 hrs before *S. oneidensis* MR-1 added**	
		Ferrous form. rate (mM/hr)	R-squared value	Ferrous form. rate (mM/hr)	R-squared value
50 mM Ligands	Control	0.076 ± 0.011	0.994	0.056 ± 0.042	0.842
	Oxalate	0.353 ± 0.003	1.000	0.417 ± 0.066	0.992
	Malonate	0.166 ± 0.006	1.000	0.126 ± 0.083	0.873
	Succinate	0.048 ± 0.006	0.995	0.030 ± 0.005	0.990
	Citrate	0.877 ± 0.379	0.909	0.823 ± 0.344	0.869
	NTA	0.789 ± 0.239	0.942	0.754 ± 0.293	0.914

The conclusion from this section is: 1) the respiration of ferric iron was not limited by the dissolution of ferric iron from ferric oxyhydroxide.

4.3.5 Corrosion Rate Measurements of Oxidized Steel with S. oneidensis MR-1 and 50 mM Dioic Acids under Anaerobic Conditions

Up until this point, the experiments were individual components aimed at testing portions of the overall research hypothesis. The experiments in this section combined the parameters of the previous sections and were aimed at investigating the overall research hypothesis of whether *S. oneidensis* MR-1 respiration with 50 mM dioic acids increases the corrosion rate of steel surfaces. Testing the hypothesis was approached in

two different ways. The first experiment tested the hypothesis that adding ligands to the media incubated with *S. oneidensis* MR-1 and oxidized steel would facilitate corrosion of steel by increasing dissolution of the passivating ferric oxide layer on the steel surface. The second experiment tested the hypothesis that addition of *S. oneidensis* MR-1 to the media incubated with ligand and oxidized steel would facilitate corrosion. Both of the experiments recognize the fact that *S. oneidensis* MR-1 and ligand have specific interactions with the steel surface such as *S. oneidensis* MR-1 can form biofilm and dioic acids can adsorb to the steel surface causing passivating corrosion.

In the first method, oxidized steel was incubated in sterile media for 17 hours and then *S. oneidensis* MR-1 (OD_{600} = 0.8) was added to both (ligand and control) EuroCell systems. Five hours after the addition of the bacteria (when the surface have equivalent $E_{corrosion}$), ligands were added into the experimental test. Figure 4.21 shows the addition of *S. oneidensis* MR-1 does not change the corrosion potential ($E_{corrosion}$). However, the addition of ligand caused a measurable change in the $E_{corrosion}$ of each coupon. Upon the addition of 50 mM oxalate, $E_{corrosion}$ dropped to -790 mV from -720 mV (Figure 4.21 A). The addition of 50 mM malonate initially caused $E_{corrosion}$ to increase to -735 mV (from -750 mV) but after ~4 hours the corrosion potential decreased -760 mV (Figure 4.21 B) With the addition of 50 mM succinate, $E_{corrosion}$ decreased to -725 mV (from -720 mV) (Figure 4.21 C).

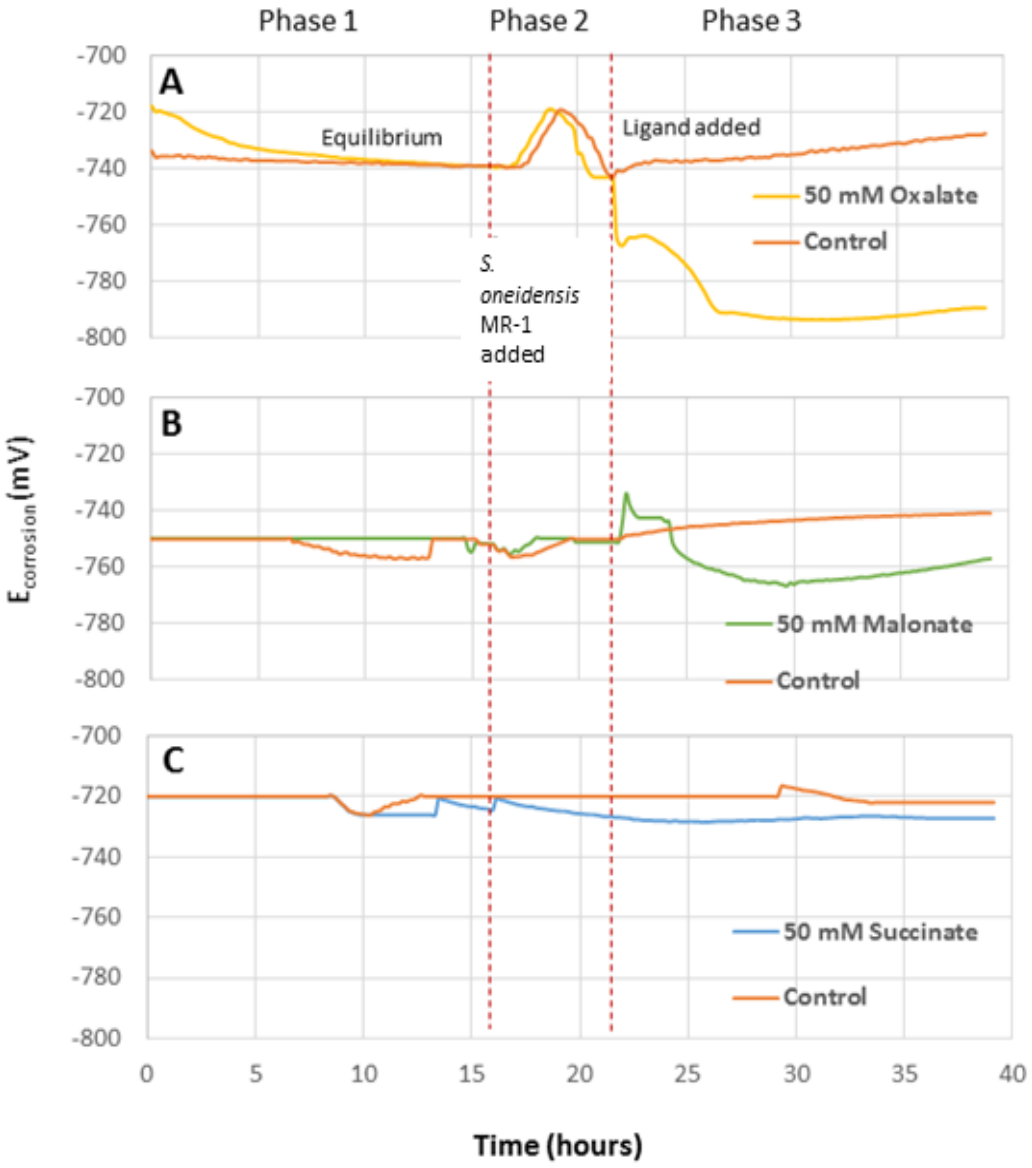

Figure 4.21 Oxidized steel coupons incubated in media under anaerobic conditions for 17 hours. *S. oneidensis* MR-1 was added to both sterile EuroCell systems at t = 17 hour and 50 mM ligands (A. Oxalate, B. Malonate and C. Succinate) added to a cell at 22 hours.

Figure 4.22 shows the change in R_p over the course of the first experiment. Relative to the control a decrease in R_p was observed upon addition of ligands, indicating a decrease in the ferric oxide passivating layer. All the experiments including controls, exhibited an increase in R_p over the time due to the formation and growth of *S.*

oneidensis MR-1 biofilm. The addition of 50 mM oxalate Figure 4.22 A) caused an initial drop in R_p to ~10 ohms (from 100 ohms), but the sample then recovered to ~ 85 ohms and then showed a gradual increase in the resistance of the sample. The value of R_p did not change immediately after the addition of 50 mM malonate (~100 ohms), but after ~2 hours R_p began to increase (Figure 4.22 B). With 50 mM succinate, the value of R_p decreased briefly (to ~ 80 ohms) twice (Figure 4.22 C), but then a similar trend to the oxalate and malonate samples was observed where R_p began to increase. This gradual passivation (increasing on R_p) suggests that it is possible a biofilm is forming on the surface of the coupons. Samples with oxalate and malonate can still cause the corrosion of the steel, and thus there is a delay on increasing R_p but they still eventually passivate.

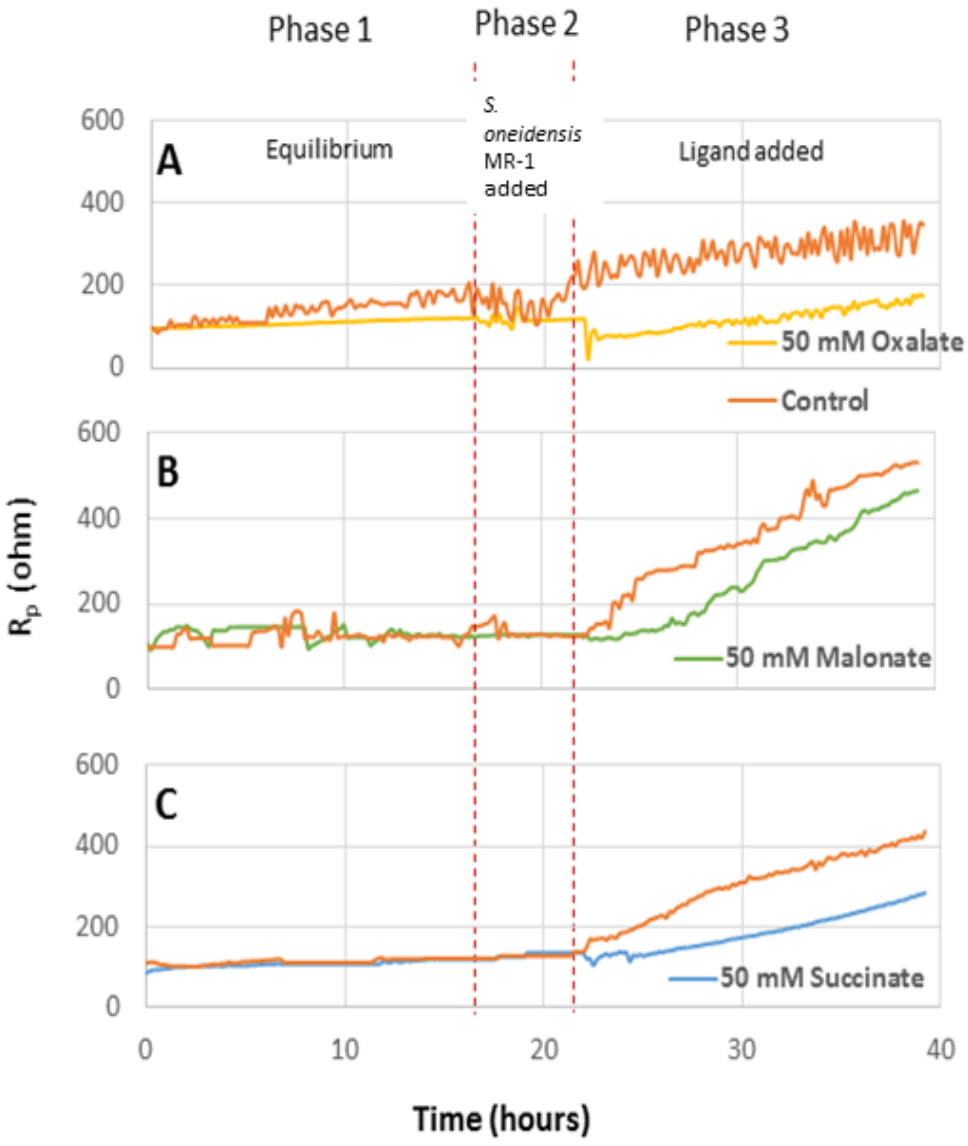

Figure 4.22 Oxidized steel incubated in sterile media under anaerobic conditions for 17 hours. *S. oneidensis* MR-1 was added to both EuroCell systems at t=17 hour and 50 mM ligands (A. Oxalate, B. Malonate and C. Succinate) were added to a cell at 22 hours.

Figure 4.23 shows the changing corrosion rate during the experiment. Again, it can be seen that the addition of *S. oneidensis* MR-1 did not affect corrosion rate for any of the ligands within 5 hours. However, the addition of 50 mM oxalate caused an immediate spike (Figure 4.23 A) in the corrosion rate (to ~125 mpy from ~25 mpy) which then stabilized back to 40 mpy before eventually constantly decreasing towards the end of the experiment. The addition of 50 mM malonate did not cause an increase in corrosion rate (Figure 4.23 B) and the sample remained around 25 mpy for the majority of the experiment before it began to slightly decrease (~18 mpy at t = 26 hr). Upon adding 50 mM succinate (Figure 4.23 C), the corrosion rate of the sample increased very slightly (~30 mpy) but then decreased again to ~15 mpy at t = 27 hr.

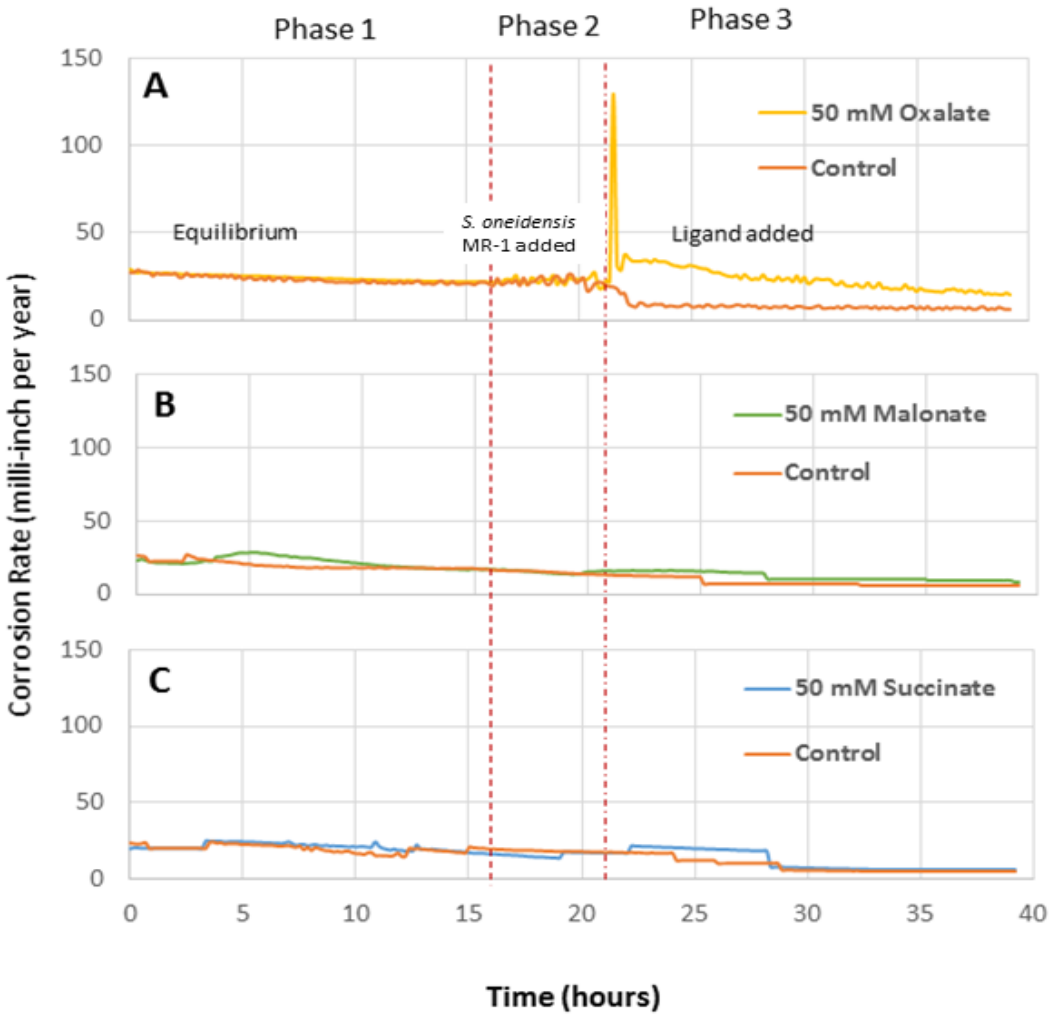

Figure 4.23 Oxidized steel incubated in sterile media under anaerobic conditions for 17 hours. *S. oneidensis* MR-1 was added to both EuroCell systems at t=17 hour and 50 mM ligands (A. Oxalate, B. Malonate and C. Succinate) added to a cell at 22 hours.

The conclusions are: 1) the addition of 50 mM oxalate appeared to increase the corrosion of the oxidized steel coupon, suggesting that its binding constant allows it to bind ferric iron from the surface oxide layer and solubilize it for *S. oneidensis* MR-1 respiration, 2) while $E_{corrosion}$ indicates that malonate and succinate caused potentials favorable for corrosion (i.e. the corrosion potential becomes more negative), overall they did not corrode the surface as well as oxalate, suggesting that their binding

constant may not have been sufficient to solubilize ferric iron from the surface, 3) while oxalate did increase the corrosion rate of the oxidized steel sample, all of the samples, including the controls, began to passivate which suggests that there may have been the formation of a surface biofilm on the steel coupons and 4) the addition of *S. oneidensis* MR-1 before the addition of ligand did not affect the corrosion properties of the steel coupons upon ligand addition.

While electrochemical methods could provide information as to the behavior of the steel coupon during the experiment, other methods were necessary to monitor the respiration of the microbe. To determine the respiration of ferric iron by the bacteria, 1 mL media samples were taken at multiple time intervals during the experiment. The time points chosen were: t = 15 hr (before addition of *S. oneidensis* MR-1), t = 18 hr (1 hour after the addition of *S. oneidensis* MR-1), t = 24 hour (2 hours after ligands were added) and t = 40 hours (the end of the experiment). Figure 4.24 shows the ferrous iron concentration for these different time points of the electrochemical experiment. Before the addition of *S. oneidensis* MR-1, the concentration of ferrous iron was ~0.1 mM on average. With the addition of *S. oneidensis* MR-1, the ferrous iron concentration in the media increased to over 0.2 mM on average, indicating that the bacteria were respiring ferric iron. The addition of 50 mM ligands showed increased respiration efficiency in 2 hours with the ferrous iron concentration having increased to 1.08 mM with 50 mM oxalate, 0.7 mM with 50 mM malonate and 0.4 with 50 mM succinate at the end of the experiment. While initially lagging malonate, by the end of the experiment the system that contained oxalate had the highest ferrous iron concentration, suggesting the highest respiration of ferric iron.

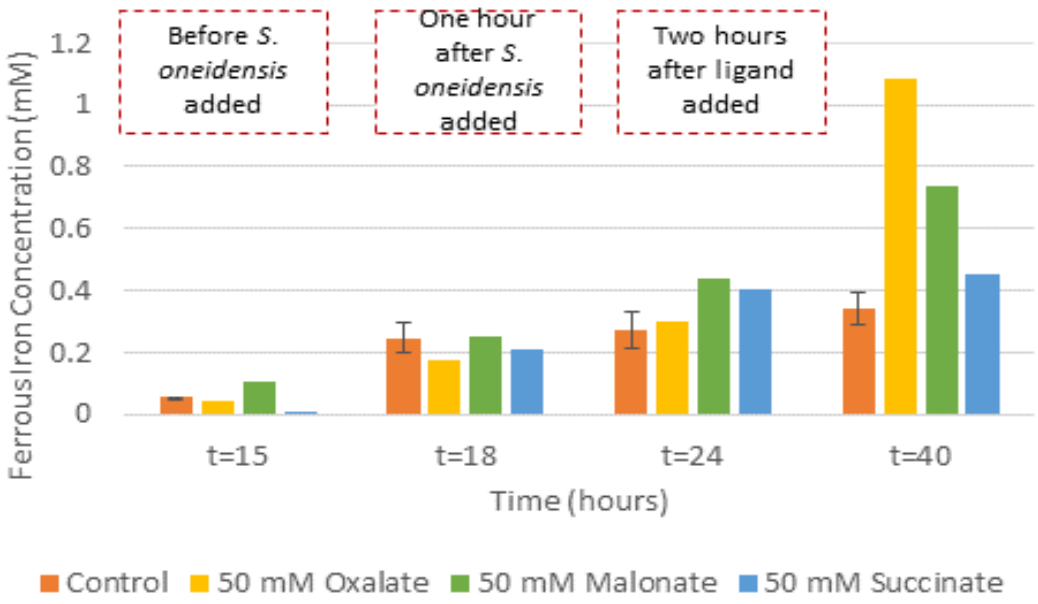

Figure 4.24 Chancing ferrous concentration during the electrochemical experiment of S. oneidensis MR-1 with 50 mM dioic acids and control (without ligand). *S. oneidensis* MR-1 was added to both EuroCell systems at t = 17 hour and 50 mM ligands (oxalate, malonate and succinate) were added to a cell at 22 hours.

To determine the effect of the ligand on the dissolved ferric iron concentration, similar measurements to those for the data in Figure 4.24 were made except that the measurement was dissolved ferric iron concentration. This was a measure of how effective the ligand was at removing ferric iron from the surface of the steel and solubilizing it for respiration by *S. oneidensis* MR-1.

Figure 4.25 shows how the dissolved ferric iron concentration changed over the course of the experiment. Before the addition of bacteria, the dissolved ferric iron concentration was at value of 0.05 mM. After the addition of *S. oneidensis* MR-1, the dissolved ferric iron concentration increased to 0.75-0.9 mM, with the sample for oxalate lagging behind the samples where malonate and succinate were to be added. After the addition of ligand (within 2 hours) the amount of dissolved ferric iron

increased for all the samples, but most noticeably for the oxalate sample, which showed a dissolved ferric iron concentration of 0.3 mM. At the end of the experiment, the concentration of dissolved ferric iron decreased to 0.2 mM and malonate had the highest dissolved ferric iron concentration at 0.27 mM. Samples incubated with succinate showed a very gradual increase in the dissolved ferric iron concentration, suggesting that there was some corrosion occurring, but the amount was minimal (0.1 mM – 0.15 mM after the addition of ligand).

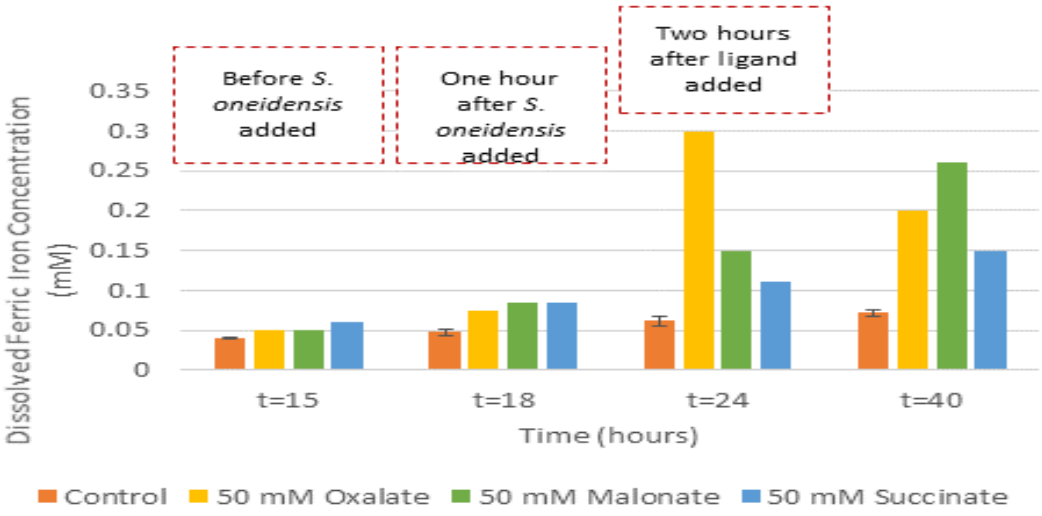

Figure 4.25 Chancing dissolved ferric iron concentration during the electrochemical experiment of *S. oneidensis* MR-1 with 50 mM dioic acids and control (without ligand). *S. oneidensis* MR-1 was added to both EuroCell systems at t = 17 hour and 50 mM ligands (oxalate, malonate and succinate) were added to a cell at 22 hours.

The conclusions from Figures 4.24 and 4.25 are: 1) the addition of ligands significantly increased the solubilization of ferric iron from the surface of the steel coupon and the ferrous iron concentration responded accordingly and 2) oxalate caused the most significant increase in dissolved ferric iron.

The two important results from this experiment were: 1) *S. oneidensis* MR-1 can dissolve ferric iron from the oxidized surface, but this amount is very small and the

presence of ligand facilitate the respiration significantly and 2) S. oneidensis MR-1 causes surface passivation due to the formation of biofilm and addition of ligands especially oxalate delay the passivation process due to removing ferric hydroxide layer.

The second method of testing the effect of ligands on steel corrosion abiotically under anaerobic conditions and then impact of addition of *S. oneidensis* MR-1 into system including ligand and oxidized steel. Oxidized steel coupons were incubated in sterile media for 7 hours and then 50 mM dioic acids were added to both cells. At the end of 17 hours, *S. oneidensis* MR-1 was added into a cell and compared with the abiotic control.

Figure 4.26 shows $E_{corrosion}$ for these samples. It was seen that the addition of ligands at 7 hours shifted $E_{corrosion}$ to a more negative potential, which indicated that there was ferric iron being solubilized from the surface. The corrosion potential dropped to -780 mV (from -710 mV) with 50 mM oxalate (Figure 4.26 A), -760 mV (from -725 mV) with 50 mM malonate (Figure 4.26 B) and -730 mV (from -725 mV) with 50 mM succinate (Figure 4.26 C). When *S. oneidensis* MR-1 was added to the system at t = 17 hours, the corrosion potential of the samples was not affected, which indicated that the microbe did not increase the dissolution of ferric iron from the steel sample. Towards the end of the experiment, $E_{corrosion}$ of all the samples increased: the sample with 50 mM oxalate increased to $E_{corrosion}$ = -780 mV, the sample with 50 mM malonate increased to $E_{corrosion}$ = -760 mM and the 50 mM succinate sample increased slightly to $E_{corrosion}$ = -740 mM. Each ligand dropped to $E_{corrosion}$ to the unique value which demonstrates their difference performance of pulling ferric iron from steel surface.

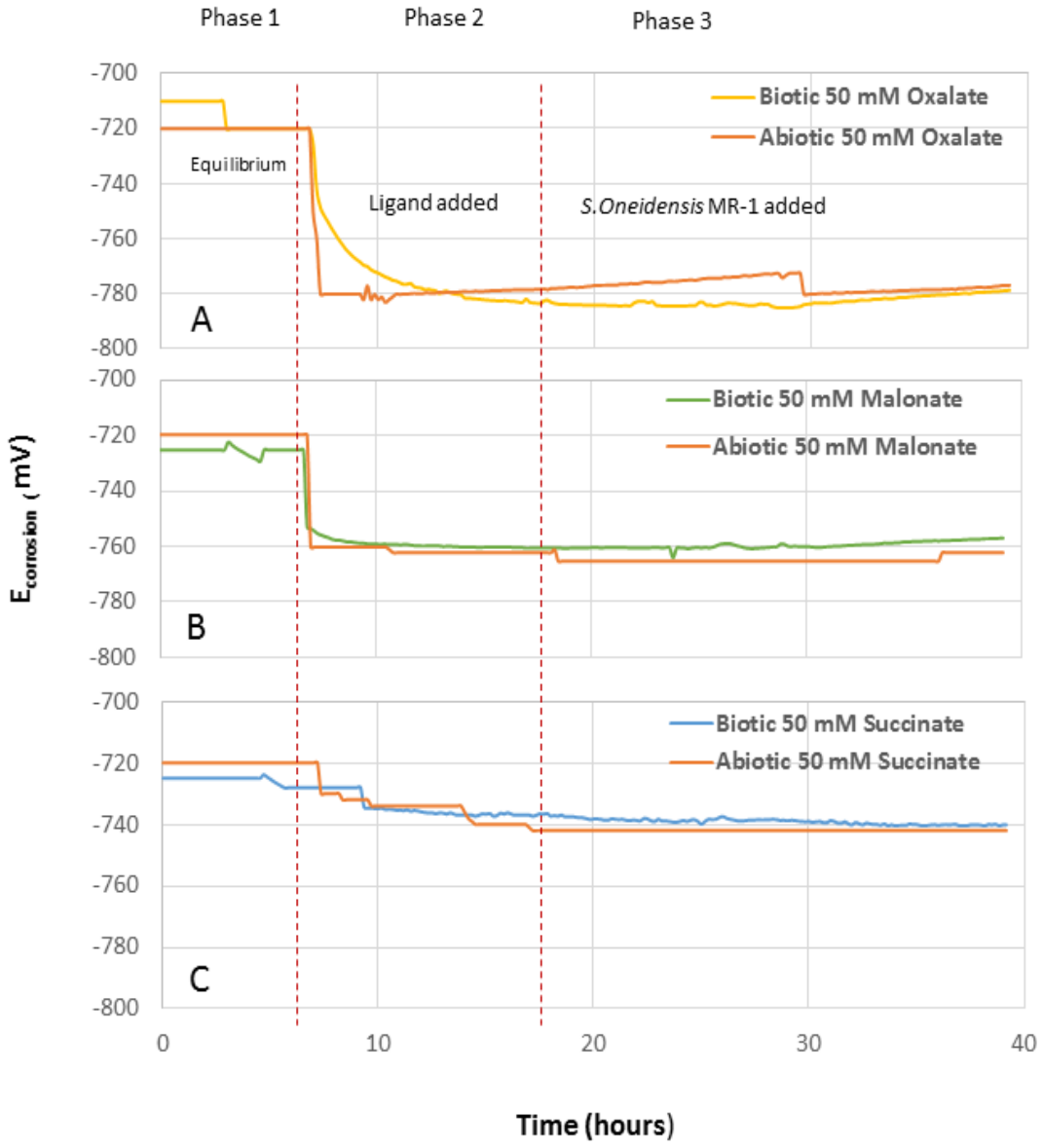

Figure 4.26 Oxidized steel coupons incubated in media under anaerobic conditions for 7 hours. 50 mM ligand (A. Oxalate, B. Malonate and C. Succinate) was added to a cell at 7 hours. *S. oneidensis* MR-1 was added to both EuroCell systems at t = 17 hours.

Figure 4.27 A shows that the addition of 50 mM oxalate caused a small decrease in the value of R_p (from 100 ohms to ~80 ohms), where it remained until the end of the experiment where it started to increase significantly after addition of *S. oneidensis* MR-1 (reaching a value of ~350 ohms by t = 40 hr). The addition of 50 mM malonate caused a sharp drop in the value of R_p (from 150 ohms to 100 ohms), which then stabilized and then began to increase upon the addition of *S. oneidensis* MR-1 (Figure 4.27 B). Upon adding 50 mM succinate to the final sample, R_p began to gradually rise from the starting value of 100 ohms (Figure 4.27 C). The addition of *S. oneidensis* MR-1 did not cause a deviation from this trend. In addition to R_p increasing for the biotic samples, it also increased for the abiotic controls, which suggests that, while a biofilm may have formed in the biotic samples as evidenced by the steep slope compared to the abiotic control samples, there must be another factor that affects the passivation of the steel surface in the presence of only the ligand.

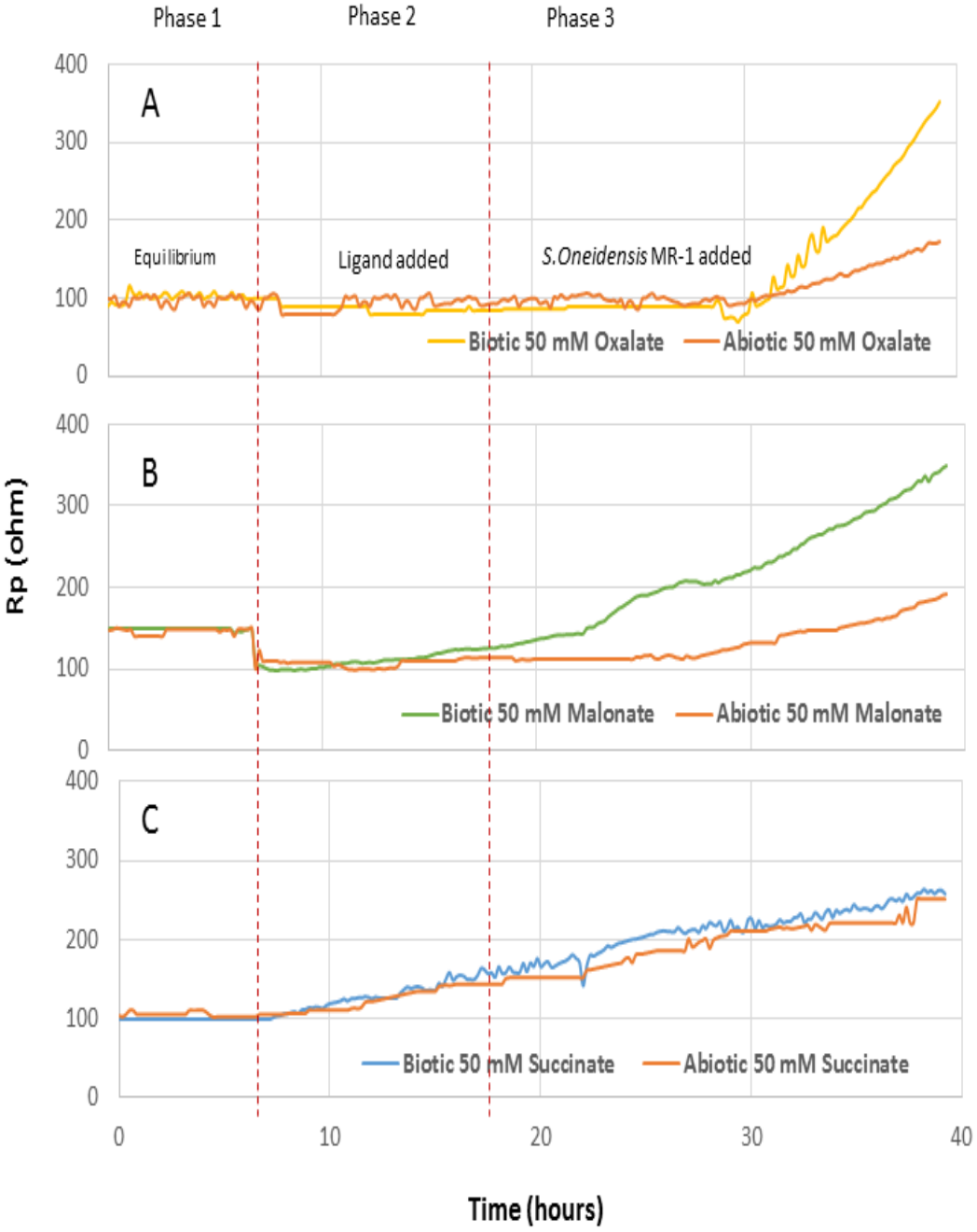

Figure 4.27 Oxidized steel coupons incubated in media under anaerobic conditions for 7 hours. and 50 mM ligands (A. Oxalate, B. Malonate and C. Succinate) added to a cell at 7 hours. *S. oneidensis* MR-1 was added to both EuroCell systems at t = 17 hours.

Figure 4.28 shows the changing corrosion rate over the course of the experiment. The addition of 50 mM oxalate did not dramatically increase the corrosion rate, which went

up to 20 mpy from 19 mpy (Figure 4.28 A). However, towards the end of the experiment (t = 25 hr) after the addition of *S. oneidensis* MR-1, the corrosion rate of the sample began to decline, indicating that the sample was experiencing passivation. Adding 50 mM of malonate caused an immediate increase in corrosion rate (from 20 mpy to 26 mpy), but the corrosion rate began to steadily decline after reaching the maximum (Figure 4.28 B), not changing with the addition of *S. oneidensis* MR-1. Upon adding 50 mM succinate, the corrosion rate of that sample did not change (Figure 4.28 C). Then, at approximately t = 13 hr, the corrosion rate began to decrease and did not change with the addition of bacteria.

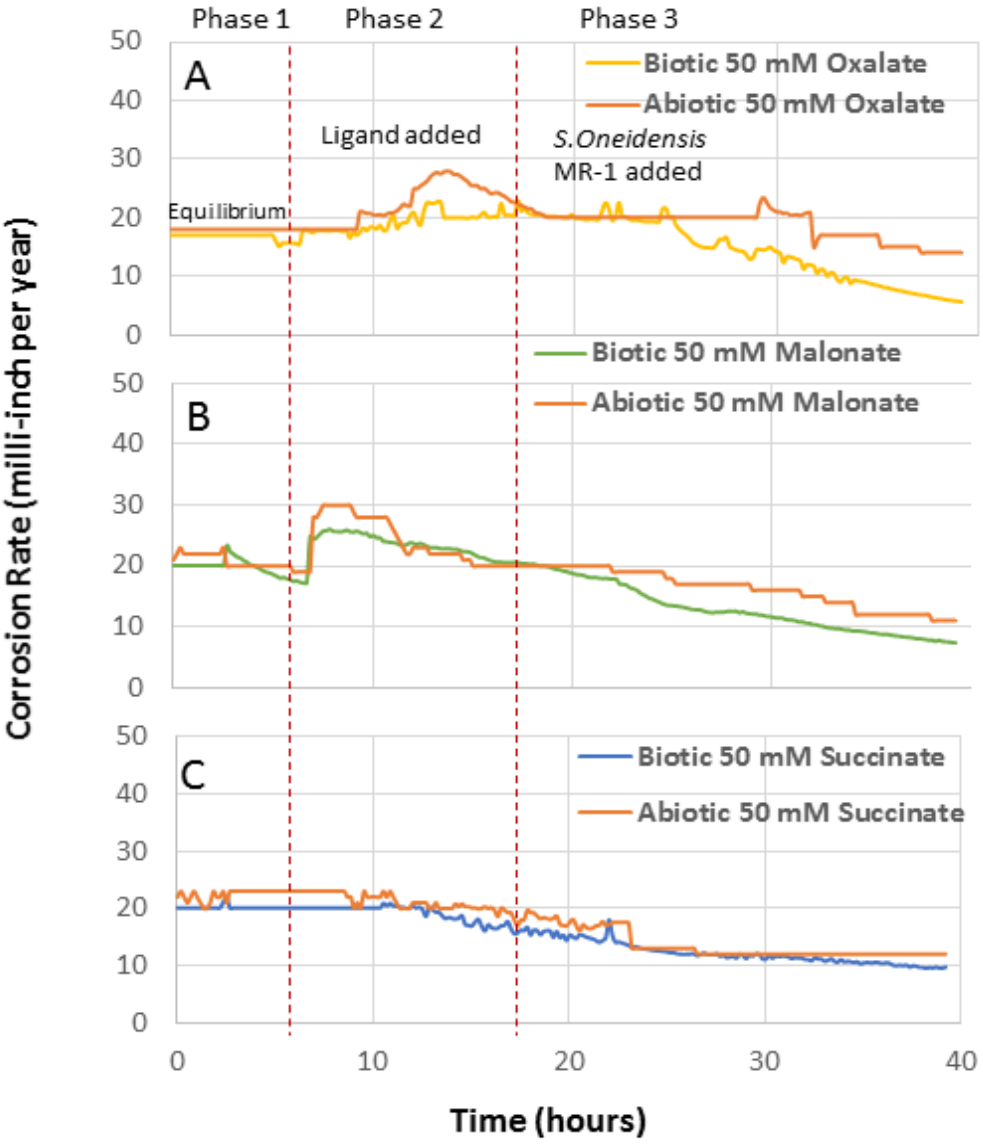

Figure 4.28 Oxidized steel coupons incubated in media under anaerobic conditions for 7 hours. and 50 mM ligands (A. Oxalate, B. Malonate and C. Succinate) was added to a cell at 7 hours. *S. oneidensis* MR-1 was added to both EuroCell systems at t = 17 hours.

The important conclusion are: 1) the addition of ligand caused an immediate decrease of $E_{corrosion}$ to different values for each dioic acid; oxalate had the lowest $E_{corrosion}$ which

indicates it removed the most ferric iron from steel surface, 2) addition of oxalate and malonate decreased the R_p but not succinate 3) abiotic succinate passivates the surface of the steel, 4) in addition to a potential biofilm formation there was another passivation layer that is forming in the control experiments due to the media and 5) the addition of *S. oneidensis* MR-1 passivated the surface and that the organic ligands play a more important role in the corrosion process.

Figure 4.29 shows the ferrous iron concentration at different time points of the electrochemical experiment. It demonstrates the presence of ligands facilitates *S. oneidensis* MR-1 respiration. There were three different time points that were chosen: t = 16 hr (9 hours after ligand addition), t = 22 hr (5 hours after the addition of *S. oneidensis* MR-1), t = 40 hours (the end of the experiment). After the addition of ligands, the ferrous iron concentration was not affected and remained at 0.1 mM on average. However, after the addition of *S. oneidensis* MR-1, the ferrous iron concentration increased to 0.55 mM for the sample with oxalate, 0.5 mM for the sample with malonate and 0.4 mM for the sample with succinate. At the end of the experiment, the ferrous iron concentration remained high, with values of 0.9 mM for 50 mM oxalate, 0.72 mM for 50 mM malonate and 0.45 mM for 50 mM succinate. This suggests that enough ferric iron is being produced for the bacteria to respire throughout the course of the experiment.

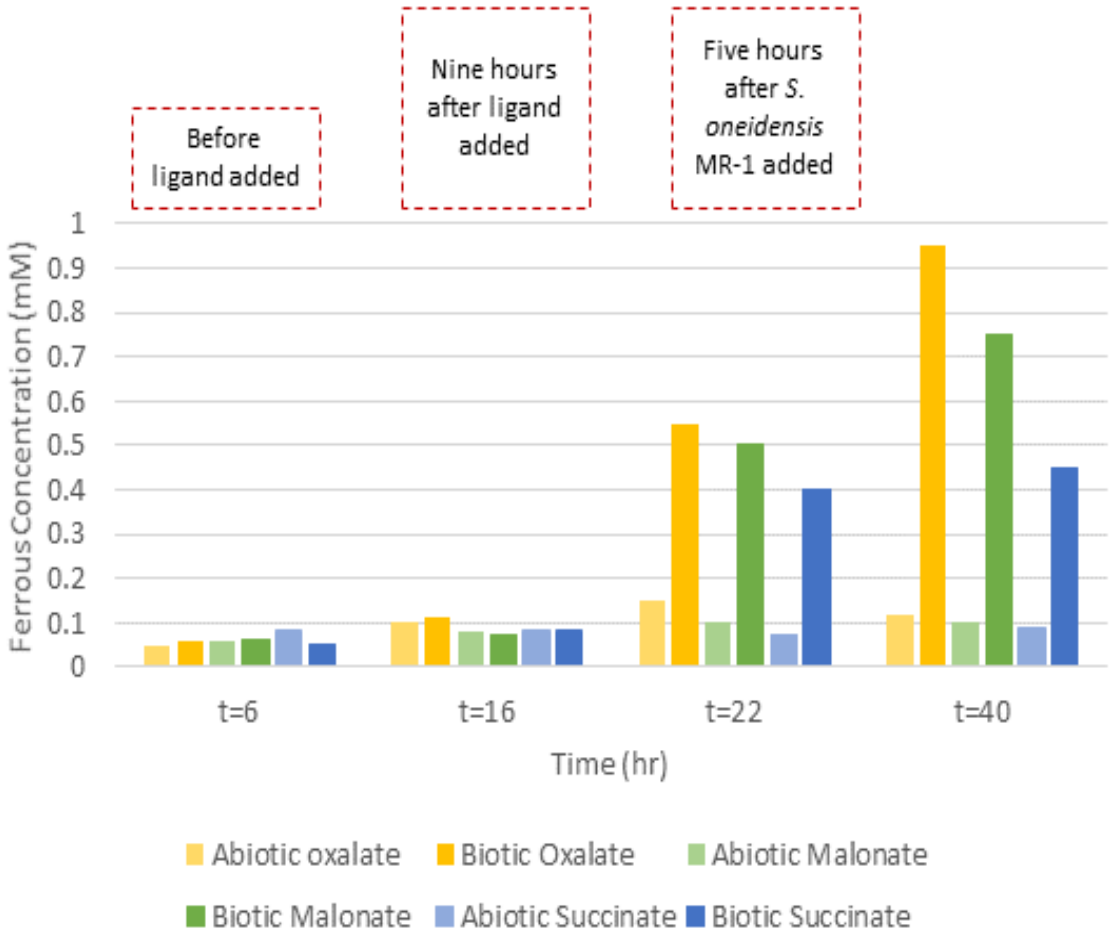

Figure 4.29 Changing ferrous concentration during the electrochemical experiment of *S. oneidensis* MR-1 with 50 mM dioic acids and abiotic control ligands (oxalate, malonate and succinate) were added to a cell at 7 hours and *S. oneidensis* MR-1 was added to a biotic cell at t = 17 hour.

Figure 4.30 demonstrates the change in dissolved ferric iron concentration at the same sampling points, which was a measure of ligand activity. At 9 hours after the addition of 50 mM oxalate, the dissolved ferric iron was 0.47 mM. It then decreased during the remainder of the experiment when at the end it was measured to be 0.1 mM. This is the opposite of the ferrous iron data and suggests that the two confirm that the ligand is immediately producing dissolved ferric iron, which is only reduced after the addition of *S. oneidensis* MR-1, which can respire the dissolved ferric iron. The trend is similar for

50 mM malonate, which started at a high concentration (0.35 mM) and then decreased as the ferric iron was consumed for respiration by the microbes. The 50 mM succinate sample had a slightly different behavior, where initially the dissolved ferric iron concentration started low (0.1 mM) and then increased to 0.2 mM by the end of the experiment. This suggests that the succinate initially passivates the steel surface and then allows for the eventual corrosion of the sample.

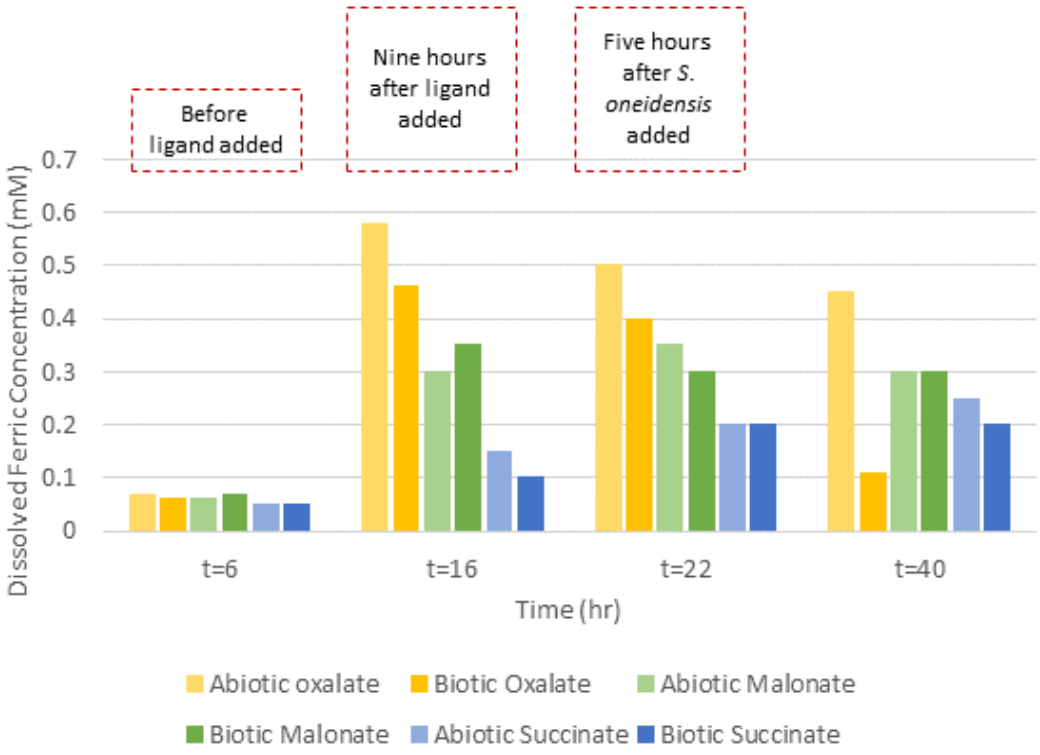

Figure 4.30 Changing dissolved ferric concentration during the electrochemical experiment of *S. oneidensis* MR-1 with 50 mM dioic acids and abiotic control ligands (oxalate, malonate and succinate) were added to a cell at 7 hours and *S. oneidensis* MR-1 was added to a biotic cell at t = 17 hour.

The important conclusions from Figure 4.29 and Figure 4.30 are: 1) the addition of oxalate and malonate caused a high amount of dissolved ferric iron to be produced,

which, when *S. oneidensis* MR-1 is added, is respired to ferrous iron and 2) succinate passivates the surface abiotically, not producing very high amounts of dissolved ferric iron though there was a slight increase in the amount of dissolved ferric iron produced after the addition of the bacteria.

The main conclusion from this experiment was: the addition of ligand increased the solubilization of ferric iron from the steel sample and corrosion was slightly increased. When *S. oneidensis* MR-1 was added to the system, it respired the dissolved ferric iron and produced ferrous iron while passivating the surface. However, in addition to potential biofilm formation there was potentially another mechanism for the passivation of the samples due to the abiotic control samples passivating as well.

The conclusion from this section then is that in the absence of ligand, *S. oneidensis* MR-1 does not affect the corrosion of a steel surface as it cannot solubilize significant ferric iron for respiration. Additionally, the addition of *S. oneidensis* MR-1 after the sample has been incubated with 50 mM dioic acid does not increase the corrosion rate, which suggests that they do not free up the ligand for additional solubilization of ferric iron.

Chapter 5 : Discussion

The overall goal of this research was to test a new proposed mechanism for the corrosion of steel facilitated by the dissolution of ferric iron by dioic acids (oxalate, malonate and succinate), which is subsequently respired by iron reducing bacteria in anaerobic production water environments (Figure 1.1). Corrosion is facilitated by the removal of the passivating layer of ferric oxide, allowing steel to be exposed to, and oxidized by, molecular oxygen during aerobic periods or events. This research was divided into an abiotic component (to investigate the effect of the dioic acids on the dissolution of ferric iron, as well as impact on steel corrosion in aerobic environments) and a biotic component (to investigate the relationship between iron reducing bacteria, dioic acids, and changes in the corrosion potential ($E_{corrosion}$) and the polarization resistance (R_p) which indicate the susceptibility of steel to corrosion). The outcome of this research is to demonstrate that microbial induced corrosion (MIC) can be facilitated by iron-reducing bacteria (IRB) under environmental conditions not amenable to sulfate-reducing bacteria (SRB), and therefore corrosion may not be properly identified and remediated.

5.1 Abiotic, Aerobic Corrosion of Clean and Oxidized Steel with Dioic Acids

The first component of the IRB MIC system requiring characterization is the abiotic interaction of the dioic acids with the steel surface to determine how the dioic acids influence the concentration of dissolved ferric iron. This is particularly important in the presence of aerobic systems, where dissolution of ferric oxide can expose steel surfaces to further oxidation by molecular oxygen, and thus facilitate corrosion. Thus, for these experiments done in aerobic conditions, clean steel surfaces as well as steel coupons

with an oxidized surface were examined. It was hypothesized that the stronger the binding constant of the dioic acid ligand (succinate: log β_3 = 6.88, malonate: log β_3 = 16.6, oxalate: log β_3 = 20.2), the greater the dissolved iron concentration, and in the presence of aerobic system, more corrosion will occur.

Our research showed no direct relationship between the ligand binding constant and the dissolution of ferric iron in an abiotic, aerobic system (Figure 4.1 and Figure 4.2). In fact, oxalate, which has the highest binding constant and was expected to solubilize the most ferric iron, solubilized less ferric iron than malonate (Figure 4.1). It has been shown in the literature that when comparing the same three dioic acids, oxalate (log β_3 = 20.2) solubilizes the highest concentration of ferric iron over malonate (log β_3 = 16.6) and succinate (log β_3 = 6.88) (Paris et al., 2013). One reason for this difference may be related to the working pH of the system, which for the previous work was 4.5 and for our work the pH was 7. At pH = 4.5, only oxalate (pKa_1 = 1.23, pKa_2 = 4.19) will be fully deprotonated as succinate (pKa_1 = 4.2, pKa_2 = 5.6) and malonate (pKa_1 = 2.83, pKa_2 = 5.69) both have pKa values above 5, thus limiting their ability to fully bind to the ferric iron due to charge interactions. As the pH increases, then succinate and malonate become deprotonated and are more available for solubilizing ferric iron.

A possible reason that oxalate does not solubilize the most ferric iron may be the adsorption of oxalate-ferric iron complexes to the surface. Ferric hydroxide species have positive surface charge between pH 4.5-7 and adsorption efficiency of oxalate might increase with increasing pH. It has been proposed that dissolved ferric iron readsorbs to the steel surface as ferric iron-oxalate complexes (Simanova et al., 2011), where they limit the bioavailability of the ferric iron. By showing that there is no direct

relationship between the dioic acid binding constant and the concentration of dissolved ferric iron for an aerobic, abiotic clean steel system. We can say that the binding constant of the ligand, by itself, is not a useful metric for measuring the corrosion of clean steel. However, this experiment has confirmed our hypothesis that the binding constants of these ligands are high enough that they are capable of solubilizing ferric iron.

The first experiments (Figures 4.1 and 4.2) were performed with a ligand concentration of 50 mM, and then we desired to find the minimum concentration of dioic acids that effect on the solubilization of ferric iron (Figure 4.3 and Figure 4.4). Varying the concentration of dioic acid between 0.01 mM and 50 mM shows an increase in the dissolved ferric iron concentration as a function of ligand concentration in the range of 1 mM to 50 mM ligand (Figure 4.3), a trend which has also been reported in the literature in the presence of 0-25 μM dioic acids (oxalate, malonate and succinate) (Paris et al., 2013). The maximum value of 50 mM ligands was selected because oxalate concentrations in production well environments was reported 50 mM (Kharaka et al., 1993). Thus, we want to work at as high of a relevant concentration as we possibly can while keeping the results meaningful to real-world systems. This is what led to the use of 50 mM ligand concentrations throughout the remainder of this work.

Succinate has the effect of passivating the surface of the steel rather than causing corrosion in that the total iron concentration is not measurable for a succinate concentration of 50 mM (Figure 4.4 and as shown in later sections, e.g. Figure 4.8 and Figure 4.23). It has the lowest binding constant of the three dioic acids as well as either of the control ligands and it dissolved less than 0.07 mM total iron at a 50 mM

concentration. However, lower concentrations of succinate had higher total iron, even being the highest of the three dioic acids at the 10 mM concentration (Figure 4.4). It has been reported in the literature that increasing the concentration (5 mM and above) of succinate decreases the corrosion of steel due to the formation of an inhibiting surface film by succinate that limits the dissolution of metal (Amin, 2006). This result of increasing concentration inhibiting the steel surface is observed in our work (again in later figures, e.g. Figure 4.8).

For the reference ligands (citrate and NTA), the expected behavior was high concentration of dissolved ferric iron (Haas & DiChristina, 2002) and those results were observed when the ferric oxyhydroxide layer was present on steel surface. These ligands chelate iron using a different mechanism than the dioic acids, where they bind to ferric iron in a 1:1 ratio while the dioic acids bind in a three dioic acid to one ferric iron (3:1) ratio. This means that for every ferric iron ion solubilized, less citrate and NTA will be required, making it easier for them to chelate and remove ferric iron than with dioic acids.

The results indicate that the ferric iron solubilization by dioic acids step of our proposed mechanism does occur and that their concentration is important to the dissolution of ferric iron. However, they also indicate that dioic acids do more than solubilize ferric iron. They likely also undergo adsorptive process and interact with the surface, which suggests that there is further complexity to this mechanism than was previously proposed. We have also learned that there is no direct relationship between the binding constant of the ligand and the amount of ferric iron that they solubilize in an aerobic and abiotic system, which means that the binding constant, by itself under the conditions

used in our experiments, is not an accurate parameter for evaluating the corrosion ability of these systems.

Since dioic acids can adsorb to clean steel surfaces and protect them from oxidation and dissolution of the resulting ferric iron, it's also important to examine how the dioic acids interact with steel surfaces already coated with a layer of ferric oxides. The purpose of these experiments is to test the component of the mechanism that involves dioic acids interacting with, and solubilizing ferric iron from the oxidized layer of the steel.

Our results show that the ligands are capable of solubilizing ferric iron from the surface of an oxidized steel coupon (Figure 4.5). However, they solubilize approx. 1.5 times less ferric iron than what was observed in the clean steel experiments. The difference between the abiotic clean steel corrosion and the abiotic oxidized steel corrosion may be due to the different adsorption properties of the dioic acids for clean steel and oxidized steel. It has been shown that organic ligands adsorb differently on clean (metallic) and oxidized steel surfaces (Kuznetsov et al., 1996). Oxidation of an iron surface changes the adsorption of organic inhibitor on surface. For example, it was shown that a "good corrosion inhibitor" might not adsorb on a clean steel surface, rendering it ineffective in medium (Kuznetsov et al., 2016). The exact opposite condition is possible where a "non-effective corrosion inhibitor" for a clean steel surface can exhibit corrosion inhibition in the presence of an oxidized layer on the metal surface (Kuznetsov et al., 2016). For our mechanism, this has implications that the presence of an oxide layer will affect the solubilization of ferric iron by causing adsorption of the organic ligand to the oxide. This will produce less soluble ferric iron available for respiration by the IRB in

the next step of the mechanism. Linear polarization resistance (LPR) assesses the impact of dioic acid ligands on the corrosion of the oxidized steel sample by measuring changes in the corrosion potential ($E_{corrosion}$) and the polarization resistance (R_p) of the steel surface as a function of ligand type and concentration.

The results of the LPR experiment with abiotic, aerobic and oxidized steel coupons provide further confirmation of the dissolved iron measurements. For oxalate, the increase in $E_{corrosion}$ (Figure 4.6 A) coupled with the increase in R_p (Figure 4.7 A) indicates that the surface is not corroding. We expect that during the corrosion of steel the metal ions are being removed from the surface, which leads to an accumulation of negative charge on the surface due to the presence of a large concentration of electrons. However, the observation that the potential and the resistance both become higher (e.g. the potential becomes less negative and the resistance increases) indicates that there is an accumulation of a positive charge on the surface, which is more resistive. The higher resistance of the sample is typically associated with the formation of an oxide layer that passivates the steel surface, but the adsorption of a ligand to the surface would give a similar result. The corrosion rate measurement also confirms that the corrosion of the sample decreases (Figure 4.8 A). This supports the dissolved ferric iron measurements for the sample incubated with oxalate (Figure 4.5).

For malonate, the decrease in $E_{corrosion}$ (Figure 4.6 B) and the decrease in R_p (Figure 4.7 B) indicate that the sample is corroding. As stated previously, we expect the process of metal ions leaving the surface (i.e. corrosion occurring) to generate a negative charge on the steel surface, leading to a more negative (decreasing) potential. This also means that the surface is less resistive to corroding due to the lack of an oxide layer building up on

the surface and a potential is more likely to be conducted on the sample, thus the decrease in R_p. The corrosion rate again demonstrates that we do indeed see increased corrosion (Figure 4.8 B), which supports the dissolved ferric iron measurements (Figure 4.5).

For succinate, the variation in $E_{corrosion}$ (Figure 4.6 C) and R_p (Figure 4.7 C) indicate that both passivation and corrosion are occurring on the surface of the steel. This suggests that initially there is passivation of the steel surface by succinate, but then it begins to corrode (Figure 4.8 C). This supports the dissolved ferric iron concentration measurements that show initially low amounts of dissolved ferric iron, but then a sharp increase towards the end of the experiment.

Mass loss measurements also show that over the course of the experiment the sample exposed to oxalate loses only 21 mg of steel compared to the ligand free control, which lost 46 mg of steel (Table 4.1). Meanwhile, the malonate samples indicate that, along with the solubilization of ferric iron, the corrosion properties of the ligand are such that they increase the corrosion of the oxidized steel sample (Figures 4.6 B, 4.7 B, and 4.8 B) with a mass loss of 70 mg and the succinate samples behave as a first a passivating ligand and then increasing the corrosion of the steel (Figure 4.8 C) with a mass loss of 44 mg. These measurements support both the LPR data and the total and dissolved iron concentration measurements shown previously.

As discussed, an increased resistance and corrosion potential are typically associated with the formation of an oxide layer on the surface of the steel. While this is likely to occur, it is also not likely that this is the explanation for the behavior of the sample with oxalate. If the formation of an oxide layer gave this result, then it would be expected

that the samples with lower binding constants would exhibit similar behaviors. However, they do not. This then suggests that it is the adsorption of oxalate to the surface of the sample that is producing this behavior. This would indicate that the oxalate is passivating the surface and preventing any further corrosion from occurring. This is not observed with malonate and succinate and could imply that their binding constants are low enough that they are more stable in solution, while the oxalate-ferric iron complex is more stable on the surface. This is potentially a problem for the biotic system in that this would prevent the solubilization of ferric iron for respiration by the IRB.

Overall the results of the abiotic component of the proposed IRB MIC mechanism indicate that in the absence of bacteria, oxalate passivates the surface, malonate corrodes the surface and succinate is a relatively neutral ligand with a small amount of corrosion. The passivation behavior of oxalate for oxidized coupons is likely due to the adsorption of the ligand to the surface, which is a process greatly enhanced in the presence of an oxide layer (Brown et al., 1999) (Simanova et al., 2011) (Kuznetsov, 2016) and suggests that pH and the adsorption of the ligand to the steel surface are also important in our proposed mechanism.

5.2 Biotic Corrosion of Carbon Steel in the Presence of *S. oneidensis* MR-1 and Dioic Acids Under Anaerobic Conditions

After dissolution of ferric iron by dioic acid ligands, the next step in the proposed IRB MIC mechanism is the respiration of the dissolved ferric iron and the subsequent freeing of the dioic acid ligand to give it the ability to readsorb to solid-phase ferric oxide and solubilize additional ferric iron for continued respiration. As seen in the

previous results, our proposed mechanism requires modification due to the adsorption of organic ligands (especially oxalate) to solid-phase ferric oxides, impacting the solubilization of ferric iron from an oxidized steel surface. The goal of these biotic experiments with *S. oneidensis* MR-1 is to determine how the respiration of these iron-reducing bacteria will be influenced by the presence of dioic acids, and if the microbes themselves, contribute to or modify the dissolution of solid-phase ferric oxide.

5.2.1 Dissolved Ferric Iron Measurements of Biotic Corrosion

The second major step in our proposed mechanism, after the solubilization of ferric iron by dioic acids, is the respiration of the solubilized ferric iron by our model organism *S. oneidensis* MR-1. This is key to the mechanism is that respiration of ferric iron to ferrous iron is proposed to free the dioic acid (since ferrous iron ions bind very weakly with dioic acids), allowing the dioic acid molecules to re-adsorb to the solid-phase ferric oxide surface and solubilize more of the ferric iron from the surface oxide layer. It is proposed that continued cycling of the dioic acids, driven by IRB respiration, will remove ferric oxide layers that passivate the steel surface, thereby making it more susceptible to molecular oxygen upon exposure to aerobic conditions.

It has been shown that *S. oneidensis* can use ferric iron as an electron acceptor from both solution and insoluable sources (Starosvetsky et al., 2016). This study found *S. oneidensis* had a 1.7 % efficiency for reducing insoluble ferric iron (Starosvetsky et al., 2016). The insoluble nature of ferric iron oxide minerals at pH 4 or more creates a metabolic dilemma for microorganisms capable of using them as terminal electron acceptors (Ehrlich, 1996) as it is energy intensive for the microbes to remove these ferric iron ions for respiration. To use insoluble ferric oxyhydroxide for respiration IRB

are required to be in direct contact with the ferric oxyhydroxide. To facilitate the respiration, the IRB produce organic chelators or electron shuttles like riboflavin as described in the literature review section (Bird et al., 2011). However, this process would be assisted by the organic ligands that are already present in the system, as is proposed in our mechanism. Our experiments show that the model organism is capable of respiring ferric iron from either ferric oxyhydroxide (Figure 4.11 and Figure 4.12) or an oxidized steel surface (Figure 4.15 and Figure 4.16). Our proposed mechanism suggests that the microbe will respire ferric iron that has been solubilized by the dioic acid, but it is also capable of respiring ferric iron using one of the mechanisms described above. This is important to keep in mind that there are other methods of microbial ferric iron respiration, any of which can occur in our system.

The rate of microbial respiration is measured by the amount of ferric iron consumed in the reaction. While with an ideal system containing a known amount of homogeneous ferric iron we can calculate the total amount of ferric iron consumed, when we are working with an oxidized coupon, the starting concentration of ferric iron is unknown and thus we can only get information about the rate of ferrous iron formation.

When we compare the homogeneous ferric oxyhydroxide particles with the actual system of an oxidized steel coupon, we can see that there are some similarities between the two systems. One of the key similarities is that the rates of ferrous iron formation between the ferric oxyhydroxide particles and the oxidized coupon are almost the same with the presence of 50 mM ligands. The formation rates differ by 8% and 3 % for oxalate and malonate respectively and the oxidized coupon has the higher rate. The difference in succinate is more profound at 3.42 times the rate of formation for an

oxidized system over the ideal ferric oxyhydroxide system. This suggests that the respiration in a system with an oxidized coupon is more favorable than with ferric oxyhydroxide. It has been shown that soluble ferric iron with organic chelators can be reduced with higher affinity by *S. oneidensis*. (Starosvetsky et al., 2016). Our experiments showed the presence of oxalate and malonate facilitated the ferric iron respiration meanwhile succinate did not really affect the respiration of ferric oxyhydroxide (Figure 4.11 and Figure 4.12) and oxidized steel (Figure 4.15 and Figure 4.16).

However, a key finding is the difference between the ligand free control samples. As there was no ligand present, the only mechanism of ferric iron solubilization and subsequent ferrous iron formation was through microbial activity. This allowed us to determine the baseline effect that the microbe itself has on the process of solubilizing ferric iron and respiring it using one of the previously mentioned mechanisms of cell secreted ligands or direct contact mechanism. What the ferrous iron formation rates tell us about the control sample with oxidized steel is that there is our model IRB do not favor solubilizing ferric iron on their own. In the presence of 50 mM ligands the rate of ferrous iron production is significantly higher than with the control samples. This further confirms that the ligand assists in the respiration process. Also notable is the fact that for the control system the rate is higher with ferric oxyhydroxide rather than the oxidized steel. As the ferric oxyhydroxide system is the most homogeneous and well controlled system, it allows for the easy solubilization and respiration of ferric iron by the microbes.

The use of 5 mM ligands was again to test the effects of concentration on the solubilization and the rate of ferric iron reduction. The observation that for this system the faster rate was with ferric oxyhydroxide suggests that at low concentrations the ligand works more efficiently with the homogenous ferric oxyhydroxide particles and that the rate of ferrous iron formation is limited in the system with the oxidized steel coupon. It should be noted that for both experiments however that, the rate values for each system at 5 mM did not vary significantly around the control value, indicating that this concentration is too low to use for further experiments. This means concentration of dioic acids are greatly important to demonstrate whether they can facilitate proposed MIC IRB mechanism.

Our results have shown that the respiration of ferric iron is greatly enhanced in the presence of higher concentrations of oxalate and malonate for both ferric oxyhydroxide (Figures 4.11 – 4.14) and oxidized steel (Figures 4.15 – 4.18), which agrees with the abiotic experiments that show increasing ligand concentration increases the amount of dissolved ferric iron. This is very noticeable when comparing Figure 4.17 and Figure 4.18, which present the total dissolved iron for each ligand. We can see that the dissolved ferric iron concentration is the same between the two experiments, but the ferrous iron concentration is higher in the 50 mM sample, indicating rapid respiration of dissolved ferric iron.

The respiration behavior has a similar trend for systems containing either ferric oxyhydroxide particles (Figures 4.11 – 4.14) or an oxidized steel coupon (Figures 4.15 – 4.18) as the ferric iron source, but the systems containing ferric oxyhydroxide have higher concentrations of dissolved ferric iron and ferrous iron. This is due to the ferric

oxyhydroxide, which provided homogenous ferric iron making the dissolution process easier as the whole particle can be dissolved. The system with an oxidized steel coupon is more complex, likely containing multiple forms of oxidized iron, thus making it more difficult for dissolution of ferric iron from the steel surface. However, there is sufficient ferric iron in these systems still to have noticeable respiration.

In order to determine if the solubilization of ferric iron was limiting to the respiration of ferric iron, we tested to see if inoculating *S. oneidensis* MR-1 twelve hours after inoculating the ligand had any effect on the rate of respiration (Figure 4.19) The observation of our work that the rate of ferric iron respiration is independent of the time that the ligand is present in the system (Table 4.3) is important as it shows that the dissolution of ferric iron is a very rapid process and thus not rate limiting. This means that the presence of 50 mM oxalate or malonate in production water would immediately provide a favorable environment for IRB to survive.

From these rates, oxalate and malonate noticeably facilitate S. oneidensis MR-1 respiration. According to Haas (2002), the ferric iron reduction rate (mM/h) is defined as a linear increase in the dissolved ferrous iron concentration over time. Ferric reduction rates are linear through ~80 – 90% of the curve, after which the rate of reduction diminishes (Haas, 2002) which is also observed in all of the respiration experiments. The fastest ferric iron reduction was observed when ferric iron was complexed with citrate (Haas, 2002), similar to the research in this thesis. As shown in Table 4.2, the ferric iron reduction rates (reported as ferrous iron formation rates) for 50 mM ligand experiments, are as follows: citrate > NTA > oxalate > malonate > succinate. This section helped to demonstrate the role of the organic ligand in the

proposed mechanism as it was shown that in the absence of the ligand, the microbe had a significantly lower respiration rate than was seen with the ligand present. This means that to see a significant effect on the solubilization of ferric iron, the ligand needs to be present in the system and in the proposed mechanism.

5.2.2 Linear Polarization Resistance Analysis of Biotic Corrosion

As we have now determined that oxalate and malonate solubilize ferric iron from oxidized steel coupons and *S. oneidensis* MR-1 are capable of respiring that ferric iron, the final parameters to test are the influence on the corrosion of the steel coupon as well as the recycling of the dioic acids for further solubilization of ferric iron from the steel surface.

The LPR experiments were performed in two ways, which allowed us to compare each parameter individually (with ligand vs. without ligand, with bacteria vs. without bacteria). The first method was experiments where *S. oneidensis* MR-1 was added before the ligand (Figures 4.21 – 4.25) and the second method was experiments where the ligand was added before *S. oneidensis* MR-1 (Figures 4.26 – 4.30).

When looking at the corrosion potential in Figures 4.21 and 4.26 for both of the methods, it can be observed that the addition of each ligand decreased the corrosion potential to the unique value for both experiments (~ -780 mV – -790 mV for oxalate, ~ -760 mV for malonate and ~ -740 mV for succinate). This change can likely be attributed to the binding constant of the dioic acid (log β_3 = 20.2 for oxalate, log β_3 = 16.6 for malonate and log β_3 = 6.88 for succinate), in which a higher binding constant allows for better binding and solubilization of ferric iron from the oxidized steel surface. Figure 4.25 supported this statement, showing the highest dissolved ferric iron

concentration with oxalate followed by malonate and then succinate. Based on this data oxalate affects the corrosion of steel more than other the other studied dioic acids. It solubilized more ferric iron from the oxidized steel surface than the other dioic acids, which caused the rapid consumption of ferric oxyhydroxide layer. The *S. oneidensis* MR-1 that were present then took advantage of the high concentration of ferric iron produced by oxalate and reduced ferric iron to ferrous iron as shown in Figure 4.24 & Figure 4.25 and Figure 4.29 & Figure 4.30. This supported the part of the mechanism that the presence of 50 mM oxalate (a dioic acid) can cause consumption of a ferric hydroxide layer from a steel surface in the presence of IRB, making the steel more vulnerable to oxidation if there is molecular oxygen in the system.

Another interesting observation was an increase in R_p when *S. oneidensis* MR-1 was present, as shown in Figure 4.22 and Figure 4.27. In method one (Figure 4.22), the addition of oxalate or malonate initially decrease R_p for a short time, likely due to a sudden rise in the solubilization of ferric iron from the oxidized steel surface. However, the consumption of the oxide layer and subsequent respiration of dissolved ferric iron over time led to an increase in R_p. Method two also showed that the presence of *S. oneidensis* MR-1 with oxalate and malonate increased Rp compared to abiotic experiments (Figure 4.27).

As stated previously, these experiments were completely anaerobic and the increase in R_p is likely not the formation of a new oxide layer on the steel surface since there is not any oxidizer present in system. It is likely that again we are observing the adsorption of the ligand to the surface. However, this time this occurs for all three ligands. This suggests that there is another mechanism that causes the passivation of the surface. This

mechanism is the formation of a biofilm on the steel surface, which would increase R_p and decrease the corrosion rate. It has been shown in the literature that biofilm formation by *S. oneidensis* MR-1 causes inhibition of steel corrosion (Videla et al., 2009), further supporting this hypothesis.

The absence of organic ligand shows that *S. oneidensis* MR-1 do not contribute much to the corrosion process, confirming the results of the rate data in Table 4.2, and that the ligand is significant in helping to solubilize more ferric iron from the steel surface for respiration by *S. oneidensis* MR-1. However, the presence of *S. oneidensis* MR-1 does not influence the effects of organic ligand on the corrosion process. This suggests that while they are using the solubilized ferric iron produced by the organic ligand, they do not directly influence or contribute to increasing the corrosion or dissolution process other than assisting in recycling the organic ligand.

LPR experiments demonstrated a key component for IRB MIC mechanism: the choice of ligand in the mechanism is important as not all dioic acids are same amount of effective to the corrosion process. These results serve to confirm that our proposed mechanism of MIC by iron reducing bacteria is overall valid. Oxalate is the best dioic acid for microbial respiration since it solubilized the highest concentration of ferric iron. From the corrosion aspect, addition of each dioic acid increased the corrosion rate in the following order: oxalate > malonate > succinate

However, our experiments showed the order of interactions (either ligand – oxidized steel or bacteria -steel) affect the corrosion behavior oxidized steel in that adding the ligand first immediately affects the corrosion of the steel, but adding the bacteria first has no effect on the corrosion process. This indicates that it is the ligand that affects the

corrosion of the steel by removing the oxide layer in the form of soluble ferric iron for respiration by the bacteria, but the bacteria themselves only serve to recycle the ligand and do not directly increase the corrosion of the steel sample. In addition, along with adsorption of the ligand to the surface causing the inhibition of corrosion which caused increased on Rp as shown in Figure 4.27, the potential formation of a biofilm passivates the surface and protects it from corrosion, indicating two potential factors that further affect our proposed IRB MIC mechanism.

Chapter 6 : Conclusion and Future Work

In this work, we have tested a newly proposed mechanism of microbially influenced corrosion of carbon steel by iron reducing bacteria. Our proposed mechanism was that dioic acids present in an anaerobic system facilitate the solubilization of ferric iron from ferric oxide layers present on the surface of the steel. The soluble ferric iron would then be available in solution and the unbound "free" iron would accessible for respiration by IRB, which use ferric iron as a terminal electron acceptor in the absence of oxygen. The unbound dioic acid can then return to the steel surface and facilitate further solubilization of ferric iron, consuming the oxide layer. The periodic cleaning and draining of the production well allows for oxygen to enter and re-oxidize the now exposed surface. Thus, the proposed mechanism contributes to increased corrosion of carbon steel.

We have concluded in our work that the proposed mechanism is indeed valid, but there are likely additional components that affect the system. We have shown that dioic acids are capable of solubilizing ferric iron from an oxidized steel surface and that this solubilization is further enhanced in the presence of our model organism *S. oneidensis* MR-1. Furthermore, we have shown that the ferric iron produced in this process is respired by *S. oneidensis* MR-1, producing ferrous iron. Finally, we have shown that the corrosion rate of oxidized steel increases in the presence of both IRB and dioic acids.

In addition to showing that our mechanism has merit, we have also learned that there are other factors affecting the IRB MIC process. One such factor is the adsorption of ligand to the surface of the steel, which would limit the availability of ferric iron for *S. oneidensis* MR-1 respiration and consequently result in decreased corrosion.

Furthermore, our results have shown that the *S. oneidensis* MR-1 might cause the formation of a biofilm on the surface of the coupon (from increasing R_p over the experiment when *S. oneidensis* MR-1 was present), which corresponds to passivation of the surface.

Future work should be invested for looking at the effects of ligand adsorption on the coupon surface. The adsorption of ligand inhibits solubilization of ferric iron, but if the ligand were on the surface and the microbes formed a biofilm, then the ligand-ferric iron complex is more bioavailable than the uncomplexed ferric iron, which would lead to an increase in ferric iron respiration.

Subsequently, the effects of biofilm formation should be investigated. As the genome of *S. oneidensis* MR-1 is well characterized and non-biofilm forming mutants have already been developed, these studies should be repeated to determine the effect of biofilm formation on the corrosion process.

Finally, the effects of oxygen input should be studied. The anaerobic work performed in this thesis showed that the corrosion rate did not increase over time and in fact decreased. It is known that there is periodic input of oxygen to the production well environment, which continuously refreshes the oxide layer, causing corrosion. These experiments could be repeated with periodic input of oxygen to investigate how the availability of the oxygen will impact the corrosion.

References

Amin, M. (2006). The Inhibition of Low Carbon Steel Corrosion in Hydrochloric Acid Solutions by Succinic Acid Part 1. Weight Loss, Polarization, EIS, PZC, EDX, and SEM Studies. *Science Dirent*, 3378-3588.

Arnold, R. G. (1990). Regulation of dissimilatory Fe (III) reduction activity in Shewanella putrefaciens. *Applied and General Microbiology*, 2811-2817.

Arnold, R., Di Christina, T., & Hoffman, M. (1988). Reductive dissolution of Fe(III) oxides by Pseudomonas sp. 200. *Biotechnology and Bioengineering*, 1081-1096.

Bird, L., Bonnefoy, V., & Newman, D. (2011). Bioenergetic challenges of microbial iron metabolisms. *Trends in Microbiology*, 330-340.

Bonneville, S., Cappellen, P. V., & Behrends, T. (2004). Microbial reduction of iron(III) oxyhydroxides: effects of mineral solubility and availability. *Chemical Geology*, 255-268.

Broadway, N., Dickinson, M., & Ratledge, C. (1993). The enzymology of dicarboxylic acid formation by Curynebacterium sp. strain 7E1C grown on n-alkanes . *Journal of General Microbiology*, 1337-1344.

Brown, G., & Henrich, V. (1999). Metal Oxide Surfaces and Their Interactions with Aqueous Solutions and Microbial Organisms. *American Chemical Society*, 77-174.

Canstein, H. v. (2008). Secretion of Flavins by Shewanella Species and Their Role in Extracellular Electron Transfer. *Applied and Environmental Microbiology*, 615-623.

Dougherty, J. (2004). A review of the effect of organic acids on CO2 corrosion. *NACE International* (p. 04376). Houston: NACE International.

Drever, J. (2004). *Surface and Groundwater, Weathering, and Soils.* Boston: Elsevier.

Dubiel, M. (2002). Microbial Iron Respiration Can Protect Steel from Corrosion. *Applied and Environmental Microbiology*, 1440-1445.

Ehrlich. (1996). *Geomicrobiology.* New York: Marcel Dekker.

Enning, D., & Garrelfs, J. (2014). Corrosion of Iron by Sulfate-Reducing Bacteria: New Views of an Old Problem. *Applied and Environmental Microbiology*, 1226 – 1236.

Fennessey, C. M. (2010). Siderophores Are Not Involved in Fe(III) Solubilization during Anaerobic Fe(III) Respiration by Shewanella oneidensis MR-1. *Applied and Environmental Microbiology* , 2425-2432.

G1-03, A. (2003). *Standard practice for preparing, cleaning, and evaluating corrosion test specimens.* West Conshohocken: ASTM.

Giacomelli, C., Giacomelli, F., Baptista, A., & Spinelli, A. (2004). The effect of oxalic acid on the corrosion of carbon steel. *Anti-Corrosion Methods and Materials* , 105.

Gram, L. (1994). Siderophore-Mediated Iron Sequestering by Shewanella putrefaciens. *Applied Environmental Microbiology* , 2132-2136.

Gunaltun, Y. M., & Larrey, D. (2000). Correlation of casses of top of the line corrosion with calculated water condensatio rate. *NACE International* (p. 00071). Houston: NACE International.

Haas, J. R. (2002). Effect of Fe(III) Chemical Speciation on Dissimilatory Fe(III) Reduction by Shewanella putrefaciens. *Environmental Science Technology*, 373-380.

Haas, J., & Dichristina, T. (2002). Effects of Fe(III) Chemical Speciation on Dissimilatory Fe(III) Reduction by Shewanella putrefaciencs. *Environmental Science Technology*, 373-380.

Hecherl, E., Kosson, D., & Cowan, R. (2003). A kinetic model for bacterial ferric oxide reduction in batch cultures. *Water Resources Research*, 1098.

Herrera, K. (2009). Role of iron-reducing bacteria in corrosion and protection of carbon steel. *Elsevier*, 891-895.

Herrera, L. K. (2009). Role of iron-reducing bacteria in corrosion and protection of carbon steel. *International Biodeterioration & Biodegredation* , 891-895.

Hinds, G. (2010). *The electrochemistry of corrosion.* Teddington: National Physical Laboratory.

Jahaverdashti, R. (2008). *Microbiologically Influenced Corrosion.* London: Springer-Verlag London.

Kato, S., & Nakamura, F. (2010). Respiratory interactions of soil bacteria with (semi) conductive iron-oxide minerals. *Environmental Microbiology*, 3114-3123.

Kawamura, K., Sempere, R., Imai, Y., Fujii, Y., & M, H. (1996). Water soluble dicarboxylic acids and related compounds in Antarctic aerosols. *Geophysicial Research and Atmospheres*, 18721-18728.

Kharaka, Y., Ambats, G., & Thordsen, J. (1993). Distribution and significance of dicarboxylic acid anions in oil field water. *Chemical Geology*, 499-501.

Kieft, T., Fredrickson, J., Onstott, T., & Gorby, A. (1999). Dissimilatory Reduction of Fe(III) and Other Electron Acceptors by a Thermus Isolate. *Applied and Environmental Microbiology*, 1214-1221.

Labinger, J., & Bercaw, J. (2002). Understanding and Exploitin C-H Bond Activation. *Nature*, 507-514.

Little, B. J. (2007). Causative organisms and possible mechanisms. In B. J. Little, *Microbially Influenced Corrosion* (p. 22). Hoboken: R. Winsto Revie.

Manivannan, R., & Rajendran. (2012). Inhibition of corrosion of carbon steel by heptane sulphonic acid and Zn2 system. *Journal of Electrochemical Science and Engineering*, 1-18.

Nanny, Mark. "Iron-Reducing Bacteria And Iron-Chelating Metabolites: Another MIC

Mechanism". 2015. Presentation.

Nanny, M., Zhou, J., Zhou, A., Avci, R., Suflita, J., Duncan, K., . . . Gao, S. (n.d.). *From Genomes to Phenomes: Systems-Level Understanding of the Molecular Mechanisms Underlying Metal Biocorrosion* (EPSCoR RII Track-2 FEC).

Okochi, H., & Brimblecombe, P. (2002). Potential Trace Metal-Organic Complexation in the Atmosphere. *The Scientific World*, 767-786.

Paris, R., & Desboeuf, K. (2013). Effect of Atmospheric Organic Complexation on Iron-bearing Dust Solubility. *Atmospheric Chemistry and Physics*, 4895-4905.

Paris, R., Desboeuf, K. V., & Journet, E. (2011). Variability of dust iron solubility in atmospheric waters: investigation of the role of oxalate organic complexation. *Atmospheric Environment*, 6510-6517.

Patil, S. A. (2013). Cisplatin-induced elongation of Shewanella oneidensis MR-1 cells improves microbe-electrode interactions for use in microbial fuel cells. *The Royal Society of Chemistry*.

Perrin, D. D. (1959). Ferric Complexation with Aliphatic Acids. *Journal of the Chemical Society*, 1710-1717.

Rivera, V. F. (2011). *Localized CO2 Corrosion in the Presence of Organic Acid.* Ohio: Vanessa Fajardo Nino de Rivera.

Ruebush, S., Icopini, A., Brantley, S., & Tien, M. (2006). n vitro enzymatic reduction kinetics of mineral oxides by membrane fractions from Shewanella oneidensis MR-1. *Geochim Cosmochim Acta*, 56-70.

S. Belkaid. (2012). Poly(4-vinylpyridine-hexadecyl bromide) as corrosion inhibitor for mild steel in acid chloride solution. *Res Chem Intermed*, 2309-2305.

Simanova, A., Loring, J., & Persson, P. (2011). Formation of Ternary Metal-Oxalate Surface Complexes on α-FeOOH Particles. *The Journal of Physical Chemistry*, 21191-21198.

Starosvetsky, J. (2016). Rust dissolution and removal by iron-reducing bacteria: A potential rehabilitation of rusted equipment. *Corrosion Science*, 446-454.

Stern, M., & Geary, A. L. (1957). Electrochemical polarization I. A theoretical analysis of the shape of polarization curves. *Journal of the electrochemical society*, *104*(1), 56-63.

Stumm, W., & Morgan, J. (1996). *Aquatic Chemistry.* New York City: Wiley & Sons.

Taillefert, M. (2007). Shewanella putrefaciens produces an Fe(III)-solubilizing organic ligand during anaerobic repiration on insoluable Fe(III) oxides. *Journal of Inorganic Biochemistry 101*, 1760-1767.

Tran, T., Brown, B., Nesic, S., & Tribollet, B. (2013). Investigation of Mechanism for Acetic Acid Corrosion of Mild Steel. *NACE Internationals* (p. 2487). Houston: NACE Internationals.

V., F., Canto, C., Brown, B., & Nesic, S. (2007). Effect of organic acids in CO2 corrosion. *NACE International* (pp. 1-4). Houston: NACE International.

Videla, H. A. (2009). Understanding microbial inhibition of corrosion. A comprehensive overview. *International Biodeterioration & Biodegradation*, 896-900.

Wiatrowski, H., Ward, P., & Barkay, T. (2006). Novel reduction of mercury (II) by mercury-sensetive dissimilatory metal reducing bacteria. *Environmental Science Technology*, 6690-6696.

Williamson, C. H., Jain, L., Mishra, B., & Olson, D. (2015). Microbially influenced corrosion communities associated with fuel-grade ethanol environments. *Applied Microbiology and Biotechnology*, 6945-6957.

Zou, R. (2007). Biofilms: strategies for metal corrosion inhibition employing microorganisms. *Applied Microbiology Biotechnology*, 1245-1253.

Appendix A: *S. oneidensis* MR-1 Minimal Media

Table A-1. *S. oneidensis* MR-1 media content

MR-1 minimal medium (modified M1 medium) with 60 mM Lactate and 25 mM Ferric Oxyhydroxide				
Chemical	FW (g/l)	Stock	for 1 L (ml)	Final concentrations
H2O			878.77 (928.77)*	(mM)
PIPES Buffer	302.5	0.5M	40	20
Ammonium chloride	53.49	4 M	7	28.04
Potassium chloride	74.55	0.5 M	2.68	1.34
Sodium phosphate monobasin	138	1 M	4.35	4.35
Magnesium chloride		1 M	1	1
Calcium chloride		1 M	0.2	0.2
Ferric oxyhydroxide	106.9	1 M	25	25
Minerals solution, 100X stock			10	LS4D
Thauers vitamins			1	LS4D
Sodium lactate (60% w/w) syrup	112.1	2 M	30	60
Tryptone 0.2 g/L			2 grams	